Progress in Polymer Science 140 (2023) 101665

Contents lists available at ScienceDirect

Progress in Polymer Science

journal homepage: www.elsevier.com/locate/progpolymsci

# Nature-inspired strategies for the synthesis of hydrogel actuators and their applications

Weijun Li[a,1,*], Qingwen Guan[b,1], Ming Li[c,*], Eduardo Saiz[c], Xu Hou[a,d,e,f,*]

[a] State Key Laboratory of Physical Chemistry of Solid Surfaces, College of Chemistry and Chemical Engineering, Xiamen University, Xiamen 361005, China
[b] School of Chemistry, University of Glasgow, Glasgow, G12 8QQ, UK
[c] Centre of Advanced Structural Ceramics, Department of Materials, Imperial College London, London, SW7 2AZ, UK
[d] Department of Physics, Research Institute for Biomimetics and Soft Matter, Fujian Provincial Key Laboratory for Soft Functional Materials Research, College of Physical Science and Technology, Xiamen University, Xiamen 361005, China
[e] Institute of Artificial Intelligence, Xiamen University, Xiamen 361005, China
[f] Innovation Laboratory for Sciences and Technologies of Energy Materials of Fujian Province (IKKEM), Xiamen 361005, China

ARTICLE INFO

*Article history:*
Received 4 November 2022
Revised 2 February 2023
Accepted 21 February 2023
Available online 26 February 2023

*Keywords:*
Responsive
Bio-inspired
Hydrogel actuator
Toughening mechanism
Smart device

ABSTRACT

Nature endows numerous organisms with the ability to realize their basic physiological activities through stimulus-responsive actuation. Inspired by these interesting biological structures, various biomimetic hydrogel actuators with excellent controllability, fast response, and toughness have been developed. Here, the principles of enabling stimulus-responsive behavior in polymer materials are first reviewed for the example of biological materials and subsequently recent progress in implementing stimuli-response behavior in bioinspired hydrogel actuators are being discussed. Particular emphasis is on the mechanisms underlying mechanical toughening of hydrogel actuators and its role in applications. The goal is to highlight recent progress, find the common threads, and discuss the fundamental differences to determine the current challenges and future directions for this field.

© 2023 The Authors. Published by Elsevier B.V.
This is an open access article under the CC BY license (http://creativecommons.org/licenses/by/4.0/)

## 1. Introduction

Various creatures in nature, such as the octopus [1–3], jellyfish [4,5], Venus flytrap [6–8], and mimosa [9–11], etc., could achieve movement, predation, reproduction and other activities through stimulus-responsive soft actuation. Based on these interesting phenomena, many attempts have been made to develop artificial responsive hydrogel actuators, including artificial muscles [12–14], smart actuators [9,15–18], and soft robots [19–22], etc. As a class of materials with highly cross-linked hydrophilic networks and a high water content, hydrogels are biologically inspired materials. By modifying their chemistry, structure, and function, it is possible to develop artificial soft actuators that respond to stimuli. However, because of the uneven distribution of networks and cross-links, the majority of typical hydrogels could be quite brittle. This brittleness precludes their practical application in actuators where they are subject to mechanical loading that can trigger failure. Designing toughening and energy dissipation processes to enhance the strength, fracture and fatigue resistance of hydrogels has long been necessary to sustain practical actuation and capabilities similar to those of natural organisms. In addition, the hydrogel actuators can also be made to achieve complex shape change and movement processes through rational responsive design. Thus, tough

*Abbreviations:* LCST, lower critical solution temperature; UCST, upper critical solution temperature; PNIPAM, poly(N-isopropylacrylamide); TiNS, titanate nanosheets; DL4P, digital light 4D printing; PAAM, polyacrylamide; AAM, acrylamide; PAAC, polyacrylic acid; AAC, acrylic acid; PNAGA, poly(N-acrylamide); LEDs, light-emitting diodes; UV, ultraviolet; NIR, near-infrared; AuNPS, gold nanoparticles; PU, polyurethane; CB, carbon black; NdFeB, neodymium iron boron; PHEMA, 2-hydroxyethyl methacrylate; PEGDA, poly (ethylene glycol) diacrylate; MF, applied magnetic fields; NMF, non-applied magnetic fields; SHSME, self-healing supramolecular magnetic elastomer; DC, direct current; PAMPS, poly(2-acrylamido-2-methylpropanesulfonic acid); RGO/Poly(PAMPS-co-AAM), reduced graphene oxide/poly(2-acrylamide-2-methylpropanesulfonic acid-acrylamide); PSPA, poly(3-sulfopropyl acrylate, potassium salt); AC, alternating current; CS, chitosan; CMC, carboxymethylcellulose; THBP, 2,2′,4,4′-tetrahydroxybenzophenone; PVA, polyvinyl alcohol; PEG, poly (ethylene glycol); NPs, nanoparticles; GO, graphene oxide; PPY, polypyrrole; IR, infrared; PEI-co-PAAC, polyethyleneimine copolymer (acrylic acid); PBI-HPEI, hyperbranched polyethyleneimine; DMAEMA, poly(N,N-dimethylaminoethyl methacrylate); MBA, N,N'-methylenebisacrylamide; RH, relative humidity; P(OEGMA-DSDMA), methacrylate-bis(2methacryloyl)oxyethyl disulfide); PS, polystyrene; P(AAM-BAC), poly(acrylamideN,N′-bis(acyloyl)cystamine); PLLADLLA, poly(L-lactide-co-D, L-lactide); AI, artificial intelligence.

* Corresponding author.
*E-mail addresses:* lwjdesky@163.com (W. Li), m.li19@imperial.ac.uk (M. Li), houx@xmu.edu.cn (X. Hou).

[1] The two authors contribute equally to this work

https://doi.org/10.1016/j.progpolymsci.2023.101665
0079-6700/© 2023 The Authors. Published by Elsevier B.V. This is an open access article under the CC BY license (http://creativecommons.org/licenses/by/4.0/)

and responsive hydrogels are especially popular due to their chemical and structural diversity [15,23–25]. These kinds of hydrogels not only show excellent flexibility and biocompatibility but are also capable of adapting themselves to complicated environments by quickly responding to external stimuli [18,26–28].

From the perspective of materials science research and practical applications, conventional stimuli-responsive hydrogel actuators are composed of simple polymer molecular structures, which exhibit various deficiencies such as weak mechanical properties (strength $<$ 50 kPa, stiffness $<$10 kPa, toughness $<$10 J $m^{-2}$), slow response (such as conventional PNIPAAM hydrogel usually taking in the range of minutes to hours.) and poor environmental tolerance, thus severely limiting their broad practical application in soft actuators. In contrast, the natural hydrogels of biological tissues featuring multi-components and multiscale hierarchical structures have outstanding mechanical performance. For example, the pinecones have high toughness modulus and strength values as 1.21 GPa and 25.24 MPa, respectively. Inspired by the extreme mechanical properties of these soft tissues, many tough hydrogel actuators possessing outstanding mechanical properties have been developed. These advances have laid a solid foundation to guide the design and processing of mechanically robust tough hydrogels, which, in turn, expand their functional applications in soft actuators [27–31]. The construction of reversible non-covalent bonds (sacrificial bonds), such as hydrogen bonds [29–32], electrostatic interactions [33–35], coordination bonds [33,35–37], supramolecular recognition [38–40] and hydrophobic associations [31,38,41–43], is of great importance to develop toughness in hydrogels. These "sacrificial bonds" could effectively enhance the mechanical properties of hydrogels, since the reversible bonds consume and dissipate a large amount of energy during breaking [44–48]. Moreover, these reversible non-covalent bonds could also endow the hydrogels with self-healing properties [44–47]. Based on this construction principle, various tough hydrogels have been developed during the past decade, including double network hydrogels [31,35,49,50] slide-ring hydrogels [43,51,52] nanoparticle-reinforced hydrogels [53], nanocomposite hydrogels [54–56] and micelle-crosslinked hydrogels [57,58], etc. The responsiveness could be obtained by further chemical design or modification of the hydrogel network structure [59–61], so that the hydrogels would undergo changes in volume or shape to achieve soft actuation when exposed to environmental stimuli involving temperature [62–64], pH [65–68], light [69–72], magnetic field [73,74], electric field [9,75,76] and redox [77–79], etc. The research on flexible, intelligent devices based on responsive hydrogels and actuation behaviors has recently received widespread attention [80–82]. Nevertheless, how to efficiently combine the responsiveness and toughening mechanism to develop tough responsive hydrogels that withstand reduplicative loads remains a critical step in practical applications. Typical construction methods include integrating hydrogels with different properties on the same device, constructing precise and controllable property distribution in a single hydrogel, and achieving programmed deformation or movement when subjected to external stimulus [83–88].

This review will introduce bio-inspired hydrogel devices that exhibit stimulus-responsive actuation behavior after being exposed to specific stimuli. Typical biological prototypes and methods to mimic natural structures will also be reviewed. In addition, we also summarize the latest developments in the development of toughening mechanism in hydrogels and their applications in smart devices and biomedicine fields (Fig. 1). This work will finish with the main conclusions and future research suggestions.

## 2. Natural examples

There are plenty of biological examples with responsive actuating behavior in nature, ranging from animals to plants and from land to ocean, providing valuable inspiration for designing artificial responsive materials.

### 2.1. Actuation based on changes in cell osmotic pressure

Many plants can trigger and control actuation by the migration of ions in cells or changes in membrane permeability after being stimulated by the surrounding environment. For instance, the Venus flytrap can instantly close their leaves to capture insects (Fig. 2A). When receiving the stimuli, the leaves of the Venus flytrap would exchange water with the environment (absorption/release of water), causing the variation of osmotic pressure, thereby generating different expansion pressure to control the “open” and “close” state of leaves. The Venus flytrap closure is caused by simultaneous outer epidermal expansion and interior epidermis contraction. The motion would not be influenced by the mesophyll. Furthermore, due to internal hydraulic pressure differential between the layers, or prestress, the traps are in a ready-to-snap state for rapid closure. The behavior of the traps after closure (when prestress was changed) suggests that water movement from the adaxial to the abaxial layers may cause the trap to become even narrower. The movement of interstitial water via the elastic tissue dampens the quick closure action of the trap internally. Exaggerated lobe bending is most likely caused by the left-over water displacement. The two distinct pieces of Venus flytrap in the puzzle of trap snapping, Once this change occurs, the geometry of the doubly-curved leaf provides the mechanism by which elastic energy is both stored and released, and the hydrated nature of the leaf induces the rapid damping that is equally crucial for efficient prey capture [7,89–92]. Similarly, mimosa can also close its leaves after being touched (Fig. 2B). However, unlike the Venus flytrap, which relies on environmental water exchange, the movement of mimosa leaves is realized by the reversible osmotic pressure changes caused by the redistribution of water molecules in cells [10,93,94].

### 2.2. Actuation based on the uneven expansion of the cellulose fibril structure

In addition to the changes in osmotic pressure, the uneven expansion of the cellulose fibril structure in the cell wall can also trigger actuation. A typical example is pinecones (Fig. 2C), composed of cellulose fibrils with two different orientations. In humid environments, the length of longitudinal cellulose fibrils increases, while the horizontal ones increase in width, causing uneven expansion in volume and eventually leading to the opening of pinecones [25,95–98]. Similarly, wheat awns have tissue types with different cell wall structures, the inside of which is called the "cap", towards the other awn; and the outside, called the "ridge", which faces towards the outside. In the cap, the cell wall has oriented cellulose fibrils almost parallel to the cell axis, making the axis of the awn less sensitive to moisture changes. However, in the lower part of the ridge, the cellulose fibrils are randomly distributed, and changes in moisture can cause isotropic shrinkage or expansion, which ultimately causes it to open/close (Fig. 2D) [99–101].

### 2.3. Actuation through the breaking/generation of weak reversible bond

Many echinoderms rely on the nanocomposite in their dermal tissue to strengthen the high aspect ratio collagen fibres with a viscoelastic matrix, achieving quick and reversible stiffness changes. For example, sea cucumbers can harden to defend against external threats (Fig. 2E) [102,103]. Researchers found that the soluble macromolecules released by the dermal cells of the sea cucumber

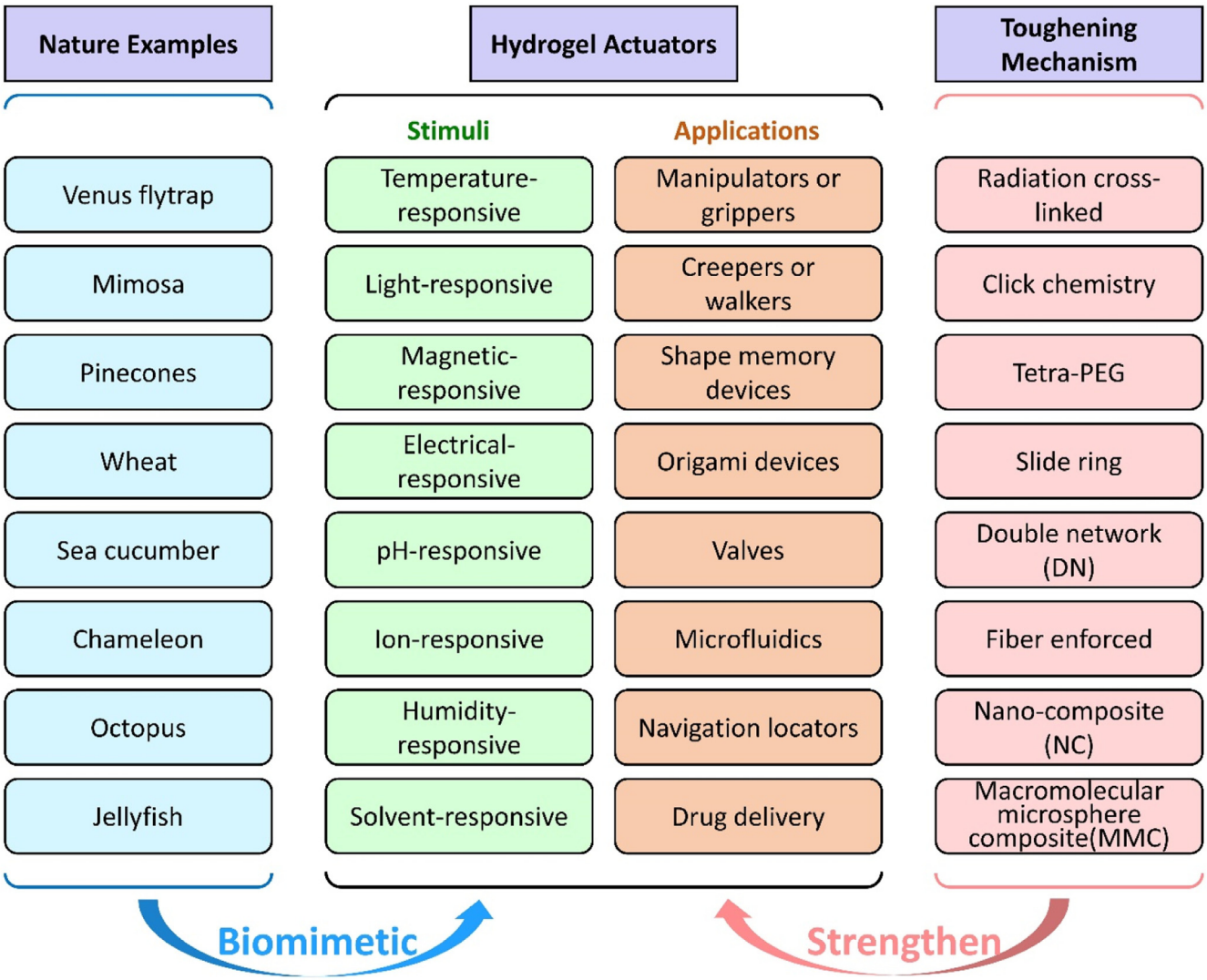



**Fig. 1.** Existing research on responsive hydrogel actuators: from natural to bio-inspired artificial switchable hydrogels, including toughening mechanisms and applications.

could promote the reversible regulation of fibre interaction in the dermal tissue [103–105]. This is mainly achieved by forming temporary, weak bonds with the proteoglycans on the surface of adjacent reinforcing fibres, which significantly increases the elastic modulus of skin tissue [103–105].

### 2.4. Actuation through microstructural changes

Stimulus-responsive structural changes, the spacing of structural units (nano-mirrors), or the average refractive index endow some organisms such as chameleons with dynamic, quick, and reversible structural colour transition behaviors. The chameleon can adjust its skin tone to help communicate and camouflage during moving to adapt to the ever-changing environment. This process takes place within a few minutes and is reversible [106–110]. As shown in Fig. 2F, under combat conditions, the adult male chameleon changes the background colour of its skin from green to yellow. This is mainly because the guanine crystals contained in the two layers of iridescent dermal cells. The iridophores in the upper layer are made up of tiny, densely packed guanine crystals with a diameter of 127.4 nm. These crystals are arranged in a triangular lattice. Guanine crystals (with a high refractive index of 1.83) combine with the cytoplasm (with a low refractive index of 1.33) to generate a photonic crystal structure. The distance between guanine crystals was on average 30% smaller in the resting state (green skin) than in the excited state (yellow skin) (Fig. 2F), while the crystal size in surface iridophores did not change. When the external environment stimulates the chameleon, its dermis is stretched to an excited state. At this moment, the lattice spacing of the nanocrystals increases, causing the preferential reflectivity to shift from short wavelengths to long wavelengths, and corresponding colour changes occur [108,110].

### 2.5. Actuation through the shrinking/stretching of soft structure

Many animals in nature also use the deformability of their soft systems to achieve effective movement in complex environments, one typical example is the octopus. The octopus' arms are provided with outstanding controllability and can stretch to twice their original length to reach into tiny cracks for preying (Fig. 2G). Besides, the octopus could also activate specific muscles to produce local stiffness, thereby exerting force on the environment. More importantly, the octopus's body is entirely soft and has no internal or external bones. The high flexibility of their arms is based on its unique muscle arrangement, which consists of three types of mus-

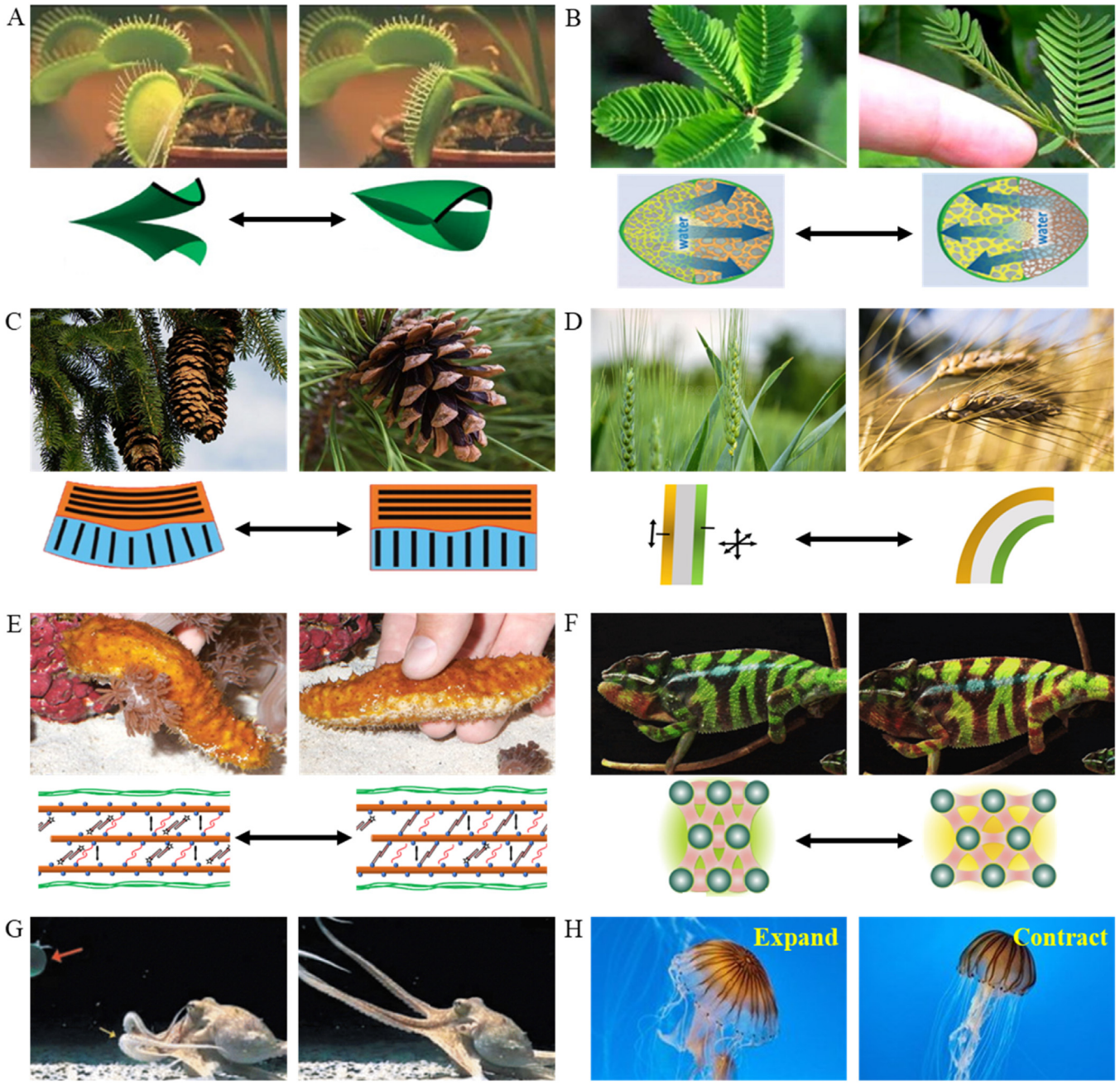



**Fig. 2.** (A) Venus flytrap in the open and closed state. [6], Copyright 2007. Reproduced with permission from John Wiley & Sons Inc. [89], Copyright 2005. Reproduced with permission from the Nature Publishing Group. (B) Mimosa leaves before and after being touched. [10], Copyright 2016. Reproduced with permission from the American Association for the Advancement of Science. (C) Pinecones in the wet and dry state. [125], Copyright 2012. Reproduced with permission from Annual Reviews Inc. (D) Wheat awn in a damp and dry condition. [101], Copyright 2007. Reproduced with permission from American Association for the Advancement of Science. (E) Sea cucumber in a relaxed and hardened state. [124], Copyright 2008. Reproduced with permission from American Association for the Advancement of Science. (F) The colour change of mature male chameleon during the challenge. [126], Copyright 2020. Reproduced with permission from the American Chemical Society. (G) The octopus stretches its arm to catch the object. [127], Copyright 2010. Reproduced with permission from the Institute of Electrical and Electronics Engineers Inc. (H) Expansion and contraction movements of jellyfish. [128], Copyright 2017. Reproduced with permission from the American Chemical Society.

cle structures: longitudinal (extending axially along the length of the arm), inclined (diagonally around the arm), and radial (vertical to the arm axis) muscles [110–113]. The longitudinal and radial muscles distributed around the central connective tissue and provide opposing contractile forces for arm elongation and shortening, while the inclined muscles produce twisting force. The synergy of these three kinds of muscles makes actions such as lengthening, shortening and bending possible, and the further combination of these basic movements result in a variety of more complex activities [1,114–116].

Unlike octopuses, Jellyfish achieve propulsion and predation through continuous bell-shaped contraction due to their unique body structure (Fig. 2H) [4,117–119]. The constant bell-shaped contraction can help Jellyfish transfer the energy generated by the periodic muscle contraction to the surrounding fluid to generate propulsion force. In addition, the high action potential of the muscle could also keep swimming muscles in an excited state and make them contract for a long time, allowing the elastic structure to fully deform in the late contraction state and store a large amount of strain energy [120–123].

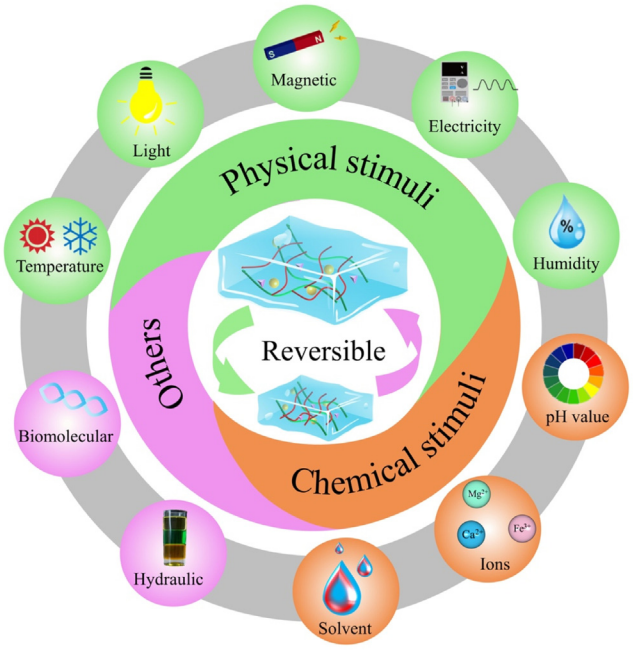



**Fig. 3.** Schematic illustration of hydrogel actuators with stimulus-responsive performance. Stimulus-responsive actuators could exhibit dramatic volume/phase changes with reversible swollen/shrunken behaviours in response to various stimuli (*i.e.*, temperature, light, magnetic, electricity, humidity, pH, ion, solvent, and others). Some photos were taken from [150], Copyright 2019. Adapted with permission from the Nature Publishing Group.

## 3. Responsive hydrogel actuators

Many natural systems are able to continuously respond and adapt to changes in their surroundings. For example, organisms can adjust their shape or position to avoid predators or achieve better nutrient acquisition by sensing stimuli (natural light, temperature changes and surrounding biochemical signals, etc.) [128]. The intrinsic principles of these response and actuation behaviors can provide advanced design concepts in fields as diverse as to flexible electronics, soft robotics, biomedicine, and other soft matter technologies. Therefore, more and more stimuli-responsive materials are widely used to develop artificial intelligence-controlled systems with deformation and locomotion capabilities. Among them, hydrogels have broad application prospects due to their biological similarity with soft biological tissues, responsiveness to various stimuli and excellent adaptability. In general, the heterogeneous structure of stimulus-responsive hydrogel actuators exhibits dramatic volume/phase transitions with reversible expansion/shrinking behaviors in response to various external stimuli, including temperature, light, magnetism, electricity, pH, ions, humidity, solvents, etc. (Fig. 3). In this section, we will discuss several representative response control methods and compare the advantages and disadvantages of these methods in detail.

### 3.1. Thermal response

One of the primary components of the extensively used and investigated artificial intelligence systems is the thermal stimulus-response system, which has demonstrated an indispensable role in the creation of hydrogel actuators. For instance, thermally responsive soft materials, such as hydrogels, can achieve corresponding actuation (actions) in response to changes of the surrounding temperature by changing their phase or volume at crucial phase transition temperatures [97,129]. Essentially, the equilibrium state of enthalpy and entropy within the hydrogel, temperature-based molecular reorganization, and interactions between polymer chains and the solvent all contribute to this solvent uptake and expulsion behavior, which leads to a macroscopic exhibit the behavior of expansion or contraction of matrix volume [130–132]. Thermally sensitive hydrogels typically have negative thermal sensitivity at the lower critical solution temperature (LCST), but as the temperature increases to the upper critical solution temperature (UCST), they change to positive thermal sensitivity [133]. The varieties and application possibilities of hydrogel actuators are further expanded by these two distinct response qualities. Then, we'll go into great depth about these two various categories and compare them.

#### 3.1.1. LCST responsive hydrogel actuators

The lower critical solution temperature (LCST) of a responsive polymer is the temperature at which all of the polymer's constituent parts become entirely miscible. The poly(N-isopropylacrylamide) (PNIPAM), one of many LCST-responsive polymers, is renowned for its low toxicity, electroneutrality, chemical stability, minimal pH dependence, near body temperature LCST (~32°C), and a wide range of tunable swelling ratios (ranging from 2-20). The PNIPAM hydrogel actuator is given as an example of a typical LCST actuator. The hydrogel will entirely dissolve in water at temperatures below LCST, and as the temperature rises, the hydrogel will progressively contract until the stability temperature is reached. The hydrogel will precipitate out of the aqueous solution at temperatures higher than the LCST (Fig. 4A). In contrast, when the temperature is gradually reduced until it falls below the LCST, PNIPAM absorbs back the liquid from the solvent in which that was originally dissolved and expands to its water-soluble state, demonstrating the reversibility of its bulk phase transition in reaction to heat [134]. In the following section, we will explain the activity behavior of this LCST responsive hydrogel actuator and use numerous examples to illustrate the overall physical mechanism of a typical LCST polymer (poly(N-isopropylacrylamide) hydrogel) actuator.

He et al. [135] reported a microstructure thermos-responsive poly(N-isopropylacrylamide) hydrogel actuator that allows for fine chemical manipulation, including turning the mechano-chemical feedback loop "On" and "Off" in addition to temperature detection and control (Fig. 4B). For example, the embedded microstructure with the catalyst-functionalized tip will move into the reagent layer when the temperature falls below the LCST, which would ignite the exothermic reaction. This hydrogel actuator then starts to expand. However, the hydrogel would contract due to heat when the exothermic chemical reaction's temperature rises over the LCST, which causes the microstructure to retract and stop acting as a catalyst to stop the process. When the temperature drops back below the LCST, the self-regulating cycle begins again (Fig. 4B). In this micro-structured hydrogel actuator, the dynamic behavior of the hydrogel in response to temperature changes is used to realize the separation of the micro-structured bilayer membrane based on the hydrogel-supported catalyst from the "nutrition" layer containing the reactants. The exact control of the "on" and "off" of chemical processes is made possible by the reversible actuation of the microstructure into or out of the nutrient layer. This concept offers a solution for programming high-precision chemical reaction devices.

A further intriguing study is a smart hydrogel actuator based on monolayer parallel aligned titanate nanosheets (TiNS) and layered thermally sensitive PNIPAM (Fig. 4C), which can exhibit temperature-controlled anisotropic deformation [136]. This work can display uniform heating-induced shrinkage and cooling-induced expansion, just like traditional homogeneous smart hydrogels based on PNIPAM. Hydrogels containing TiNS, on the other hand, display inverse thermal response functions, or differential expansion/contraction between directions parallel and perpendic-

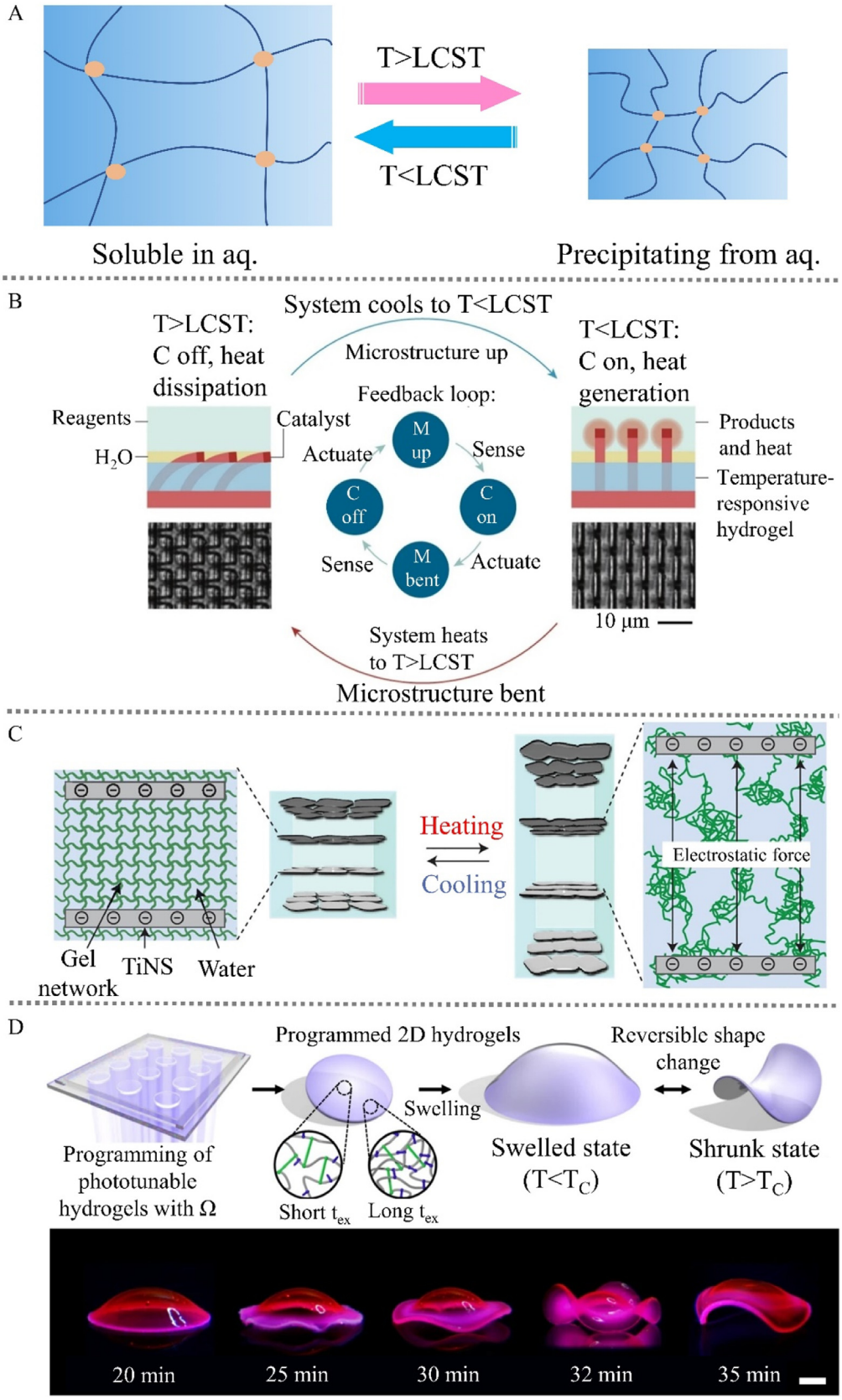



**Fig. 4.** Hydrogel actuators in response to LCST stimuli. (A) Schematic diagram of the actuation mechanism of LCST hydrogels. The term aq. is an abbreviated form of aqueous solution. [150], Copyright 2019. Adapted with permission from the Nature Publishing Group. (B) Schematic illustration of the LCST-regulated hydrogel microstructure with a self-regulating mechanochemical adaptive reconfigurable performance. [135], Copyright 2012. Reproduced with permission from the Nature Publishing Group. (C) Schematic illustration of a PNIPAM/TiNS hydrogel actuator based on thermal-responsive deformation. [136], Copyright 2015. Reproduced with permission from the Nature Publishing Group. (D) Schematic illustration and pictures of 3D-structured LCST gel actuators. Scale bars, 5 cm. [137], Copyright 2018. Reproduced with permission from the Nature Publishing Group.

ular to the TiNS plane. Temperature-dependent electrostatic repulsion between TiNS, which reduces internally released water molecules, causes an increase of the electrostatic permittivity of PNIPAM. This research offers new options for this kind of hydrogel and shows how more complex PNIPAM-based LCST gel actuators can be designed.

As another illustration, Nojomi et al. [137] created 3D-structured LCST gel actuators with pre-programmed motion morphologies using digital light 4D printing (DL4P). The overall density of the 4D printed patterned PNIPAM network was changed by digital light to produce hydrogel actuators with varying crosslinking densities and deformability. The hydrogel precursors were exposed to digital light while monitoring the exposure time ($t_{ex}$). The amount and rate of macroscopic swelling and shrinkage are reduced because of the hydrogel network's crosslink density increasing with exposure time. They got preprogrammed 2D hydrogel disks and distorted them into numerous intricate 3D morphologies using this effective adjustment (Fig. 4D top). The structure shows a reversible shape change between the expanded and shrunken states during at the temperature of the bulk phase transition ($T_C$, 32.5°C). The method encodes specified metrics and geographically and temporally relevant expansion/shrinkage in PNIPAM-based smart hydrogels, allowing the created 3D structures to display programmable time-ordered motion in their reduced form (bottom in Fig. 4D). Such fabricated 3D deformable structures enable programmable morphology and motion, which may pave the way for the design and fabrication of soft-engineered systems for soft robotics, actuators, and artificial muscles.

*3.1.2. UCST responsive hydrogel actuators*

Unlike LCST hydrogel actuators, UCST hydrogel actuators expand as the temperature rises. The majority of the polymer matrices employed in UCST hydrogel actuators are polyacrylamide (PAAM) and polyacrylic acid (PAAC), which have diffusion network characteristics in general [138]. The hydrogel network's volume contracts due to a strong interaction between the acrylic acid (AAC) and acrylamide (AAM) chains when the temperature is below UCST; when the temperature is above UCST, AAC-AAM interactions become stronger. The hydrogel's volume increases because of the quick dissociation of the hydrogen bonds between the networks. In order to alter the hydrogel's characteristics and achieve the necessary functionality, additional copolymerization or modification can be carried out in the UCST copolymer molecular segments [139–142]. The UCST hydrogel actuator's mechanism of action is covered in detail and with specific examples in the following sections.

By using asymmetric photopolymerization, Zhao et al. [143] created a bilayer hydrogel actuator with a PAAM/PAAC layer with UCST effect and a PAAM layer without responsive function. The hydrogel actuator experiences spontaneous deformation when the temperature falls below UCST because of the numerous hydrogen bonds that form between the two polymers, PAAM and PAAC, causing the layer to shrink. In contrast, the pure PAAM layer maintains its original state independent of the temperature (Fig. 5A). Moreover, the driving amplitude of this hydrogel actuator can be further achieved by adjusting the composition ratio of the two layers. This idea of asymmetrically distributed polymer hydrogen bonding can be used to create various UCST hydrogels and inspire fresh developments in the field of intelligent actuators.

Additionally, there have been increased efforts to create smart hydrogels with LCST and UCST sensitive characteristics [144,145]. Using poly(N-acrylamide) (PNAGA) layers and PNIPAM layers, for instance, Sun et al. [146] created a temperature-driven hydrogel actuator that demonstrated the traits of dual response control of UCST and LCST. Thus, a variety of sophisticated deformation processes can be accomplished (Fig. 5B). The two layers of polymers in this hydrogel can exhibit completely different thermally responsive expansion and contraction characteristics at low and high temperatures thanks to the complementary temperature response behavior of the two distinct polymers at UCST and LCST. This hydrogel actuator can respond quickly to temperature changes and recover quickly from them. This hydrogel actuator can be used for a variety of tasks requiring sensitive response characteristics thanks to its stable and effective response properties, such as grasping, transporting, releasing objects, or acting as circuit switches (for example, turning light-emitting diodes (LEDs) on and off).

In the system described above, the hydrogel is actuated by its constant volume contraction or expansion, specifically by absorbing or releasing water at a responsive temperature. This behavior necessitates that the actuator be submerged in the corresponding solution to achieve a flexible and stable actuation behavior, but this restriction restricts the potential for more applications of hydrogel actuators. To address this issue, Chen et al. [147] reported a bilayer hydrogel actuator made of a P(AAC-co-AAM) layer and a PNIPAM layer that was inspired by the mimosa plant (Fig. 5C). When the surrounding temperature is lower than LCST, the PNIPAM hydrogel layer retains a significant quantity of water whereas the P(AAC-co-AAM) layer loses some of the water, causing the bending deformation of the UCST hydrogel side. The LCST hydrogel (PNIPAM layer) loses water when the temperature is higher than both the LCST and the UCST, and this water discharges into the UCST hydrogel layer (P(AAC-co-AAM) layer), causing volume collapse and causing the device to bend in the direction of the LCST hydrogel. This hydrogel actuator can realize the actuation execution in open air environment by internal moisture transfer, thus freeing the hydrogel actuator from the limitation that it must be restricted to the corresponding solvent to realize the actuation function, and providing ideas for the development of other hydrogel actuators for more application scenarios.

## 4. Light response

Light stimulation has become another hot stimulation method due to its long-distance, fast, non-contact, and sensitive characteristics. In general, photo-responsive hydrogel actuators are driven by reversible cross-linking processes and photothermal excitation, both of which can be accomplished by doping the photoactive components into the hydrogel matrix to produce distant photoexcitation behavior (Fig. 6A). The two most popular techniques for creating reversible cross-linking reaction mechanisms in photo-responsive hydrogel actuators are photoisomerization and photo-cycling. In order to drive and deform hydrogels, photoisomerization of hydrogel actuators refers to the induction of photo-initiators like azobenzene (cis to trans change) and spiro-pyran (open/closed loop) under light irradiation. In contrast, the photo-cycling control technique (e.g., cross-linking and de-cross-linking behavior of p-hydroxybenzoyl and triphenylmethane groups upon exposure to light) is utilized to achieve reversible shrinkage and swelling behavior of hydrogels [148–150]. Benefiting from the development of light-responsive hydrogel actuators, many typical applications have been developed, such as self-healing hydrogels, remote-controlled soft robots, molecular machines, and controlled drug release [151–153]. The sources of light stimulation can generally be classified into several types based on differences in wavelength and energy, such as natural light, ultraviolet (UV), near-infrared (NIR), and infrared light. Then, we'll introduce three different types of light-driven hydrogel actuators—natural light, ultraviolet light, and near-infrared light—and go into great depth about each of their individual driving mechanisms.

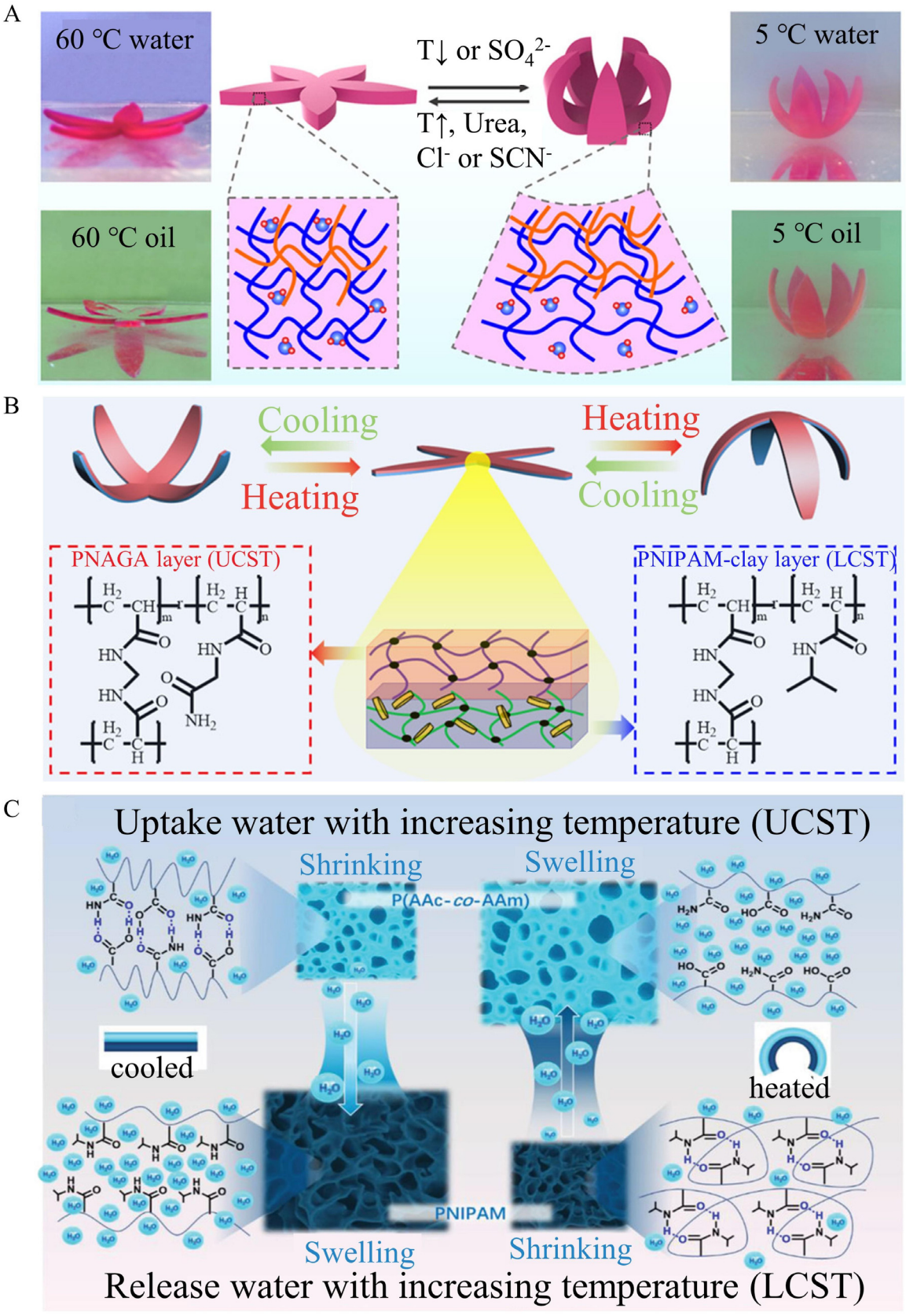



**Fig. 5.** Hydrogel actuators in response to UCST stimuli. (A) Schematic illustration of the UCST-regulated hydrogel microstructure with a self-regulating mechanochemical adaptive reconfigurable performance. [143], Copyright 2019. Reproduced with permission from the American Chemical Society. (B) Schematic illustration of a hydrogel actuator based on thermal-responsive deformation with PNAGA layer and PNIPAM-clay layer. [146], Copyright 2020. Reproduced with permission from the American Chemical Society. (C) Schematic illustration of double layer hydrogel actuator with UCST layer and LCST PNIPAM layer. [147], Copyright 2018. Reproduced with permission from the Royal Society of Chemistry.

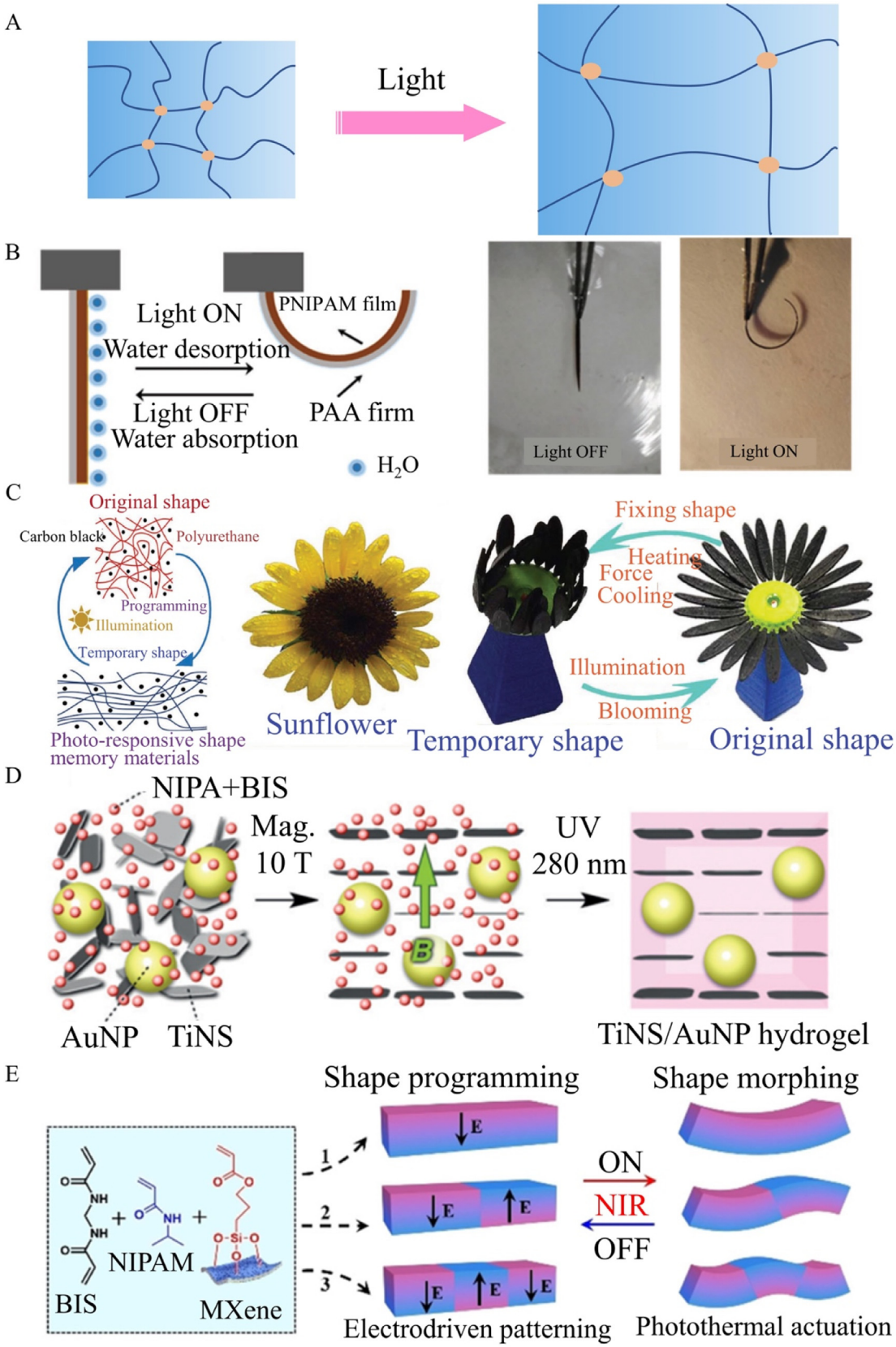



**Fig. 6.** Hydrogel actuators in response to light stimuli. (A) Schematic diagram of the actuation mechanism of light responsive hydrogels. [150], Copyright 2019. Adapted with permission from the Nature Publishing Group. (B) Schematic illustration of the light-regulated dual hydrogel layers. [154], Copyright 2017. Reproduced with permission from John Wiley & Sons Inc. (C) Schematic illustration of hydrogel actuator with sunflower-like properties to response the natural light. Scale bars, 2 cm. [155], Copyright 2017. Reproduced with permission from John Wiley & Sons Inc. (D) Schematic illustration of a TiNS/AuNPS hydrogel actuator based on UV-responsive deformation. [156], Copyright 2018. Reproduced with permission from John Wiley & Sons Inc. (E) Schematic illustration of NIR light responsive MXene hydrogel actuator. [157], Copyright 2021. Reproduced with permission from John Wiley & Sons Inc.

### 4.1. Natural light responsive hydrogel actuators

Natural light is one of the most readily available sources of stimulation and has a wide range of applications in real life. The hydrogel can be directly placed under natural light or fluorescent lamps to drive the process. It can be accomplished without any sophisticated light source equipment. In light of this, a lot of research has concentrated on smart hydrogels that are precisely activated by sunlight. In one of these interesting studies, Xia et al. [154] constructed a PNIPAM-AuNPS/PAAM thin-film hydrogel actuator doped with visible-light-responsive photothermal gold nanoparticles (AuNPS). The photothermal nanoparticles inside this hydrogel actuator produce heat when stimulated by external light through their own photothermal effect. When the temperature rises above the LCST of the PNIPAM layer, the hydrogel begins to contract, resulting in bending deformation as a result. As shown in Fig. 6B, when the NIPAM-AuNPS/PAAM actuator was immobilized in a buffer solution and exposed to visible light, the AuNPS in the hydrogel network was able to absorb the radiant energy and transform it into thermal energy, raising the temperature of the hydrogel matrix to facilitate rapid bending. The actuator returns to its normal vertical position when the light is switched off. The reversible actuation performance of natural light shows critical value in the remote and precise control of the process.

Similarly, Chen et al. [155] used polyurethane (PU) and carbon black (CB) as printing doping materials to create natural light-responsive hydrogel actuators. They created light-triggered shape memory composite artificial multi-layer sunflowers that were inspired by sunflowers. These sunflowers included sunflower petals, sunflower stamens, flower stems, and polylactic acid printed vases that were produced from black photosensitive shape memory materials (Fig. 6C). Like a natural sunflower, the artificial sunflower has a comparable precise driving procedure. Carbon black can continually absorb solar energy and transform it into heat energy when exposed to light. The petals of the sunflower shift from being closed to being open at a temperature of 30°C ($T_g$). The petals' softness and elasticity in this stage enable them to follow moving light. Furthermore, the deformation of this sunflower is reversible. For example, the artificial petal will return to the initial closed condition and maintain its shape when the temperature of the sunflower is gradually reduced below $T_g$ in the absence of an external light source. It will then display the deformation behavior once more when there is an external stimulus. The development of this photosensitive biomimetic hydrogel actuator provides a new idea for fabricating more complex photo-responsive actuators.

### 4.2. Ultraviolet light responsive hydrogel actuators

Unlike natural light stimuli, ultraviolet (UV) light is also widely used in response to its driving molecules and compounds to achieve effective light-driven reversible shape changes and displacements. For example, Aida et al. [156] developed a PNIPAM hydrogel actuator with TiNS and AuNPS, where the TiNS had a diameter of 17 nm (as shown in Fig. 6D). This hydrogel actuator, specifically, is a UV-responsive anisotropic hydrogel actuator created by spontaneous polymerization of AuNPS (a photothermal agent), N,N'-methylenebisacrylamide (a crosslinker), and TiNS (a photo-responsive agent) homogeneously dispersed in a solution of N-isopropylacrylamide (polymer monomer). At a wavelength of 445 nm, the hydrogel actuator displays effective photothermal conversion performance (5.6 $Wcm^{-2}$ power density). As a result, after UV light irradiation, the hydrogel's surface temperature can rise quickly to 85°C, at which point the hydrogel matrix begins to extend and expand to produce the necessary deformation. The hydrogel naturally cools below LCST and contracts back to its initial length in 6 seconds after the laser is switched off. Additionally, the hydrogel actuator's ability to achieve a dynamic crawling process is enabled by the hydrogel matrix's repeating expansion and contraction when the laser light is repeatedly turned on and off. The dynamic crawling operation is realized by the hydrogel actuator. The reversible driving stimuli for this hydrogel can be regulated by a switching laser, providing options for future UV light-driven hydrogel actuators.

### 4.3. Near infrared light responsive hydrogel actuators

Near-infrared light has also been widely used in the construction of responsive hydrogel actuators due to its easy access and high energy properties. Li et al. [157] recently announced the development of an MXene hydrogel actuator with programmable deformability driven by near-infrared light. By combining photopolymerizable MXene nanomonomers with PNIPAM hydrogel, an in situ radical copolymerization created the hydrogel (Fig. 6E). The concentration gradient of MXene nanosheets' electric field can be modulated to control the thickness of the structured hydrogel. By using patterned electric field photopolymerization, they were able to create a variety of geometrically formed anisotropic hydrogel actuators, such as the U, J, S, and W as well as more intricate flower-shaped ones. Among them, the flower-shaped anisotropic hydrogel actuators may produce a precise driving mechanism for deformation with an evolutionary behavior resembling the blossoming and closing behavior of genuine flowers. The hydrogel actuator can also be employed as a four-arm soft gripper to perform a number of complicated tasks, including grabbing, lifting, lowering, and releasing objects while being stimulated by programmed near-infrared light. This method's attractiveness is that it makes it easier for near-infrared light stimulation to be used in more scenarios. The abovementioned light-controlling techniques can offer fresh perspectives on the creation of more intelligent hydrogel machines or actuators by giving them the ability to perform actions that are more complicated and adaptable for brand-new multifunctional applications. Although there have been several attempts to create photoresponsive hydrogels in various domains, most of the current systems are only suitable for straightforward application research. Some significant issues, such as the creation of photochemical reactions, investigations of photodynamics, and the biocompatibility of light-responsive hydrogels, need to be resolved in order to broaden their practical application. Although many challenges need to be addressed, the potential for the development and implementation of light-responsive hydrogel actuators is bright.

## 5. Magnetic response

In contrast to light/thermal responsive actuators, magnetic responsive actuators are more useful in some application scenarios, such as in the fields of minimally invasive surgery and targeted drug delivery. They remain biocompatibility under high magnetic field fluxes and can be remotely activated by a magnetic field for a brief period of time. This class of hydrogel actuators achieves responsive behavior primarily by incorporating external paramagnetic or ferromagnetic additives into the polymer matrix. The resulting magnetic field stimulation response is distinguished by a rapid, large deformation drive as well as remote controllability (Fig. 7A). According to their magnetization properties, magnetic additives can generally be divided into two groups: soft magnetic (such as metallic iron [158], alloys, and oxides [159,160], which exhibit high magnetization and saturation magnetization), and hard magnetic (such as neodymium iron boron particles (NdFeB), which are most distinctively characterized by a large magnetic hysteresis and can therefore be used as a permanent magnetic field) [161–163]. Typically, such magnetically responsive hydrogel actuators do

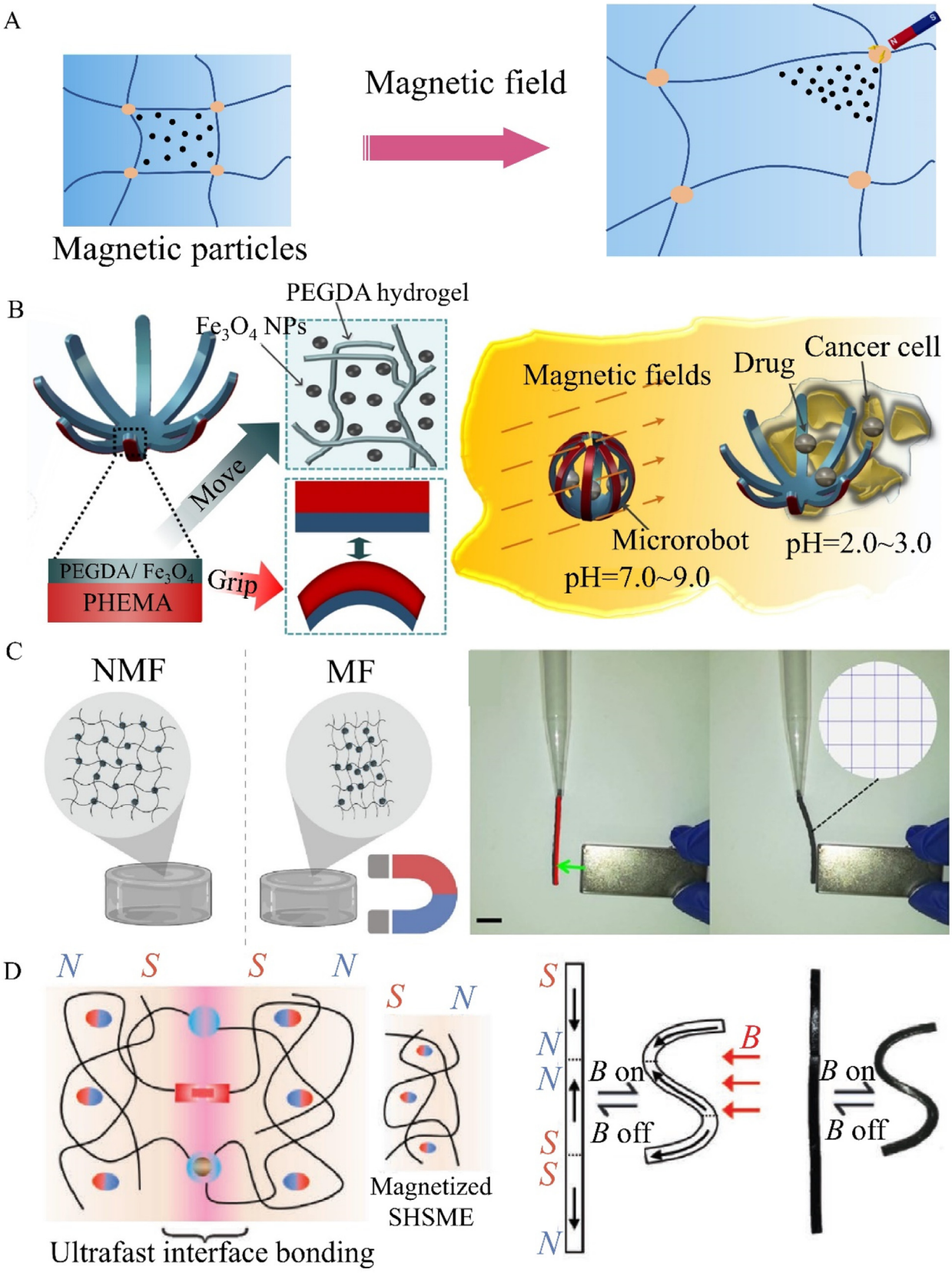



**Fig. 7.** Hydrogel actuators in response to magnetic stimuli. (A) Schematic diagram of the actuation mechanism of magnetic responsive hydrogels. [150], Copyright 2019. Adapted with permission from the Nature Publishing Group. (B) Schematic illustration of the magnetic-regulated dual hydrogel layers. [165], Copyright 2016. Reproduced with permission from IOP Publishing Ltd. (C) Schematic illustration of magnetic responsive hydrogel actuator. Scale bars, 2 cm. [166], Copyright 2020. Reproduced with permission from Elsevier Science Ltd. (D) Schematic illustration of a NdFeB magnetized hydrogel actuator. [167], Copyright 2021. Reproduced with permission from John Wiley & Sons Inc.

not need any additional cross-linking agents during their synthesis; instead, the magnetic particles will naturally create covalent or synergistic cross-links with the gel's polymers. Next, we will introduce the synthesis and actuation process of magnetically responsive hydrogel actuators with $Fe_3O_4$ particles and NdFeB particles as the main magnetic dopants.

### 5.1. $Fe_3O_4$ particles responsive hydrogel actuators

As was previously noted, magnetic compounds are typically physically incorporated directly into the hydrogel network. The magnetic additives in the hydrogel matrix function as magnetic receptors and can be affected by external non-uniform magnetic field forces when subjected to an external magnetic field gradients [164]. This is demonstrated by the magnetic additive moving forward or backward. This motion finally results in a graded distribution that is commensurate with the external magnetic field, which in turn propels the deformation and motion of the hydrogel structure. Here, the $Fe_3O_4$ particles were used as a representative of soft magnetic additives to illustrate the relevant functions and mechanisms of action. Fig. 7B shows a hydrogel actuator with a bilayer response system that is both pH-responsive and magnetically driven [165]. It consists of a layer of 2-hydroxyethyl methacrylate (PHEMA), which is pH-responsive, and a layer of poly (ethylene glycol) diacrylate (PEGDA-$Fe_3O_4$), which is doped with iron oxide particles. Thus, using an electromagnetic drive system and this dual-responsive hydrogel actuator as a micro-robot, it is possible to achieve drug collection and release in solutions with various pH values. The anticancer drug beads are first captured by the soft micro-robot at pH=9.58, and then they are transferred to the corresponding tumor tissue by the electromagnetic driving system. Once the soft micro-robot has successfully targeted the tumor, it can release the pre-capture with accuracy because the pH of the tumor tissue is lower than normal (pH=2.6). In conclusion, under specific circumstances, this soft microrobot may grip and release pharmaceuticals thanks to its electromagnetic driving mechanism and in cooperation with the pH shift in the environment. This study may pave the way for additional research into similar topics. For instance, if the external magnetic field and actuator are further tuned, the composite soft body actuator may be able to achieve multi-modal motion over a range of challenging terrains.

Another intriguing example is that Podstawczyk et al. [166]. who reported a magnetic hydrogel actuator created by employing a mixture of PAAC dispersion solution as a printing slurry together with magnetic nanoparticles, alginate and methylcellulose hydrogels in 3D printing. In this instance, the magnetic nanoparticles and the PAAC embedded in the hydrogel function as cross-linkers. Electrostatic interactions hold the cross-linked PAAC to the polymer backbones, such as alginate and methylcellulose, and the incorporation of magnetic nanoparticles enables the deformation of the printed hydrogel microstructure when exposed to an external magnetic field. The greatest degree of bending achieved by the hydrogel strip with applied (MF) and non-applied (NMF) external magnetic fields is shown in Fig. 7C. This maximum degree of bending is governed by the density of the magnetic particles inserted, allowing bending angles from values of 24° to 106°. The development of new stimulus-responsive drug delivery devices is inspired by the capacity of this magnetic hydrogel actuator to accurately control the degree of expansion of the flexible material by changes in the external magnetic field. Drugs may be put into the hydrogel's grid structure, for instance, and their release may be regulated by altering the external magnetic field, which in turn alters the hydrogel's grid structure's dimensions.

### 5.2. NdFeB microparticles responsive hydrogel actuators

Hard magnetic hydrogel actuators that are magnetically responsive frequently have good programmability and enable more intricate shape transformations than soft magnetic hydrogel actuators with limited programmability. Neodymium iron boron particles are one of the most widely used hard magnetic materials (NdFeB). When hard magnetic particles are mixed with a soft polymer matrix, soft actuators are created that have hard magnetic properties (such as high correctability and transparency) as well as mechanical softness and flexible deformability, thus showing excellent promise and value for applications. As a typical example, Cheng et al. [167] reported a self-healing supramolecular magnetic elastomer (SHSME), which exhibited high mechanical strength (Young's modulus of 1.2 MPa) and rapid self-healing ability (300% tensile strain after 5 s of repair at ambient temperature) due to the strong dynamic network and abundant reversible chemical bonds within the elastomer. A schematic depiction of the quick chemical bonding that occurs between two magnetized SHSME sheets is shown in Fig. 7D. Based on this interfacial bonding capacity, the local structural magnetization distribution within the SHSME is successfully adjusted. The SHSME rod is made up of three short magnetized SHSME units, as seen in Fig. 7D, and when exposed to a consistent external magnetic field, the entire SHSME rod goes through a quick and predictable shape change process. The operation of this magnetron soft drive is also reversible; upon removal of the magnetic field, the hydrogel instantly transforms back into a rod shape. Notably, the SHSME frame not only enables modular customization of structure and function but also recycling and reuse through thermal deformation. The aforementioned findings imply that this SHSME soft robot is capable of complicated geometries and adaptable modular assembly, indicating intriguing applications for strategic tasks like dismemberment-navigation-assembling in limited places.

## 6. Electrical response

Hydrogel actuators that respond to changes in the external environment by expanding or contracting when exposed to solvent-induced or externally applied electric fields are referred to as electric field responsive hydrogel actuators, electrolyte hydrogel actuators, or electroactive hydrogel actuators [168]. Utilizing an electric field as an external stimulus has the special benefit of allowing for exact voltage/current control through software programming, which may be used to regulate the motion and behavior of the hydrogel actuator. The main mechanism of an electrically responsive hydrogel actuator typically depends on the distribution/arrangement of ions within the hydrogel's swelling medium and the ionic motion of the electric field (Fig. 8A). These factors can be influenced by the relative positions of the electrodes (e.g., monomer concentration and pore size) and the hydrogel's solvent properties (e.g., ionic strength) [169]. In particular, when exposed to an external electric field, free ions inside the hydrogel migrate in a specific direction, causing a non-uniform ion concentration inside and outside the gel and generating osmotic pressure, which causes the hydrogel actuator to swell or shrink [170]. Electro-responsive hydrogel actuators can have tremendous potential in applications like bioengineering and biomedicine based on the qualities of quick, accurate, and repeatable electric field control. Two typical electro-responsive hydrogel actuators (direct current responsive and alternating current responsive hydrogel actuators) are being currently researched, and we discuss them separately because of the difference in their external control current sources.

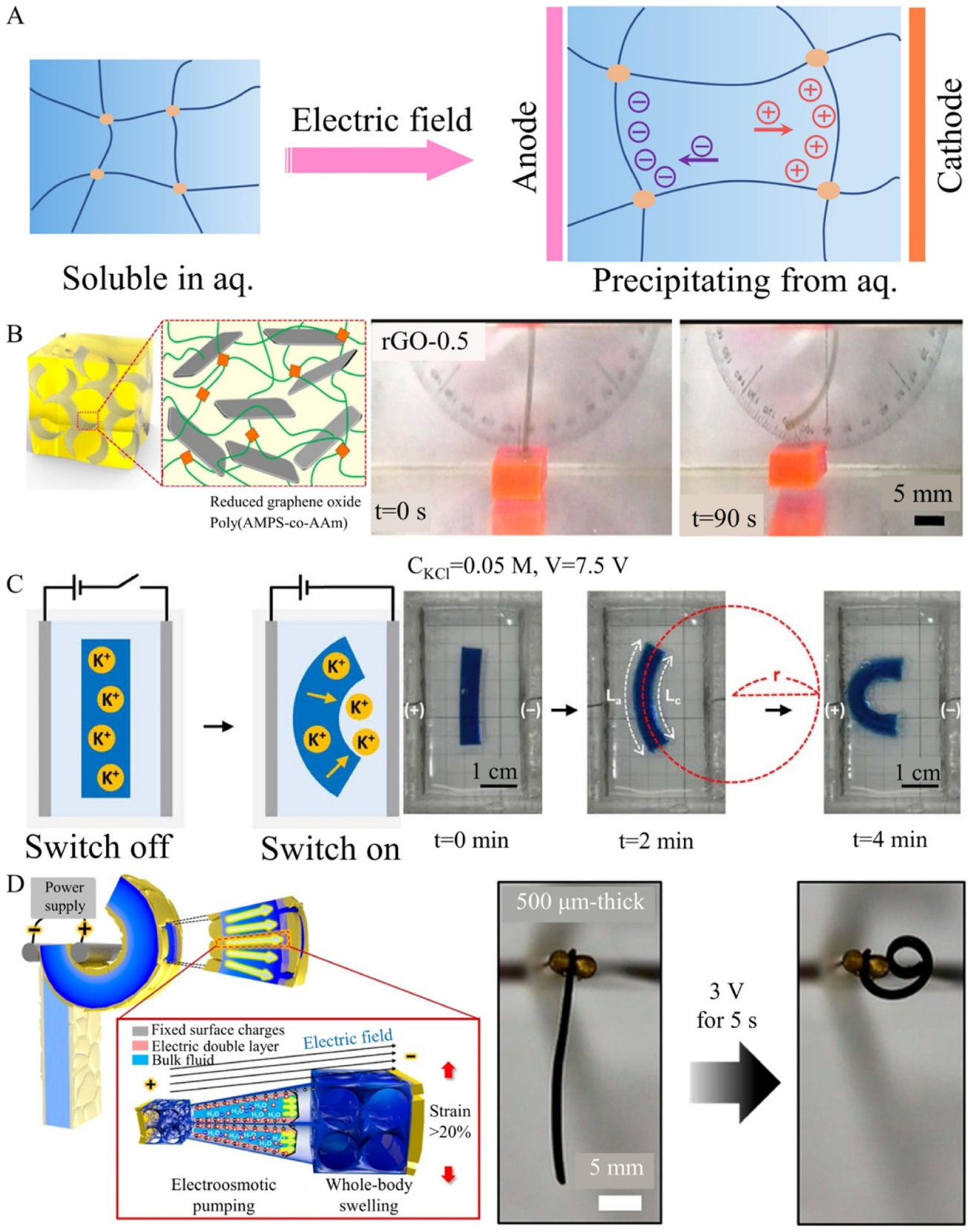



**Fig. 8.** Hydrogel actuators in response to electric field stimuli. (A) Schematic diagram of the actuation mechanism of electric responsive hydrogels. [150], Copyright 2019. Adapted with permission from the Nature Publishing Group. (B) Schematic illustration of the electric-regulated (DC) RGO- Poly(AMPS-co-AAM) hydrogel actuator. [171], Copyright 2017. Reproduced with permission from the American Chemical Society. (C) Schematic illustration of an DC-electric responsive hydrogel actuator. [172], Copyright 2019. Reproduced with permission from IOP Publishing Ltd. (D) Schematic illustration of AC-electric responsive hydrogel actuator. [173], Copyright 2020. Reproduced with permission from the American Chemical Society.

### 6.1. Direct current responsive hydrogel actuators

In various miniature/miniaturized devices, direct current responsive hydrogel actuators are frequently found because the majority of small power supplys provide direct current (DC) electrical impulses. For creating DC-responsive hydrogel actuators, poly(2-acrylamido-2-methylpropanesulfonic acid) (PAMPS) polymer is one of the most widely used materials because this monomer can be fully ionized in a variety of aqueous solutions from pH=2 to 12, giving PAMPS hydrogel actuators good DC response. For example, Chu et al. [171] reported a novel reduced graphene oxide/poly(2-acrylamide-2-methylpropanesulfonic acid-acrylamide) (RGO/Poly(PAMPS-co-AAM)) composite hydrogel actuator with excellent DC response and mechanical properties. This hydrogel actuator has strong electrical conductivity due to the uniform dispersion of reduced graphene oxide nanosheets, which helps with ion transport inside the hydrogel and controls the osmotic pressure inside/outside the hydrogel (Fig. 8B). Additionally, the hydrogel's mechanical characteristics and compressive strength are improved by the hydrogen bonding connection between the RGO nanosheets and the polymer chains, giving this hydrogel actuator exceptional and quick reversible deformation capabilities. As seen in Fig. 8B, the RGO-0.5 hydrogel actuator can lift a significant amount of weight-0.4 g-in the electrolyte solution in just 90 seconds. The hydrogel's actuation capabilities are greatly improved by the doping of the RGO nanosheets, in addition to its electro-responsive and mechanical attributes. Although this hydrogel actuator has a high deformation capacity and a quick response time, its large size and requirement to be in solution for actuation also restrict the range of possible applications.

In addition, Sun et al. [172] constructed a DC hydrogel actuator based on poly(3-sulfopropyl acrylate, potassium salt) (PSPA) by 3D printing. The actuators based on this approach usually have customizable structures and volumes. The hydrogel actuator is positioned between two electrodes in a KCl solution, as shown in Fig. 8C. When the external circuit is closed, the ion concentration at the interface between the two sides of the hydrogel will differ due to the electric field, which in turn creates an electric osmotic pressure at the interface. The cations of the hydrogel migrate into the electrolyte solution to reach electrical neutrality in the hydrogel. Consequently, the hydrogel actuator responds to the electric field by bending toward the negative pole (Fig. 8C). Although the hydrogel actuator only had a 1 mm $min^{-1}$ ion transport rate when driven by 7.5 V DC and took 10 minutes to fully drive the deformation of the hydrogel sample, it was able to drive bending within 4 min at 7.5 V and 0.05 M KCl solubility (Fig. 8C). These findings show how adaptable and controllable the DC hydrogel actuator is. Biosensors and artificial muscles can both be made from this electrically responsive hydrogel since its shape change resembles that of muscular tissue. However, due to the typically low DC voltage, the associated actuation would be slower, which could restrict its further advancement and application.

### 6.2. Alternating current responsive hydrogel actuators

Due to their quicker and more effective actuation capabilities, alternating current responsive hydrogel actuators have also been developed and studied extensively. Ko et al. [173] recently created a voltage-permeable, swell-driven hydrogel actuator using an acrylic-based hydrogel as a porous membrane and a storage medium for ionic liquids. This actuator has a low working voltage, quick actuation, and can achieve motion with several degrees of freedom (Fig. 8D). In particular, a significant volume of hydraulic fluid stored inside the hydrogel starts to flow quickly when an alternating current (AC) working voltage of roughly 3 V is given to the open electrodes at both ends, causing the hydrogel to expand and deform and enabling actuation. The major source of power for this hydrogel actuator is the expansion of the hydrated ionic fluid energized by the AC voltage. The AC voltage may be altered to alter the motion's amplitude, which offers a concept for the creation of various programmable soft electronic devices. Although the material shows great potential for application in the field of muscle reconstruction, the need to connect external circuit devices such as wires for electrical actuation makes the whole device too cumbersome and bulky, so further improvements are needed.

## 7. pH response

In addition to the various physical stimuli mentioned above, chemical stimuli can also achieve controllable driving of hydrogel actuators. Here, we will discuss two of the most common chemical stimuli as typical cases, including pH-responsive and ion-responsive hydrogel actuators. The osmotic pressure difference across the hydrogel network is influenced by pH changes in the system, which are known to drive pH-responsive hydrogel actuators. The majority of pH-responsive hydrogel actuators have side groups that can ionize in solution on their polymer backbone. These side groups can be categorized into anionic and cationic side groups depending on the sort of charge they acquire following ionization. In particular, the anionic side group hydrogel actuator has the characteristic of dissociating the side chain groups at pH higher than its acid dissociation degree (pKa). The anionic side group hydrogel shrinks when the pH value is lower than its acid dissociation degree (pKa). In contrast, cationic side-based hydrogels swell at pH values below pKa and shrink above pKa (Fig. 9A) [174,175]. We will discuss the specific driving process and behavior of the anionic side-group and cationic side-group hydrogel actuators, respectively.

### 7.1. Anionic side-group hydrogel actuators

Here, Zhang et al. [176] have created a natural cellulose-based hydrogel with layers of chitosan (CS) on the left and cellulose/carboxymethylcellulose (CMC) on the right. Such anionic side group sensitive bilayer hydrogel actuators are used to demonstrate the pH-responsive control capability of these actuators. As seen in Fig. 9B, the hydrogel actuator's CMC layer, which contains a lot of carboxyl groups, undergoes side-group dissociation at relatively high pH (pH >3.8). As a result, the hydrogel layer loses its proton, which makes the bilayer hydrogel bend in the direction of the CS layer (red layer). In contrast, when the CS layer of the double-layer hydrogel is bent in the opposite way, the amino group is protonated at low pH (pH = 3.8) due to the high expansion rate of the CS layer. When pH = 3.8, the swelling of the CS hydrogel layer is consistent with that of the CMC hydrogel layer, and thus is in a stable state (vertical state) that is not biased to either side. Based on the above characteristics, they further constructed a series of new soft actuators with mechanical working ability that can be triggered by pH. These actuators can not only realize reversible and repeated controlled deformation, but also realize various complex shape changes including rings, flowers, spiral bamboo and capsules, showing potential applications in areas such as soft grippers, smart encapsulators and artificial muscles.

### 7.2. Cationic side-group hydrogel actuators

Following that, we'll go through how cationic side-based hydrogel actuators function and their various applications. A prominent example is the pH-responsive poly(acrylic acid) (PAAC) hydrogel microtube-based cationic side-based hydrogel actuator proposed by Wu et al. [177] When the pH of the solution changes

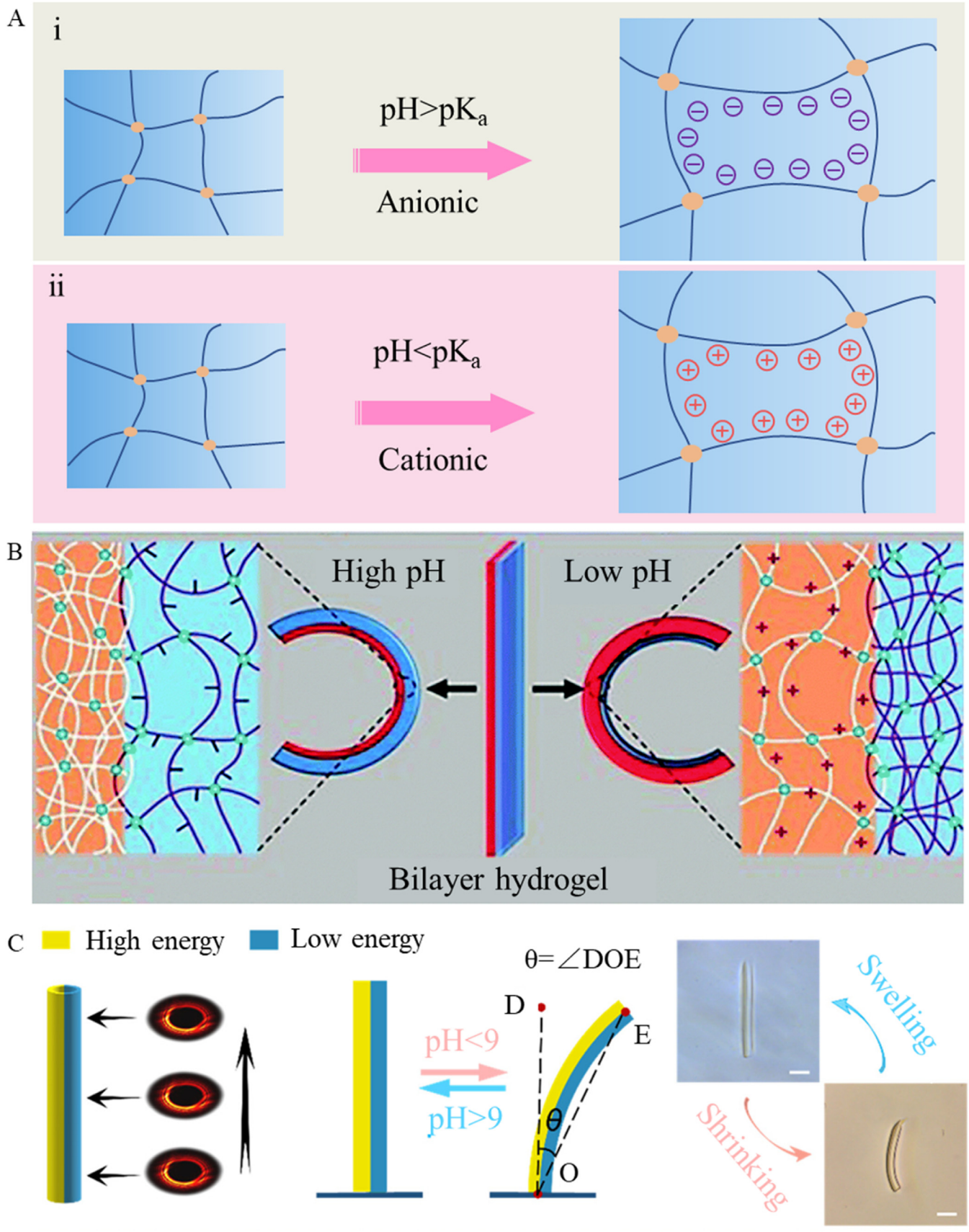



**Fig. 9.** Hydrogel actuators in response to pH stimuli. (A) Schematic diagram of the actuation mechanism of pH responsive hydrogels. [150], Copyright 2019. Adapted with permission from the Nature Publishing Group. (B) Schematic illustration of the anionic side-group pH-regulated bilayer hydrogel actuator. [176], Copyright 2017. Reproduced with permission from the Royal Society of Chemistry. (C) Schematic illustration of a cationic side-group pH responsive hydrogel microstructure actuator. [177], Copyright 2020. Reproduced with permission from the American Chemical Society.

within a certain range, this microtubule can respond to pH and accomplish asymmetric expansion/contraction, which can display a dynamic evolution of reversible bending and upright states within 1 s. For instance, when the pH of the solution is below 9, the carboxyl groups on the side chains of acrylic acid are protonated in response to the pH change of the solution, and the microtubules rapidly change from the upright state to the bent state. When the pH of the solution is above 9, the microtubules return to the upright state (as shown in Fig. 9C). The authors also suggested a method for processing and splicing dynamic holograms that can produce more intricate pH-responsive microstructures, such as S- and C-shaped microtubules and chiral twisted structures in about 10 seconds. Such micro-hydrogel actuated tubes can be used to capture and release polystyrene particles and neural stem cells. These cationic side-based hydrogel actuators have been widely exploited as biosensors and drug delivery systems due to their exceptional pH responsiveness. However, disadvantages such as switchable actuation process that are difficult to regulate and laborious control procedures carried out in dry environments should be addressed for industrial applications.

## 8. Ion response

Ion response is another method of chemical regulation. In this article, we primarily cover salt-responsive hydrogel actuators, which may expand and contract in response to changes in the solution's salinity, offering additional possibilities for actuation in subsea applications. Many pH-responsive hydrogels are also salt-responsive, with internal polyelectrolyte networks that expand in pure water and contract in salt solutions, mostly as a result of variations in osmotic pressure within the hydrogel matrix. In low salinity solutions, hydrogels produce a high charge density on the backbone due to the dissociation of ionizable groups in solution. This causes intermolecular repulsion within the matrix, which in turn allows the molecular spacing to increase and ultimately manifests as a volume expansion of the hydrogel [178]. In general, salt-responsive hydrogels consist of zwitterionic polymers whose salt responsiveness can be tuned by adding different types and concentrations of salts [179]. Using $Fe^{3+}$ and $Na^{+}$ responsive hydrogel actuators as specific cases, we will next investigate and go into great depth on the driving behavior of ion-responsive hydrogel actuators.

### 8.1. $Fe^{3+}$ responsive hydrogel actuators

Generally speaking, actuation behavior can be produced by the precise binding of chemical groups such hydroxyl groups by $Fe^{3+}$ ions. Recently, Chen et al. [180] employed PAAC to chelate with $Fe^{3+}$ ions to produce PAAC-$Fe^{3+}$ temporary complexes, which gave the anisotropic structure of the complete hydrogel material salt ion solution-driven behavior. The hydrogel film displayed varying degrees of arching through contact with various filter papers at 1 minute when the contact area with the $Fe^{3+}$ ion-containing filter paper was changed, as illustrated in Fig. 10A. A three-dimensional flower-shaped hydrogel's state of blossoming can also be managed with this control. The internal process is that when the hydrogel is immersed in an ionic solution, $Fe^{3+}$ enters the hydrogel and chelates with AAC to create three-tooth crosslinks, which reduces the rate of swelling on one side of the hydrogel and causes it to bend. Due to the creation of more chelated crosslinks inside the hydrogel as the $Fe^{3+}$ level rises, the anisotropic structure of the hydrogel actuator becomes more obvious and exhibits more bending. Additionally, the fluorescence of the composite hydrogel actuator may be cleverly altered by varying the $Fe^{3+}$ content. Information hiding and presentation are both possible with this fluorescent hydrogel in ionic solution, therefore the hydrogel has a lot of promise for use in information storage.

### 8.2. $Na^{+}$ responsive hydrogel actuators

In addition to the case of the stimulus of $Fe^{3+}$ ions, we will also discuss the role and functionality of $Na^{+}$ ions in the hydrogel actuator. For instance, Du et al. learned the construction principle of touch deformable plants in nature, and successfully realized the controllable three-dimensional deformation of calcium crosslinked sodium alginate hydrogel by combining the surface-oriented arrangement of microarray structure with top-down gradient crosslinking design. In a typical experiment, they [181] created patterned microchannels by photolithography, filled the microchannels with pre-gel solution, then dipped the patterned pre-gel into a $CaCl_2$ solution to create ionic crosslinks and exfoliated it to create hydrogel film actuators. As seen in Fig. 10B, the microchannels were introduced along different directions in hydrogel sheets that are then submerged in a $CaCl_2$ solution to produce a controlled 3D alteration of the hydrogel structure around the microchannels. The hydrogel diaphragm mentioned above can be formed into a complex petal shape. A six-petal flower structure was created, and the hydrogel was treated with 0.1 M $Na^{+}$ ions, five petals had blue dye partially applied to them to fully mimic the opening and closing of flowers, and other petals had the letter "R" written on the surface without microchannels. After 3 minutes of immersion, the closed petals with the letter "R" started to slowly open, and after 7 minutes, the flower was fully formed. The flower with six petals closed into a "R"-shaped full bud after being submerged in 0.1 M NaCl solution for nine minutes. The entire procedure can clearly show the many blossoming stages, and the letter "R" marking on the petals may capture the hydrogel's reversible inner and outward deformation process. By further controlling the deformation parameters, this technology enables high precision patterning and response process control while opening up new avenues and providing fresh direction for the control of polymer shape in the future. In summary, this ion-responsive hydrogel actuator demonstrates great research and application value.

## 9. Humidity response

Natural phenomena have provided us with numerous ideas and methods for controlling soft machines. One of them is the use of air humidity as a stimulus-response mechanism, like in the pine cone discussed above, which may open its scales when the air is dry and close them when the air is moist [182]. Wheat exhibits a similar function to release its seeds [101]. Humidity is an easy-to-implement control strategy, and thus hydrogel actuators responsive to humidity have great potential in a wide range of upcoming engineering applications [183].

To explore the functionality of humidity-responsive hydrogel actuators, Sun et al. created poly(ethylene glycol) diacrylate (PEGDA) 3D micro-structured hydrogel actuators with excellent humidity response by using highly hygroscopic PEGDA as the main chain combined with 3D printing. They exhibited good morphological structure and stable geometry [184]. In this instance, the researchers printed hydrogel flowers, and when the printed hydrogel flowers were immersed in water or the ambient humidity was increased, the water molecules diffused into the highly hygroscopic PEGDA hydrogel molecular network to expand the internal microstructure. As seen in Fig. 11A, when the hydrogel that resembles a flower is submerged in water, it continuously absorbs water, which is evident by the size of the flower growing noticeably larger within a few seconds. After absorbing water, the diameter of the flower can expand by about 155%. After removing the flower from the water, it gradually contracts back to its original size. This

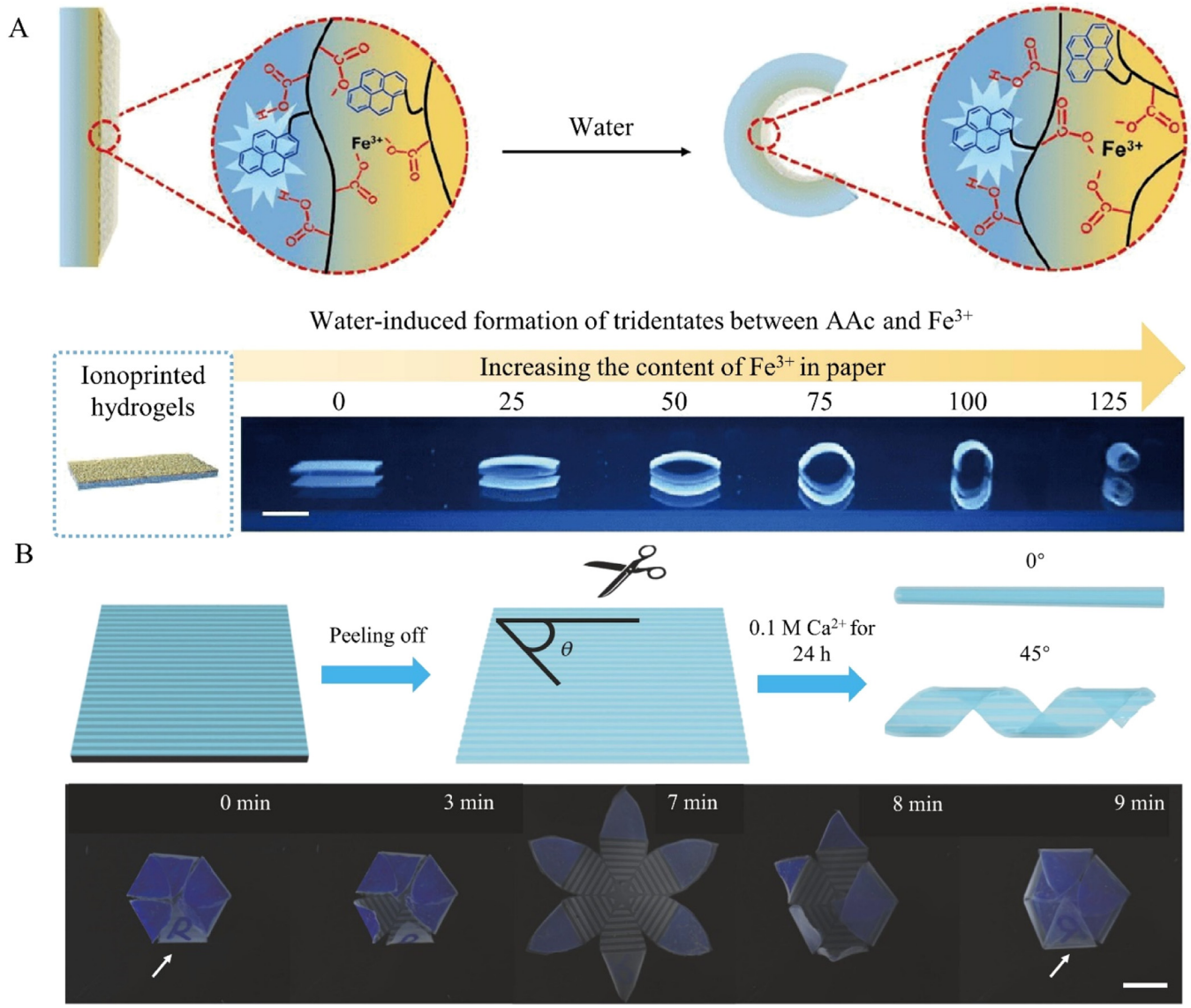



**Fig. 10.** Hydrogel actuators in response to ion stimuli. (A) Schematic illustration of the $Fe^{3+}$ regulated hydrogels actuator. Scale bars, 1 cm. [180], Copyright 2019. Reproduced with permission from the Nature Publishing Group. (B) Schematic illustration of an $Na^{+}$ ion responsive hydrogel actuator. Scale bars, 1 cm. [181], Copyright 2019. Reproduced with permission from American Association for the Advancement of Science.

process can be repeated numerous times without causing damage. In addition to placing the flowers directly into water, raising the environment's humidity will also cause the gel to expand; when the humidity drops, the flowers will immediately revert to their previous size. The hydrogel microstructure maintains good stability throughout the 10,000 repetitions of the swelling and dissolving process. This composite hydrogel microstructure may bring wider applications in the construction of actuators or soft robots.

Similarly, a wet-responsive hydrogel actuator described by Zheng et al. [185] using polyvinyl alcohol (PVA) grafted with 9-anthracenecarboxylic acid and co-blended with the UV shielding agent 2,2′,4,4′-tetrahydroxybenzophenone (THBP) and then crosslinked. This actuator can be programmed and modulated to take on various complex shapes as needed. In addition to other things, the anthracene group enables intricate patterning and reversible actuator programming through controlled UV detection. The internal expansion of the hydrogel fluctuates with the density of the crosslinking network when the external humidity changes, leading to deformation behavior because the crosslinking gradient is created by adding THBP. Fig. 11B depicts the variation in this hydrogel actuator's actuation performance in a humidity field of heated water vapor; as the ambient relative humidity increases from 20% to 90%, the actuator quickly bends in the direction of the side that has been exposed to UV radiation; when only UV radiation is present, no bending behavior is produced in the hydrogel actuator. In addition, the authors also created a soft walking robot that can bend directly downward and upward under the stimulation of humidity intervals. During this time, the leading edge, which has higher friction, acts as a fixed end, while the trailing edge advances due to the difference in friction between the leading and trailing edges, resulting in a complex line of controlled motion. Therefore, this research is expected to provide new opportunities for the development of high-performance, stable and reprogrammable actuators.

## 10. Solvent response

Many functional applications have been achieved due to the fact that hydrogels resemble human tissues and contain large amounts of water inside. Various related actuating and memory behaviors are shown in the presence of some organic solvents be-

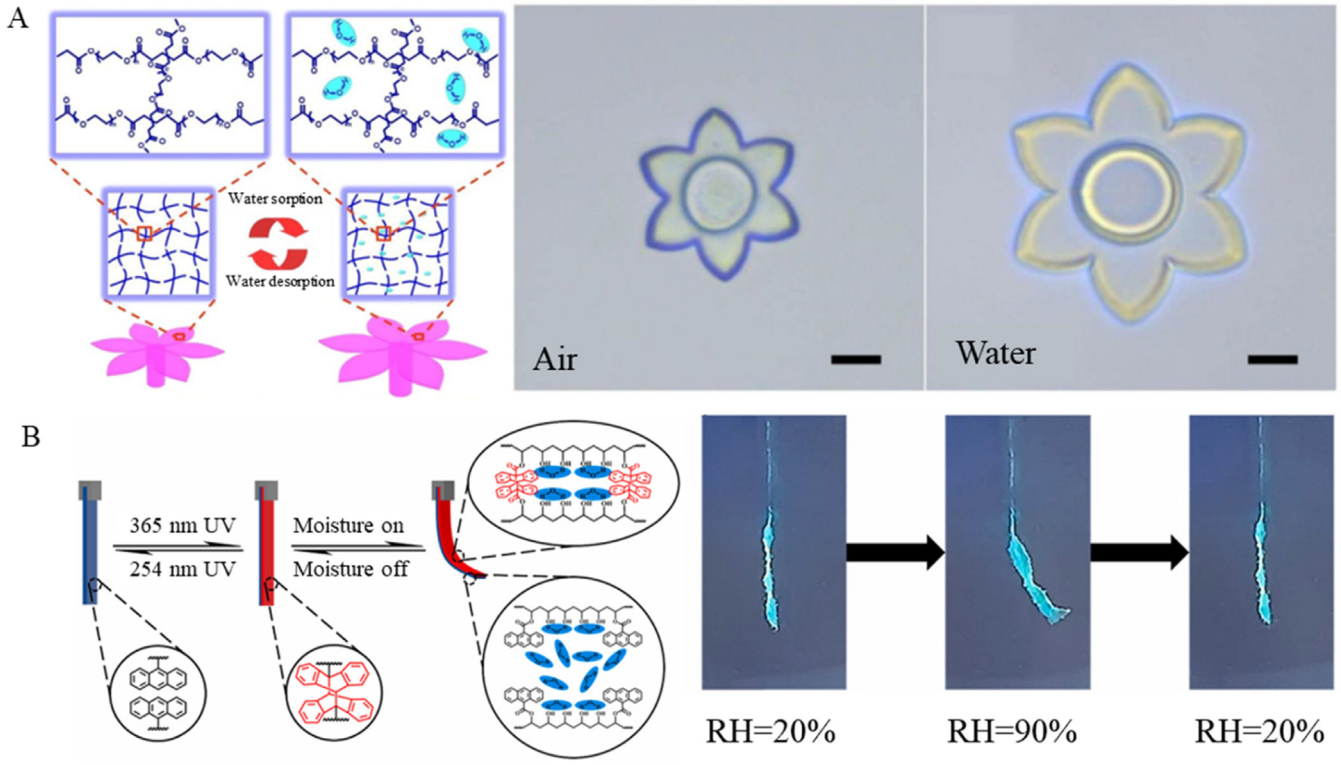



**Fig. 11.** Hydrogel actuators in response to humidity stimuli. (A) Schematic illustration of the humidity-responsive actuation of programmable hydrogel based on 3D printing. Scale bars, 10 μm. [184], Copyright 2018. Reproduced with permission from Elsevier Science Ltd. (B) Schematic illustration of PVA gradient cross-linked humidity-responsive actuator. [185], Copyright 2021. Reproduced with permission from Elsevier Science Ltd.

cause of the interaction between the solvent and the water and ions inside the hydrogel, which is also a typical response performance. In the following content, we will focus on the effect of solvent on the behavior of hydrogel actuators. Glycol and acetone will be the main focus of this section.

### *10.1. Glycol responsive hydrogel actuators*

Under solvent stimulation, Chen et al. [186] developed a smart hydrogel actuator that could react to both water and ethylene glycol. In order to create a blue fluorescent quantum dot polymer gel layer, the researchers combined vinyl-functional carbon quantum dots with acrylamide (AAM) and acrylic acid (AAC) radical copolymerization. The 3M VHB elastomer layer was then joined to the gel layer to create a non-symmetrical double layer actuator. As a result of the carboxyl groups in the chemically cross-linked poly(AAC-AAM) gel partially ionizing in the high dielectric constant water, which causes electrostatic repulsion between polymer chains, the hydrogel layer of the actuator swells in aqueous solution; the elastic layer is also deformed. In water, the straight double-layer actuator stripes progressively twisted into curved stripes over the course of 60 min, as illustrated in Fig. 12A, and then gradually reverted to their original straight state in ethylene glycol. Similarly, throughout this phase, the hydrogel actuator may be accompanied by a notable fluorescence color change (from dark blue to rose). Solution diffusion governs the entire process and is responsible for controlling how the shape and color change in response to the same stimuli (i.e., water-glycol exchange). As shown in Fig. 12A, the straight double-layer actuator stripes gradually twisted into curved stripes within 60 min in water, and then gradually returned to a straight state in ethylene glycol. Likewise, the hydrogel actuator can be accompanied by a significant fluorescence color change (from dark blue to rose) during this process. This change in shape and color is highly synchronized and the entire process is controlled by solvent diffusion and triggered by the same stimuli (i.e., water-glycol exchange). As a result, this intelligent fluorescent hydrogel actuator may be used to create a swimming gel robot that works in tandem with shape deformation, color change, and directional movement and employs the fluorescence change as an alarm reminder function while coping with external risks. In conclusion, this gel actuator's synergistic color-changing and mutation characteristics may serve as a model for future multifunctional soft robotics and color-changing biomimicry.

### *10.2. Acetone responsive hydrogel actuators*

In addition to the glycol-responsive hydrogel actuators mentioned above, we will also introduce the acetone-responsive hydrogel actuators here. Recently, Gong et al. [187] demonstrated a technique for fusing hydrogels with elastomers utilizing a glass fiber interface that permits solvent control effects on composite textiles. Here, they created a three-layer elastomer/glass fabric/hydrogel layer using the interaction of the fabric and soft elastomer, and the hydrogel filled in the middle through electrostatic interaction with the glass surface, as shown in Fig. 12B. The hydrogel layer in the composite can provide in a solvent-swelling response. They alter the elastomer inclusion ratio to reduce the elastic layer's modulus due to the gradual swelling process, making the composite more prone to bending. As shown in Fig. 12B, the composite material remains flat in deionized water and when moved between acetone or 2.0 M salt solutions bends and deforms in opposite directions. This composite actuator describes a fresh concept that could guide the design of more sophisticated polymorphic or trimorphic actu-

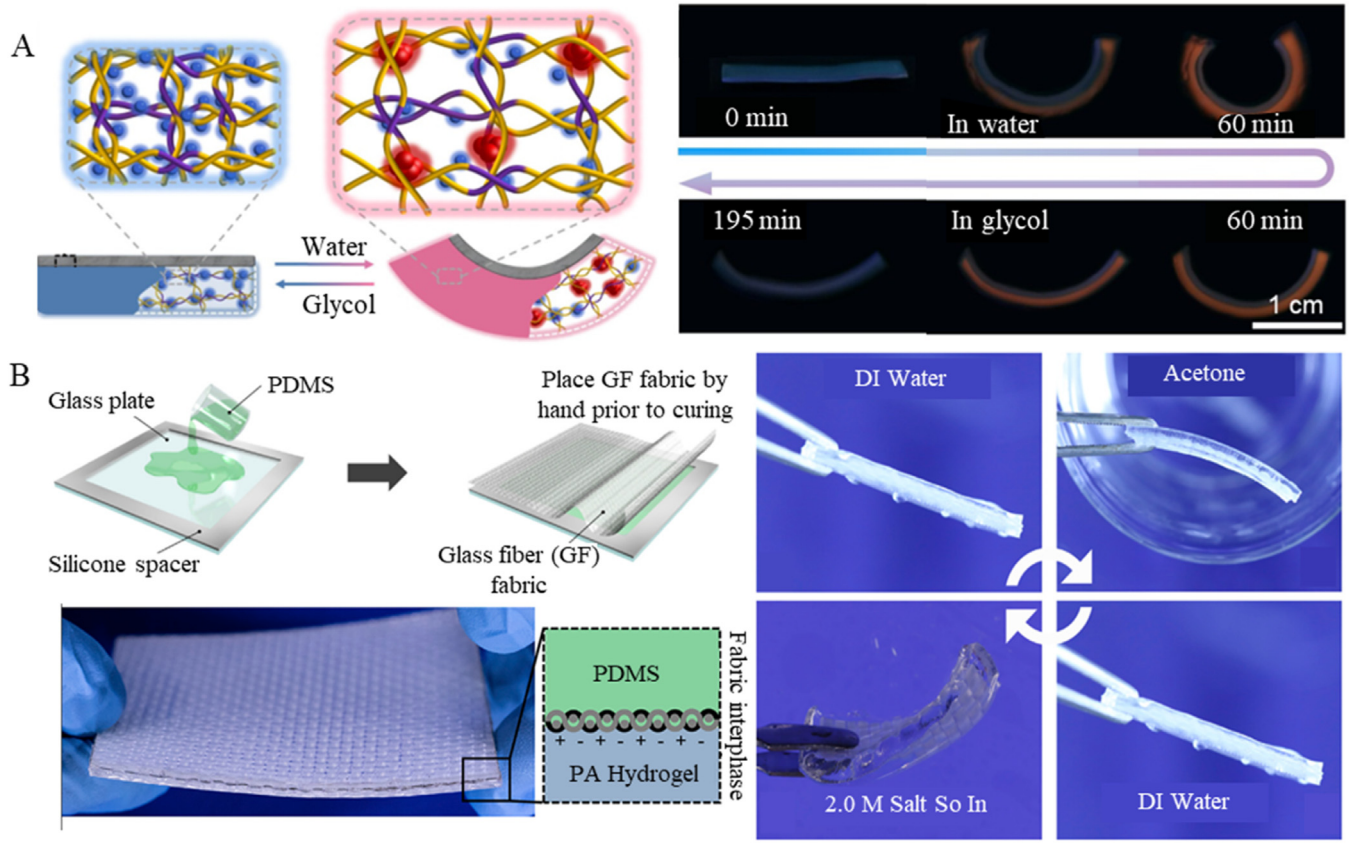



**Fig. 12.** Hydrogel actuators in response to solvent stimuli. (A) Schematic illustration of the glycol-responsive carbon dots hydrogel inspired by octopus. [186], Copyright 2021. Reproduced with permission from John Wiley & Sons Inc. (B) Schematic illustration of hydrogel/elastomer laminates bonded via fabric interphases for acetone-responsive actuator. [187], Copyright 2019. Reproduced with permission from Elsevier Science Ltd.

ators. In conclusion, solvent-responsive hydrogel actuators have a very broad range of application scenarios and its own distinctive control methods, but these methods also have some limitations, such as slow responses, sensitivity to outside influences (like solvent), and environmental issues brought on by solvent volatilization, etc.

## 11. Other response

In addition to the above-mentioned various stimuli, other types of physical or chemical stimuli, such as hydraulic or e activated by biomolecules, are also used to trigger hydrogel actuators [188,189]. Under typical conditions, the distinctive polymer network design is capable of realizing the function of reversible and controllable shape modification. Here are several examples to discuss the deformation of hydrogel actuators controlled by these two stimulating methods.

### *11.1. Hydraulic responsive hydrogel actuators*

The hydraulically responsive hydrogel actuators have larger actuation forces than other hydrogel-based actuators and are shape-modulated in response to changes in external hydraulic pressure. Zhao et al. [22] created cross-linked dissipative networks in tough hydrogels and built hydraulic hydrogel actuators out of polyacrylamide (PAAM) and alginate. To achieve an equilibrium condition, the hydrogel actuators had to be submerged in water for 48 hours. Additionally, they employ 3D printing to create complex-structured hydrogel actuators that can support numerous hydraulic drive cycles. The behavior of this hydrogel actuator is driven by external hydraulic pressure, as shown in Fig. 13A. The driver deformation can reach greater than 1 N, and the response time is faster (much lower than one second). This hydrogel is also highly transparent, making it useful to build actuators that can camouflage under water (e.g. in fishing operations). This approach provides new ideas for the next generation of bionic robots in marine biology.

### *11.2. Biomolecular responsive hydrogel actuators*

Biomolecule-responsive hydrogels are a significant advance in contemporary biomaterials [190]. DNA-responsive hydrogels are the most representative biomolecule-responsive hydrogels; however, the volume expansion of DNA-responsive hydrogels is small (in the 10-20 percent range). These values are significantly lower than the ones achieved with pH or temperature-responsive materials, limiting the scale and precision of deformation and motion. Cangialosi et al. [191] proposed a hydrogel actuator made of DNA hairpins to overcome this limitation. They varied the hydrogel's volume expansion deformation by sequentially adding different DNA hairpins, increasing the volume up to 100 times that of the original DNA-responsive hydrogel (Fig. 13B). Next, the authors explored the different control processes of the hydrogel actuators within the framework of various DNA sequences. For instance, they created a hydrogel flower with petals that had distinct DNA sequences from the other two groups so that they can react differently to DNA stimuli by changing how they deform. All petals can be folded up in the case of two different sets of DNA sequences,

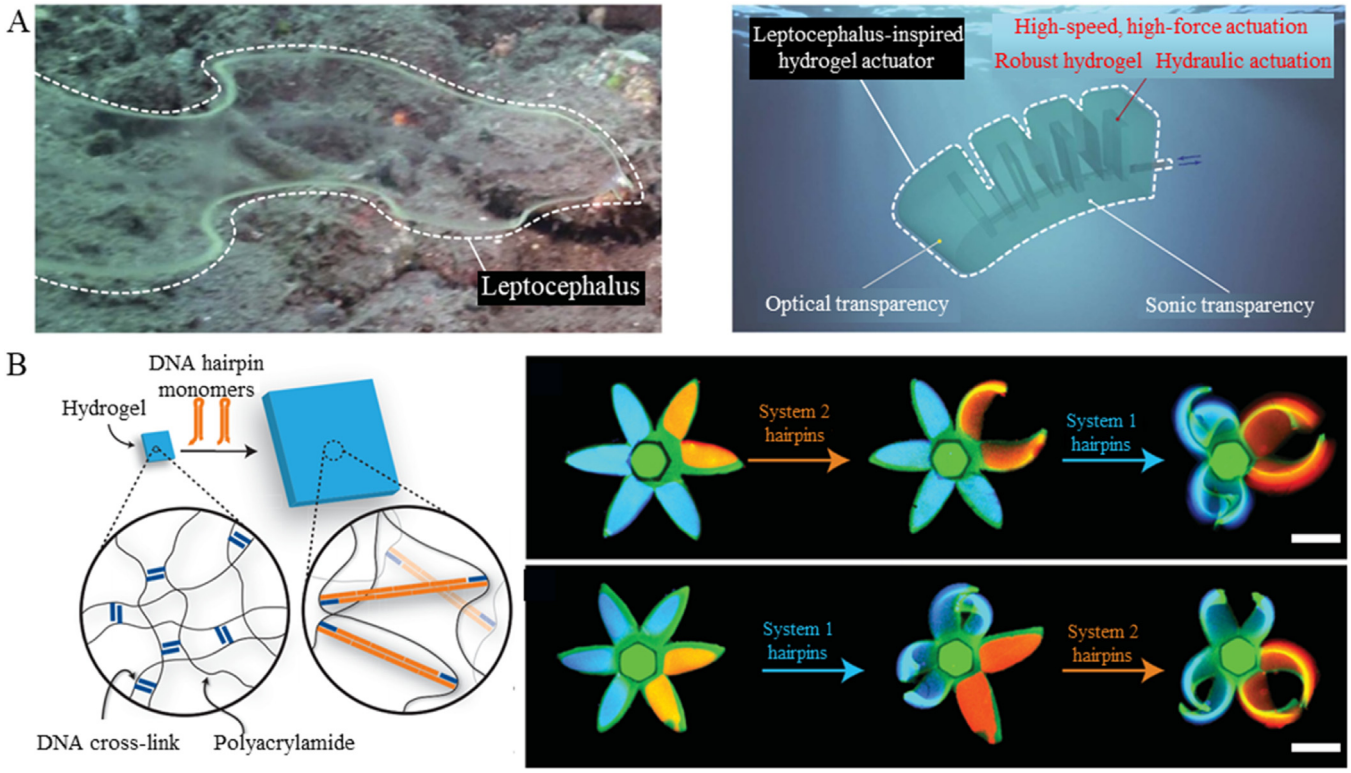



**Fig. 13.** Hydrogel actuators in response to other stimuli. (A) Schematic illustration of the hydraulic-responsive hydrogel actuators and robots in water. [22], Copyright 2017. Reproduced with permission from the Nature Publishing Group. (B) Schematic illustration of DNA-responsive hydrogel actuator. Scale bars, 1 mm. [191], Copyright 2017. Reproduced with permission from American Association for the Advancement of Science.

and each set of sequences can achieve a distinct regulation of the folding behavior for the petals, realizing a difficult procedure by which the petals can be folded step by step. More complicated structures, such tentacles, claws, and legs, can be curled and activated simultaneously or sequentially depending on their placement on the hydrogel device. This provides a new direction for novel biomolecular responsive actuators.

## 12. Toughening mechanism

### *12.1. Fracture toughness & fracture energy*

Emerging tough hydrogel actuators allow for repetitive and large strain deformation during cyclic driving and motion, thus enabling their practical application. Therefore, tough hydrogels will support the implementation of hydrogel actuators [192]. Here, the toughening mechanisms of functional hydrogels will be systematically discussed and summarized. Typical examples include the use of molecular and structural engineering approaches to achieve stress homogenization or building energy dissipation into stretchable hydrogels. In addition, the molecular engineering-based network structure design of homogeneous hydrogel actuators and structural engineering-based design of heterogeneous hydrogel actuators are also described. The mechanical properties of hydrogels, and in particular their ability to sustain stress without breaking, often determine their technical potential in the fabrication of actuators. In addition it has been shown that when subjected to cyclic loads (as could be the case during repeated actuation), hydrogels may suffer a gradual property degradation due to fatigue as well as nucleation and growth of cracks that cause the material to fracture [193].

The property that determines the ability of a material to resist the growth of defects that could eventually lead to failure is its toughness. Unlike conventional elastic materials, hydrogels exhibit large, non-linear strains up to their breaking point [195]. As a result, linear elastic fracture mechanics cannot be used to describe their behavior. The most commonly used magnitude to characterize hydrogel toughness is the fracture energy (the energy to advance a crack per unit of area: $\Gamma$) that is usually divided as the sum of two contributions: the intrinsic fracture energy, $\Gamma_0$, that is the energy required to break the polymer chains and the energy dissipated in the regions around the crack, $\Gamma_D$. They can be calculated as follows:

$$\Gamma_0 = \Sigma_0 nU$$

where "n" is the number of "monomer units", "U" is energy required to break the "single monomer unit", and "$\Sigma_0$" is the number of "chains per unit area".

$$\Gamma_D = 2V \int_0^h w_D d_y$$

Where "$w_D$" is the "energy dissipation per unit volume", "V" is the "volume fraction of the hydrogel", "h" is the "height of the process zone", and 2 represents "the crack on both sides".

One source of dissipation arises from the large deformations sustained by the polymer chains in the region around the crack (the process zone) (Fig. 14). The material in this process zone is first loaded and then unloaded when the crack progresses. As the deformation of the material in the process zone exceeds the linear elastic limit, it stress-strain curve exhibits an hysteresis loop with the consequent dissipation of energy [194,196]. The size of this process zone varies depending on the hydrogel from a few nanometres to millimetres. In addition, hydrogels reinforced by fibres or particles may develop a bridging zone behind the crack tip that can also contribute to the dissipation of energy and increase $\Gamma_D$.

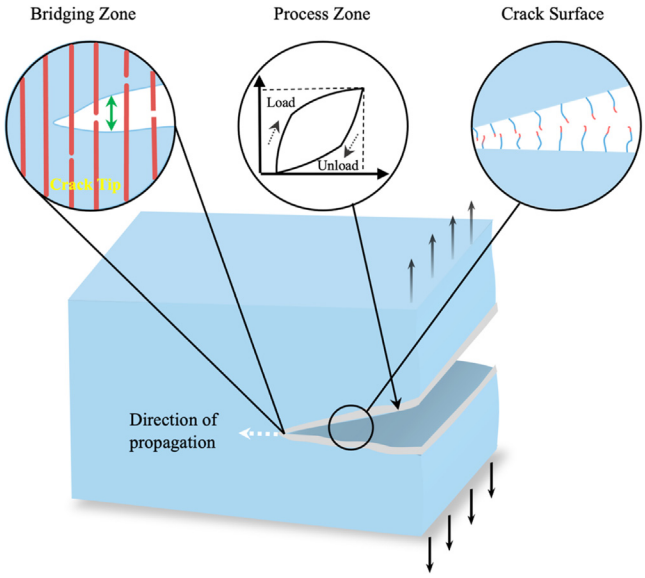



**Fig. 14.** Schematic illustration of crack propagation in a hydrogel. [197,198], Copyright 2020. Adapted with permission from John Wiley & Sons Inc.

### *12.2. Construction of tough hydrogels*

In general, due to their high water content and low number of bonds per unit of area the intrinsic fracture energy of hydrogels is relatively low ($\Gamma_0 \approx 10$ J m$^{-2}$, which is comparable to glasses and smaller than that of common elastomers that are of the order of 50 J m$^{-2}$) [199]. The intrinsic fracture energy will also depend on the swelling ratio of the hydrogel as the increase in swelling leads to a decrease in the number of polymer chains per unit of cross-sectional area, thereby causing the intrinsic fracture energy to decline [201]. In addition, various additional factors including the irregular distribution of crosslinking points of polymer chains, and the variation of their length can further decrease $\Gamma_0$ [200] and, in general, be detrimental to the mechanical performance. Due to the differences in reactivity between monomers and crosslinkers, the structure of the polymer network tends to be heterogeneous. For instance, the monomers and crosslinkers will form denser cross-linked microgels at the early stage of the reaction, and then connect to a larger network based on the cross-linked microgels, resulting in an heterogenous hydrogel [199]. It is also difficult to ensure that crosslinking of polymer chains occurs at equal intervals when monomers react with crosslinkers, leading to a wide range of chain lengths in the final product [200]. The heterogeneity of the materials can lead to points of stress concentration when subjected to external forces what could be detrimental. On the other hand, for polymers with constant monomeric unit and crosslinking density, the value of intrinsic fracture energy is relatively constant across the material.

To increase significantly the fracture energy of hydrogels, it is necessary to increase the dissipation contribution, $\Gamma_D$. This means that increasing the contribution of the stress-strain hysteresis in the process zone has been the main focus on the development of tougher hydrogels [202]. Considering the properties and design constraints of the material, the approaches used in practice to increase the toughness of hydrogels while maintaining structural integrity after undergoing large deformations are usually divided in three types (Table 1):

i) Increasing gel homogeneity. In a homogeneous gel the load can be distributed uniformly over a large fraction of the chains to reduce the formation sites of microcracks due to the presence of inhomogeneities. In this way it should be possible to increase the strain in the process zone without fracture and therefore to increase the dissipation generated by the stress-strain hysteresis. Inhomogeneous hydrogels may be more prone to stress concentration cracking in general and cracks could propagate more easily through the less cross-linked regions leading to a decrease in toughness. (Fig. 15A, B);
ii) Introducing additional mechanisms to promote energy dissipation such as addition of sacrificial units that will increase dissipation in the process zone or fibres that can increase the dissipation due to bridging and pull-out behind the crack tip (Fig. 15C);
iii) Combining the first two mechanisms to prepare hydrogels with high toughness, such as using multifunctional crosslinkers (micro/nanoparticles (NPs)) to control the distance of mutual crosslinking between polymer chains to form a homogeneous network, while taking advantage of additional energy dissipation coming from the bond breakage between particles and polymer chains (Fig. 15D).

## 13. Applications

The above-mentioned reversible shape transition abilities and stimulus response modalities are directly related to the prospective applications of hydrogel actuators. In the previous section, several bionic response hydrogel actuators were discussed in terms of how the response and actuation behavior is controlled, and some potential application scenarios were briefly reviewed. Soft actuators and robots have been developed with increasing sophistication and are currently employed in a number of applications due to advances in material design and manufacturing technologies. Hydrogel actuators have been employed in fixtures, soft actuators, soft robotics, biosensors, tissue engineering, artificial muscles, electronic skins, and soft actuators [228–230]. Many of these applications are still in the conceptual stage (Fig. 16). In this section, we will go into great depth about the potential real-world uses for hydrogel actuators, ranging from soft actuators and fluid control to medical engineering.

### *13.1. Responsive soft actuators*

#### *13.1.1. Manipulators or grippers*

One of the most promising applications of hydrogel actuators is as relatively complex multi-arm robots or clamps. The hydrogel actuator may capture items when subjected to one or more stimuli and then release the object in response to a different stimulus. These responsive actuators has been widely used as smart actuators in robotics, flexible sensors, mobile medical and surgical biopsy tools, which are strongly related to their shape programming [223]. This application is still in its early stages. So far, a frequently utilized actuator that can grip and release is a promising soft clip holding. Taking advantage of this opportunity, Yuk et al. [22] designed a hydraulic soft and transparent fixture with optical and acoustic camouflage in order to capture and release live goldfish (Fig. 17A). To generate natural camouflage akin to fibers in optical and acoustic environment, they used hydrogel actuators with great optical and acoustic transparency in water. This hydraulic hydrogel actuator has a high water content that provides nearly identical optical and acoustic qualities to water for natural concealment, and the hydraulically powered actuator display fish-like movements (Fig. 17A). Therefore, the camouflaged hydrogel actuator can capture and release live fish in the water, its optical transparency maintains its camouflaged state when the hydrogel is tightly held against the goldfish in the tank, its flexible actuation control can successfully capture and grasp the goldfish, and the internal flexibility of the hydrogel actuator can release the captured goldfish without harming it. Although this fixture for an un-

**Table 1**
Manufacturing of tough hydrogels classified according to the toughening strategies.

| | Toughening Strategy | Trigger | Advantage | Shortcoming | Reference |
|---|---|---|---|---|---|
| | Radiation crosslinking | $\gamma$-radiation, X-ray, HV, UV, heat | Facile approach<br>Good mechanical properties, gel fraction, swelling ratio, and<br>Absence of toxic reagents<br>Antimicrobial, biodegradable and biocompatible characteristics<br>Independent of monomer reactivity and concentration | Uncontrollable and uncertain reaction<br>Difficult and time-consuming optimization<br>Long-term radiation exposure can lead to loss of toxicity and biocompatibility | [195,203,204] |
| Combination of uniform stress distribution and mechanical | Click chemistry | Reactive precursors with specific functional groups and their interaction with light ($h\nu$), pH, or temperature | Simple process<br>Spontaneous formation and mild condition<br>High yielding<br>Easily removable by-products<br>Stereospecific<br>Tunable mechanics, gelation and the degradation rate<br>Wide in scope<br>Bio-orthogonal<br>Improved biocompatibility | Low biocompatibility of degradation products<br>Low vivo stability, specificity, and reaction rate<br>Complex synthetic routes<br>Potential side reactions<br>Limited chemical component | [205–208] |
| | Tetra-PEG | Cross-end coupling of two symmetrically end-modified PEG macromonomers | Remarkable mechanical properties<br>Ideal and homogeneous polymer network<br>Efficient and tunable cross-coupling reaction<br>Low expansion pressure<br>Negligible defects and tangles<br>Hydrophilicity, stability, biocompatibility and biodegradability<br>Excellent fatigue resistance | Limited by available monomers and polymers<br>Strong entanglement of prepolymers hinders the study of polymer gels at the molecular level | [209–211] |
| | Slide ring | Cyclic molecules are covalently cross-linked to form cross-links that can slide along the chain, and topological confinement at the chain ends prevents "slip rings" from falling off | Generation of crosslinking agent topology interlock<br>No cross-linking point on the polymer chain<br>Adjustable ring coverage and axial chain length<br>Extraordinary mechanical properties<br>Reversible self-healing<br>Extensive swelling ratios<br>Uniform tension | Restricted cyclic molecules and polymers | [212,213] |
| | Fibre-reinforced composite | Embedding a stretchable fibre or filler into a hydrogel matrix | Retainable inherent stratified structures/<br>Enhanced compression and wear characteristics;<br>Biochemical modification<br>Enhanced biocompatibility | Impossible to mimic the microstructure and composition of the extracellular matrix of tissues | [214–217] |
| Introducing energy dissipation mechanism | Interpenetrating polymer networks | Two or more cross-linked polymer chains interconnected by non-covalent means | Complicated and controllable mechanical properties<br>More functional combinations | Difficult to release the encapsulated bioactive molecules<br>Susceptible quality | [218–220] |
| | Double network | Two networks with different mechanical properties are cross-linked by covalent/non-covalent bonds to form a fully/semi-interpenetrating polymer network | Highly designable sacrificial bond regimes and scales<br>Excellent mechanical properties<br>High water content<br>Self-healing ability<br>3d printability and injectability<br>Enhanced ductility<br>Biocompatibility | The cumbersome and time-consuming synthesis<br>Unattainable complex shapes<br>Complex and time-consuming synthesis<br>Requires high reproducibility control<br>Breaking of covalent bonds leads to irreversible destruction and mechanical degradation<br>Low water content | [221–223] |

(*continued on next page*)

**Table 1** (*continued*)

| | Toughening Strategy | Trigger | Advantage | Shortcoming | Reference |
|---|---|---|---|---|---|
| Combination of uniform stress distribution and mechanical energy dissipation mechanism | Nanocomposite | Nanomaterials act as highly functional crosslinking points to connect multiple polymer chains | Unlimited to molecular crosslinking points<br>High uniformity<br>Excellent swelling ability<br>Outstanding toughness<br>Enhanced stimulus sensitivity<br>Easily structural modification<br>Uniform stress distribution | Relatively low inorganic clay content<br>Lower mechanical properties<br>Self-repair ability<br>Affectable characteristics by nanoparticle selection<br>Low biocompatibility and biodegradability | [224–226] |
| | Macromolecular microsphere composite | Control of cross-linking density and mutual cross-linking distance by the presence of covalent cross-linking between polymer chains and polymer microspheres | Overcome the classical limitations of organic crosslinkers<br>Enhanced energy dissipation and self-repair processes | Uniform performance<br>Unrecovered ruptures | [200,227] |

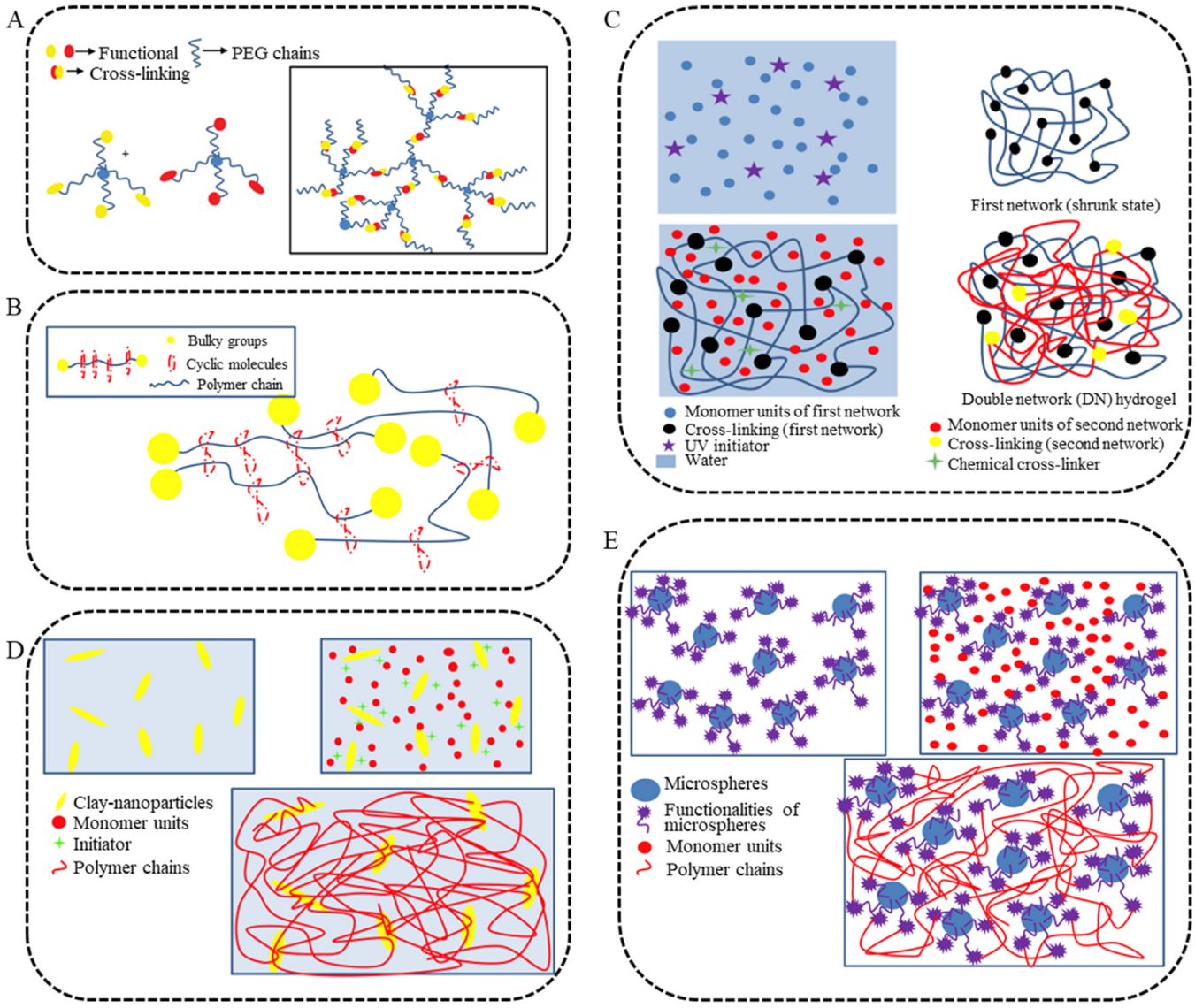



**Fig. 15.** Schematic illustration of toughing mechanism in a hydrogel. [192], Copyright 2018. Reproduced with permission from John Wiley & Sons Inc. (A) Structure of tetra-PEG (poly (ethylene glycol)) tough hydrogels. (B) Structure of sliding cross-linked tough hydrogels. (C) Structure of DN tough hydrogels. (D) Structure of clay-based nanocomposite tough hydrogels. (E) Structure of microsphere-reinforced tough hydrogels.

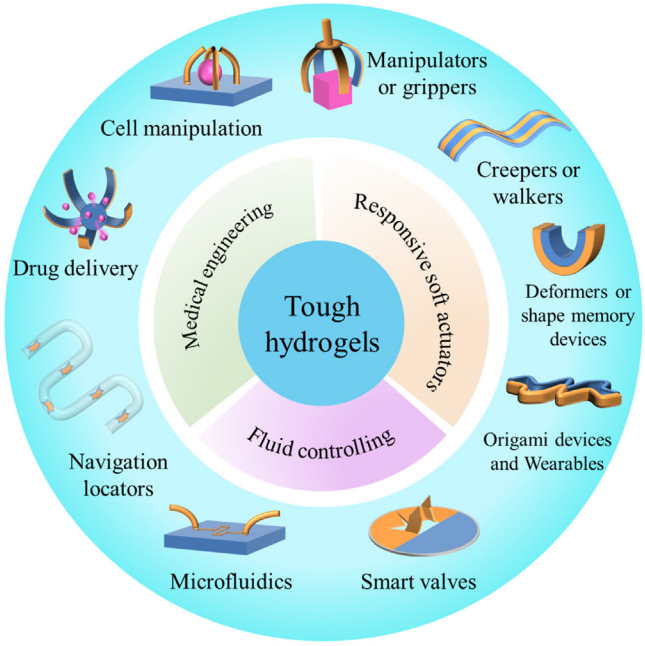



**Fig. 16.** Schematic illustration of the potential applications of the hydrogel actuator. [231], Copyright 2019. Adapted with permission from the Nature Publishing Group. [239], Copyright 2018. Adapted with permission from Elsevier Science Ltd. [242], Copyright 2019. Adapted with permission from American Association for the Advancement of Science. [246], Copyright 2019. Adapted with permission from Elsevier Science Ltd. [253], Copyright 2019. Adapted with permission from the American Chemical Society. [254], Copyright 2019. Adapted with permission from the American Chemical Society. [177], Copyright 2020. Adapted with permission from the American Chemical Society.

derwater living manipulator provides a starting point for further research, its single stimulus control constraint prevents it from being used for more complex applications.

In order to create more robotic hands for application scenarios, Liu et al. [231] added graphene oxide (GO)/polypyrrole (PPY) to create a programmable patterned GO/PPY dual-responsive hydrogel actuator. This actuator demonstrated excellent responsive actuation performance under temperature and infrared (IR) light stimulation. As shown in Fig. 17B, they created a smart gripper with a cross structure that was modeled after an eagle's claw. The GO/PPY gripper, which has excellent mechanical gripping characteristics, can bend and successfully pick up rectangular, square polymeric foams after stimulation by high humidity stimulation and release the weight and return to its initial state at low humidity, where the weight is 38 times heavier than the GO/PPY gripper. This is similar to how an eagle can catch its prey with its claws. This work provides an effective method for building hydrogel actuators that can work in many fields and will open up new opportunities for smart hydrogel actuators.

A similar humidity-responsive hydrogel actuator was created by Zhou et al. [232] They used $Eu^{3+}$ ionic polyethyleneimine copolymer (acrylic acid) (PEI-co-PAAC) and poly(ethylene glycol) diacrylate (PEGDA), which demonstrated humidity-sensitive properties and accomplished object localization and recognition under UV stimulation. They also exploited the aforementioned features to design and create a double-layer hexagonal hydrogel for hiding jellyfish in order to realize the process of gripping and releasing underwater objects (Fig. 17C). They investigated the underwater application in more detail and discovered that the hydrogel gripper can hold items up to 4.5 cm in diameter and 25 grams in weight, making this dynamic camouflage hydrogel useful for catching live goldfish. The gripper is opaque in daylight when it is open, but after catching the goldfish and closing, it is instantly identifiable by glowing under UV light and can thus be easily located by a person or machine. This hydrogel actuator demonstrates more options and practical applications for underwater soft grippers.

The functional flexibility of the above-mentioned actuators is severely constrained because they are employed for grasping and releasing by fixing one end and then gripping and releasing the targeted item. Another kind of unfixed soft actuator has been created in order to overcome this restriction, and this unrestricted little soft robot can offer more gripping and releasing options in complex settings. According to Wang et al. [233], a hydrogel actuator with a bilayer asymmetric structure was created by 4D printing. The printing hydrogel ink contained nanotype vesicles, synthetic lithium saponite, N-isopropylacrylamide, N,N'-methylenebisacrylamide, and phenyl lithium-2,4,6-trimethylbenzylphosphonate. Among them, nanotype vesicles can release $O_2$ through photothermal catalytic decomposition of $H_2O_2$, and synthetic lithium saponite is used to regulate the print quality, so this hydrogel actuator has the ability to release $O_2$. In order to implement the process of transfer and release, the printed hydrogel sheets were put together into a four-arm hydrogel actuator, as illustrated in Fig. 17D. The hydrogel actuator was gradually submerged in water heated to 50°C, and as the time of immersion increased, it caught the rubber block attached to the rope and securely wrapped it. The operation of moving the wrapping was accomplished by tugging the rope. In addition, the bend/release trigger shape of this hydrogel actuator is replaced with a bionic plant flower and a hydrogel manipulator, both of which are simple to use for closing/opening and grasping/capture operations of the targeted object under thermal stimulation. Based on this approach, a number of more sophisticated hydrogel actuators have recently been created. They can be employed as smarter fixtures and offer further chances to get beyond the drawbacks of conventional fixtures under challenging environments [234,235].

### *13.1.2. Creepers or walkers*

Crawling or walking can be translated into periodic stimulation, bending movements, and exciting real-world application scenarios. The intriguing movement of earthworms in nature has sparked experts' interest in the subject. In order to control the unidirectional expansion and contraction of the hydrogel under the stimulation of an external light source and achieve the actuator's crawling behavior, Aida et al. [156] developed a cylindrical anisotropic crawling hydrogel actuator. This actuator is made up of a thermally responsive polymer network and a two-dimensional nanoelectrolyte. As shown in Fig. 18A, when the hydrogel at the right end is exposed to the 445 nm laser beam, the irradiated area gradually thins, lowering the amount of friction with the capillary wall and causing a minor lift to occur on the right side of the hydrogel actuator. The gel in the area where the irradiation point is shifted toward the left end eventually extends or thins, forming a frictional shape, producing a crawling motion like to that of an earthworm, and the entire hydrogel column moves from left to right. When the reverse procedure is carried out repeatedly, the hydrogel column can also realize the directional crawling and adjustment of the shift direction process. the hydrogel column may also crawl and shift directions. Since near-infrared light (NIR light) can penetrate biological tissues, the system can work inside living organisms through external control, i.e., it can be applied to clinical drug delivery and wound detection, among other things. When the internal gold nanoparticles (photothermal agent) are replaced with gold nanorods, the hydrogel can also be remotely controlled by NIR light. The example provides concepts for potential future application opportunities by demonstrating the behavior of precise remote control and crawler movement.

The crawling process of the inchworm is also widely studied and imitated. Its movement process can be divided into two steps

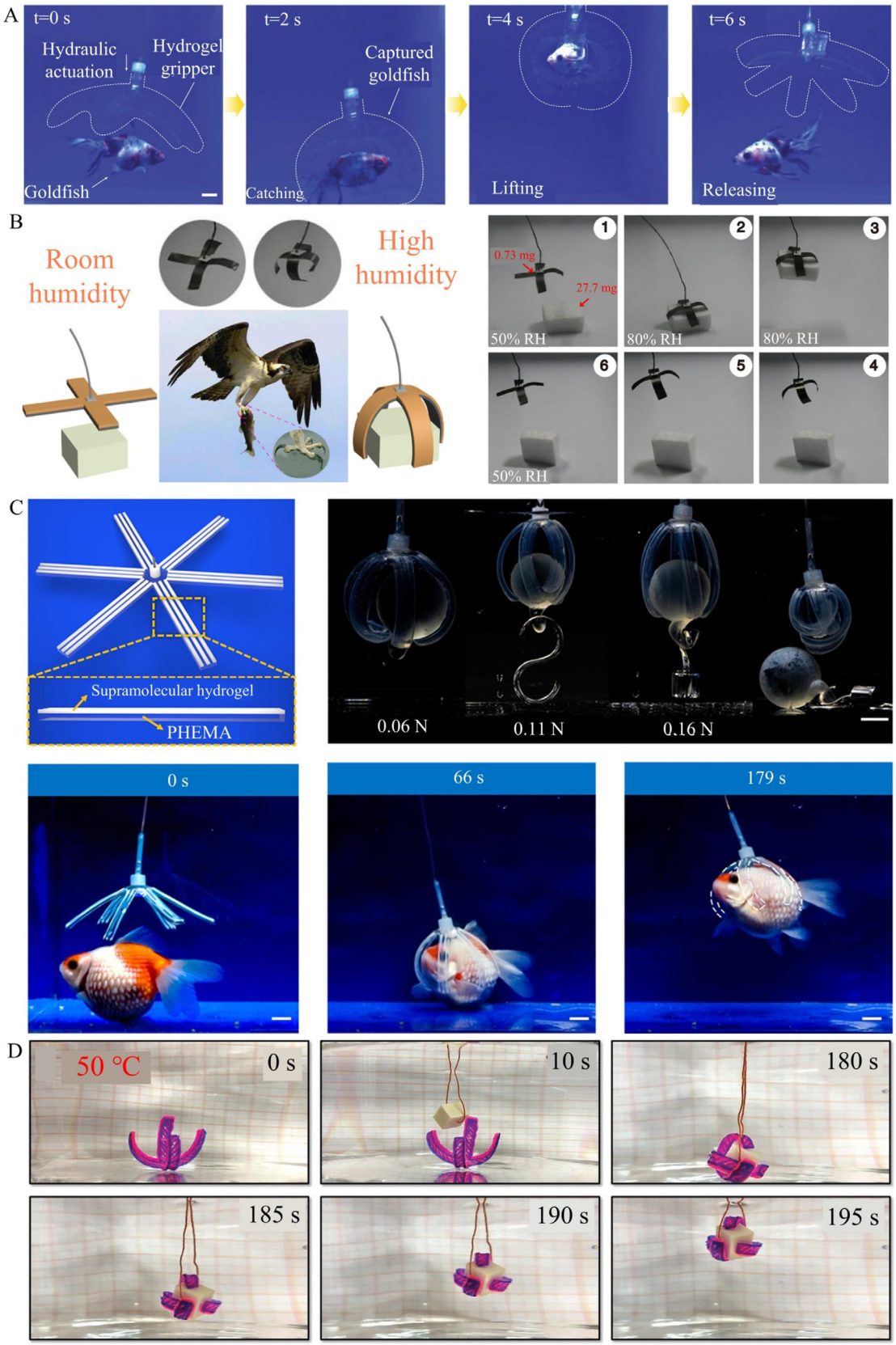



**Fig. 17.** Hydrogel actuators acting as manipulators or grippers functionality. (A) Images of the hydrogel gripper used to capture goldfish. Scale bars, 1 cm. [22], Copyright 2017. Reproduced with permission from the Nature Publishing Group. (B) Photos of the GO/PPY hydrogel gripper mimic the eagle claw. [231], Copyright 2019. Reproduced with permission from the Nature Publishing Group. (C) Schematics and photos of 3D printed supramolecular hydrogel acting as gripper. Scale bars, 10 mm. [232], Copyright 2020. Reproduced with permission from the American Chemical Society. (D) Examples of temperature responsive hydrogel actuator acting as gripper. [233], Copyright 2021. Reproduced with permission from John Wiley & Sons Inc.

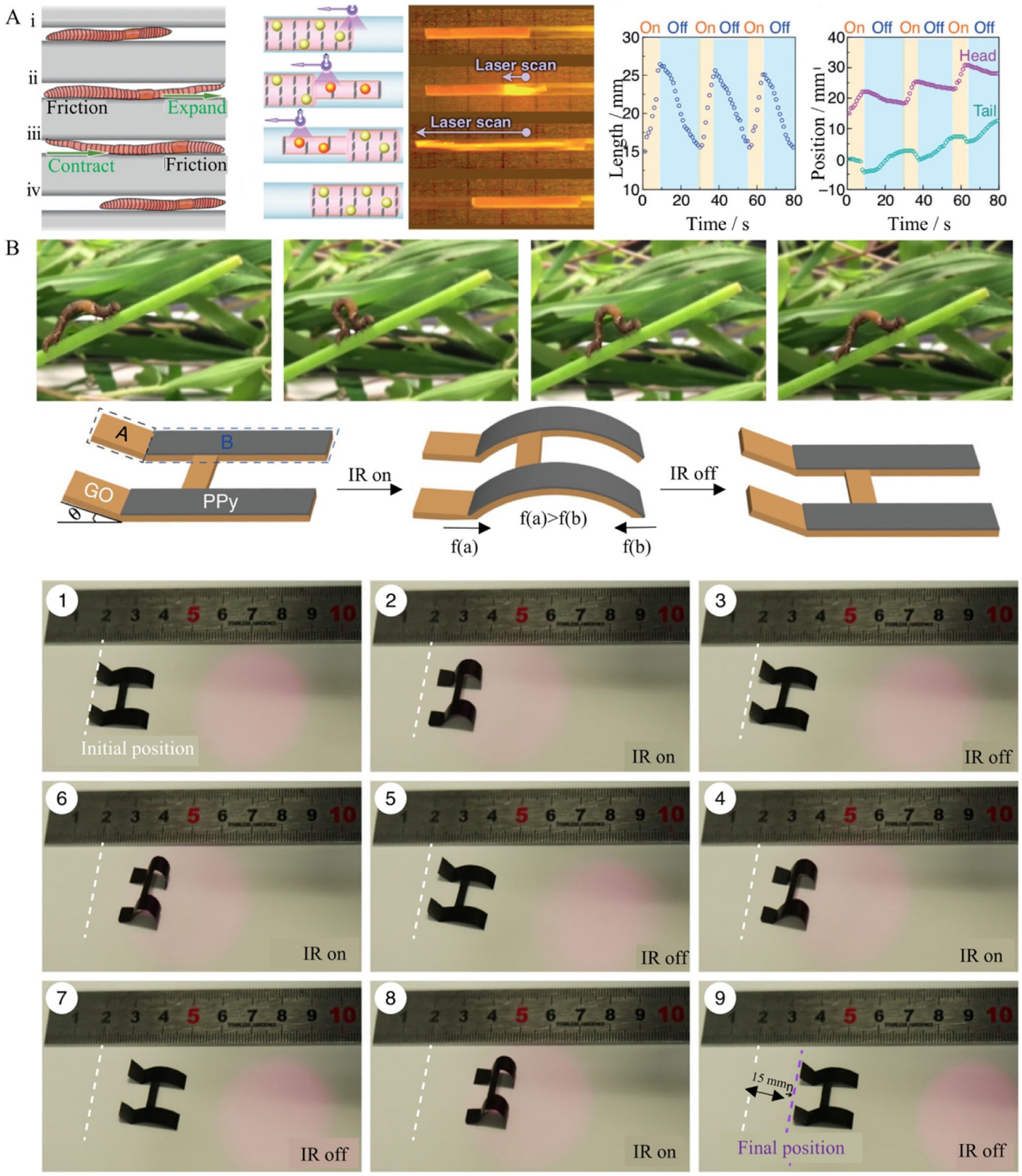



**Fig. 18.** Hydrogel actuators acting as creepers or walkers' functionality. (A) Schematics and photos of light responsive earthworm-like hydrogel acting as creepers. [156], Copyright 2018. Reproduced with permission from John Wiley & Sons Inc. (B) Schematics and images of the movement of the inchworm and light responsive GO/PPY hydrogel soft walking robot. [231], Copyright 2019. Reproduced with permission from the Nature Publishing Group.

(Fig. 18B): (1) the front foot holds on to the branch while the body curls up (2) after grasping the branch, the front part of the body moves forward thereby driving the whole body forward. Inspired by the inchworm motion, Liu et al. [231] prepared a double-layer hydrogel actuator with two sections, one of which has the ability of horizontal and angle adjustment (the ability to modify the angle (A)), and the other of which is made of graphene oxide (GO)/polypyrrole (PPY) hydrophilic tape (B). The soft pedestrian robot's B component bends when stimulated by infrared light, and part A is in close touch with the horizontal plane. Part B will re-

sume its straight form when the infrared light fades, rubbing the horizontal plane and propelling the entire body forward. With the help of external light control and modifying the length of continuous stimulation, this soft walking robot shows how to crawl over vast distances. The aforementioned findings demonstrate that, with careful planning and precise environmental control, it is entirely possible to create intelligent walking machines. To create creeping or moving hydrogel actuators, more stimulation modalities and responsive materials are also used, along with more intricate designs, carefully managed bending and twisting, programmed materials, quick and efficient control techniques, and a wider range of potential application scenarios [236,237].

*13.1.3. Deformer or shape memory devices*

There are many materials in nature that can respond to external attacks or changes in the environment and produce complex morphological changes or position shifts depending on their internal anisotropic structure. Inspired by these natural materials, researchers have designed biomimetic hydrogel actuators with a variety of intelligent actuation properties [237,238]. Recently, Zhao et al. [239] designed and assembled three-layer hydrogel actuators, consisting of inner, middle, and outer layers, and precisely mimicked the shape and arrangement of chrysanthemum petals. The pistil and stem of the chrysanthemum are made of real flower parts and polydimethylsiloxane rods, respectively (Fig. 19A). By further introducing external infrared light stimulation, it was shown that as the infrared spots gradually spread from the inner to the outside layer, when the light stimulation is provided to a layer, the petals of under light stimulation layer will cluster towards the stamens. The NIR light spot gradually covered the entire flower as the irradiation time increased, and the petals were tightly packed around the stamens, indicating a fully closed state. When the light spot was removed, the closed chrysanthemum gradually stretched back to its original form, simulating the full opening of the flower. Additional stimulation can result in the following closure and flowering step. This work provides references and research ideas for future studies on devices able to switch between an open and close state.

In another pioneering work, Chen et al. [240] described a macroscopically anisotropic biphasic hydrogel actuators that coordinates shape deformation and color change. It was made from layers of hyperbranched polyethyleneimine (PBI-HPEI) fluorescent hydrogel combined with supramolecular host-guest polymers via thermally responsive oxides, and it demonstrated pH-dependent shape deformation and color change. Such hydrogel actuators can also be built with sophisticated shape transformations based on the same methodology, in addition to simple shape deformation. As seen in Fig. 19B, the hydrogel actuator layer is encased in a layer of hydrogel that displays responsive deformation behavior actuated by external light stimuli, stretching the shape and producing a flowering-like process. This layer of responsive hydrogel also exhibits pH responsive fluorescence color changes. This hydrogel actuator can thus mimic some naturally moving animals, providing intriguing directions for further research.

Similarly, Zhao et al. [143] created an asymmetric bilayer hydrogel actuator employing a PAAM/PAAC bilayer hydrogel actuator that has a double network structure in the top layer and a single network structure in the bottom layer. AAM creates a single network layer, whereas AAC photopolymerizes only to a particular irradiation depth due to low UV penetration, producing a bilayer structure. The medium of a bilayer PAAM/PAAC hydrogel can be swapped between its two layers thanks to the UCST-type bulk phase transition behavior displayed by this hydrogel actuator, enabling applications that are not bound by the environment. When the top of the hydrogel is triggered by UV light, whether in a medium of water or paraffin oil, this hydrogel flower can open at 60°C and close at 5°C (Fig. 19C). The reverse process will take place during the heating process. However, hydrogels have variable reaction times in various media, taking roughly 10 minutes in water baths and 50 minutes in oil baths. This asymmetric hydrogel actuator may therefore drive amphibiously, which will increase the range of applications.

Tang et al. [241] created magnetic hydrogel soft structures using 3D printing to create more intricate shape-deforming hydrogels. In order to create a directly printed magnetic hydrogel, a hard magnetic filler (NdFeB) was included into the hydrogel matrix and nanocolloids were used to change the rheology of the precursors. Then, numerous intricate shapes were 3D printed. The printed parts were used to assemble a hydrogel lotus flower, which continuously distorted to alter its overall shape as the external magnetic field changed. The magnetic hydrogel lotus that was 3D printed in Fig. 19D is seen completely bloomed when there is no magnetic field. When a magnetic field is supplied, the hydrogel lotus spreads out completely on the plane, and when an upward magnetic field is utilized, the lotus is totally closed; however, when a downward pair of magnetic fields is employed, the lotus opens. With a high reaction efficiency, this change can occur in as little as 0.1 s. These hydrogel actuators describe the potential for hydrogel actuators to function as crawlers and shape memory devices through various forms of external field control and shape design. They also demonstrate complex change processes through assembly and design, which offers fresh concepts for related and intriguing future research.

*13.1.4. Origami devices and wearables*

The origami structure combines the simplicity of the plane manufacturing method and the geometric complexity that can be achieved. An intriguing experiment is hydrogel origami, Zhao et al. [239] used graphene oxide (GO) particles to create a hydrogel material that was responsive to NIR driving and acted as a photothermal sensor. Next, they created a six-part prototype box, adhering hydrogel sheets at the joints. Fig. 20A shows the carton unfurled in a way that ensures a fully folded state by having each part's origami angle achieve a hinge angle of at least 90 degrees. The intended carton prototype was folded as illustrated in Fig. 20A, folding each portion in turn under NIR light. A responsive hydrogel actuator was used to achieve the desired deformation outcomes by applying it to the actuator's periphery in accordance with the intended folding process. Three NIR light beams were employed to highlight the appropriate hydrogel box components, ensuring accuracy and consistency. The unfolded hydrogel box was then gently folded in the intended order while being stimulated by NIR light. The folded box resumed its unfolded state and displayed repeatable and controllable features after the external stimulus was removed for further 15 s. This offers a fresh concept for the remote management of intricate behaviors.

In contrast to the comparatively sluggish shape transformation process of typical hydrogels, the leaves of coriander grass can close swiftly in nature to capture insects in less than a second. In order to create gradient composite hydrogel actuators, Nie et al. [242] employed UV light to stimulate GO radical production and begin the polymerization of poly(N,N-dimethylaminoethyl methacrylate) (DMAEMA monomer) and N,N'-methylenebisacrylamide (MBA; cross-linker) (Fig. 20B). The composite hydrogel responds to NIR light as a result of GO's photothermal action. Due to the initial twofold gradient effect, the hydrogel sheet dramatically bends to one side when NIR light is shone on it. This composite gel actuator also displays responsive behavior when submerged in water. Based on this characteristic, it is possible to achieve extremely complex morphological changes, as shown in Fig. 20B. When exposed to various NIR stimulation beams, the hydrogel sheet curls, and when the hydrogel is further submerged

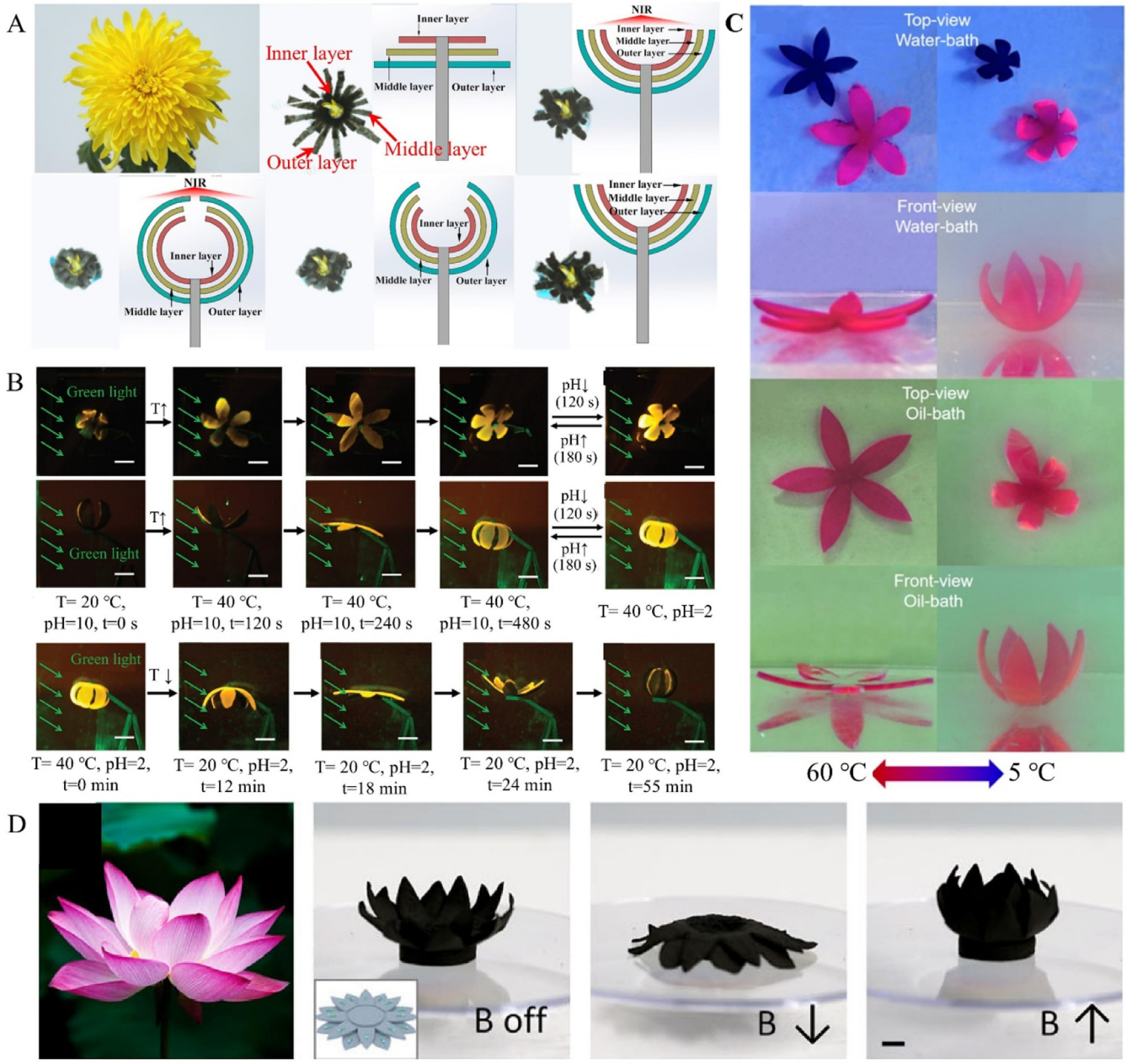



**Fig. 19.** Hydrogel actuators acting as deformers or shape memory devices functionality. (A) Schematics and photos of the NIR-driven bionic hydrogel chrysanthemum. [239], Copyright 2018. Reproduced with permission from Elsevier Science Ltd. (B) Photos of the colour-tuneable fluorescence anisotropic hydrogel actuators acting as shape transformer. Scale bars, 5 mm. [240], Copyright 2018. Reproduced with permission from John Wiley & Sons Inc. (C) Photos of multiple-responsive UCST-type hydrogel flowers with self-actuation behaviour. [143], Copyright 2019. Reproduced with permission from the American Chemical Society. (D) Examples of magnetic hydrogel lotus under actuation. Scale bars, 5 mm. [241], Copyright 2021. Reproduced with permission from John Wiley & Sons Inc.

in water, a variety of complex folding forms can be demonstrated by varying the immersion time. They created complicated folding and programmable cube folding structures based on this behavior, which can accomplish complex origami behavior through external stimulus. Additive manufacturing could enable hydrogel actuators that display more intricate origami features and precise structural modifications for biomedical instruments including soft robotics, adaptive optics, and energy systems, among other applications.

Materials able to provide a useful interface with the skin should exhibit low stiffness and easy deformation, which makes hydrogel actuators very suitable, e.g., in wearable devices. For instance, employing hydrogel biofilms generated from the most prevalent E. coli cells and coupling them with natural emulsions as moisture-inert materials, Wang et al. [243] developed actuators with outstanding humidity-responsive behavior. When the actuator films were exposed to a dry environment (relative humidity (RH), 15%), shrinkage due to cell dehydration caused the films to bend, however when exposed to high humidity, the films flattened instantly. They have created wearable devices for high-intensity workers, such as sports and soldiers, to fit their needs in order to prevent frostbite or to work at high temperature, which is an appealing application field. Sportswear with variable breathing can be created, which can be used to modify the level of comfort by altering the fabric's temperature to modify the shape (Fig. 20C), and further control the area of exposed skin, thereby modulating the level of comfort of the human body under different environments. This intelligent

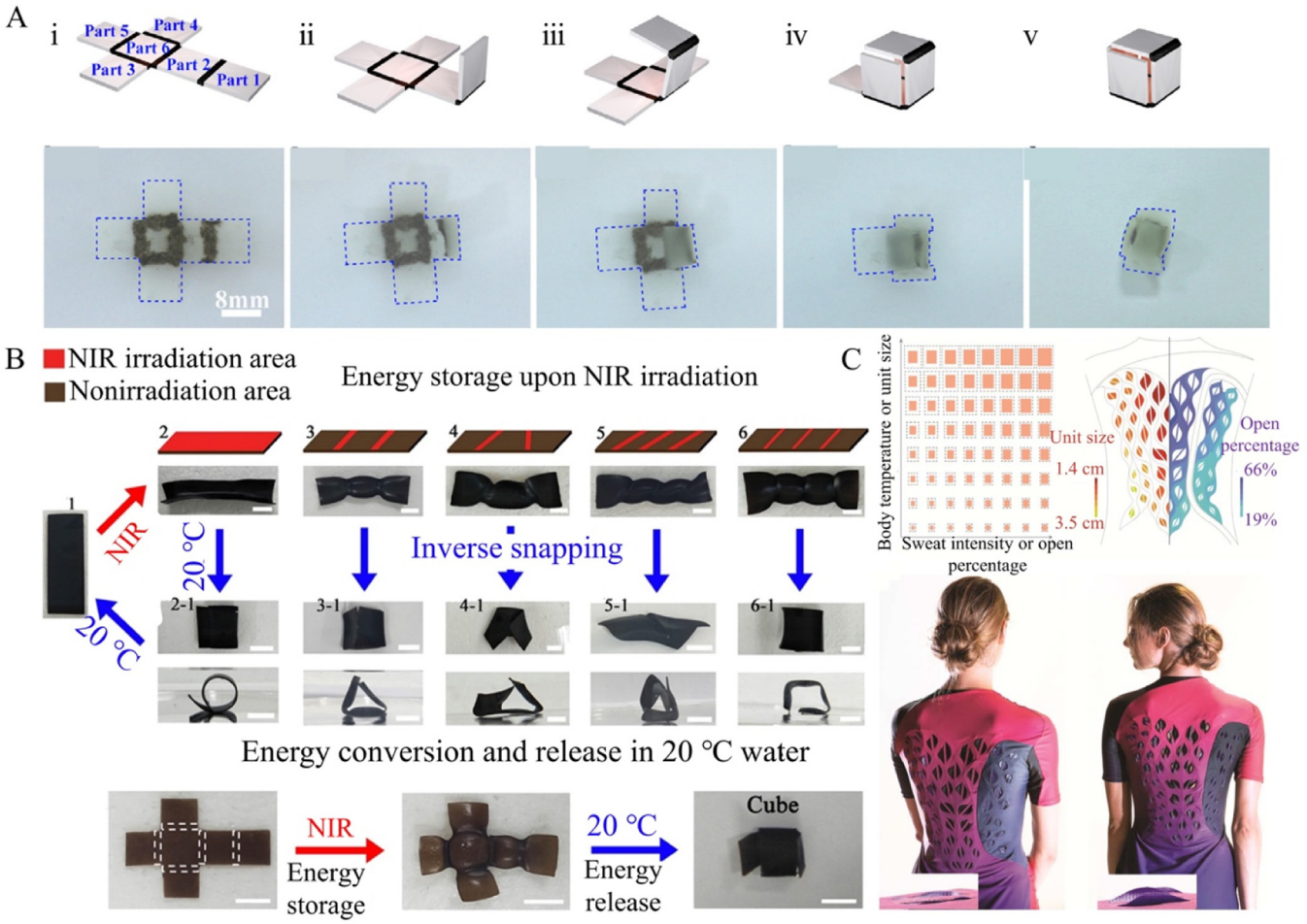



**Fig. 20.** Hydrogel actuators acting as Origami devices and wearables functionality. (A) The mechanism and performance of hydrogel actuator acting as Origami devices. [239], Copyright 2018. Reproduced with permission from Elsevier Science Ltd. (B) Schematics and photos of the dual-gradient composite hydrogel serving as complex shaped Origami devices. Scale bars, 1 cm. [242], Copyright 2019. Reproduced with permission from American Association for the Advancement of Science. (C) Schematics and images of sweat responsive ventilation flaps actuators used on garment prototype. [243], Copyright 2017. Reproduced with permission from American Association for the Advancement of Science.

clothing can improve air convection with large area ventilation for quick dehumidification when the body is hot and perspiring. The high opening rate ensures a dynamic fabric response with breathability that can subtly reflect and respond to the physical state and enhance the control of the substrate's core temperature. After five minutes, when test subjects started to feel damp, the flap of the fabric opened, effectively removing perspiration from the body and lowering the temperature between the body and the fabric. Similarly, Rivera et al. [244] developed a hydrogel-textile bilayer actuator for usage as a weather-triggered adaptive comfort fabric garment for autonomously altering functions in complex situations, leaving the body in a comfortable state.

### *13.2. Fluid controlling*

#### *13.2.1. Smart valves*

Hydrogel actuators make ideal options for valves in fluidic devices due to their habit of changing shape in response to stimuli. Direct insertion of hydrogel blocks as controls for smart valves is the easiest application. As shown in Fig. 21A, Yu and colleagues' [245] proposed a bionic hydrogel valve. This hydrogel control valve allows for exact control of fluid pH, flow direction, and fluid condition (flow or static state) and may be used to start, halt, and regulate fluid flow in microfluidic channels. In order to control fluid flow, they used photopolymerization to create pH-sensitive hydrogel blocks that swell at high pH, contract at low pH, and undergo volume displacement at pH around 5. Back pressure causes the valve to close, preventing backflow, while forward pressure causes the valve blades to open, permitting fluid to pass. As a result, the valve has the ability to function under particular circumstances and can be utilized as a one-way balancing valve. This function is similar to that of a check valve in a mammalian vein. This offers a fresh concept for a brand-new hydrogel control valve.

In order to achieve a more complex valve control system, Wei et al. [246] presented a bilayer structure comprising "curtain-like" and "petal-like" hydrogel discs that may be separated into several stripes and reveal "openings" under NIR light. Fig. 21B illustrates the closed and open states of the hydrogel valve with and without NIR irradiation. This bilayer hydrogel disk is fixed in the channel and then locally distorted under irradiation. The NIR light stimulation causes the PNIPAM layer to contract, opening the channel, which leads the four segments to bend and deform one after the other. A folded open portion can be regulated to have two (1.75 W), three (2.50 W), or four (2.76 W) light sources by modifying the light's intensity and irradiation area, allowing different energies to be chosen to initiate the hydrogel's deformation and channel-opening states. For a single arm and a multi-arm deformation, respectively, the horizontal-to-vertical bending deformation takes around 90 and 30 seconds to complete. In a similar manner, the "petal" hydrogel actuator can be opened and closed by

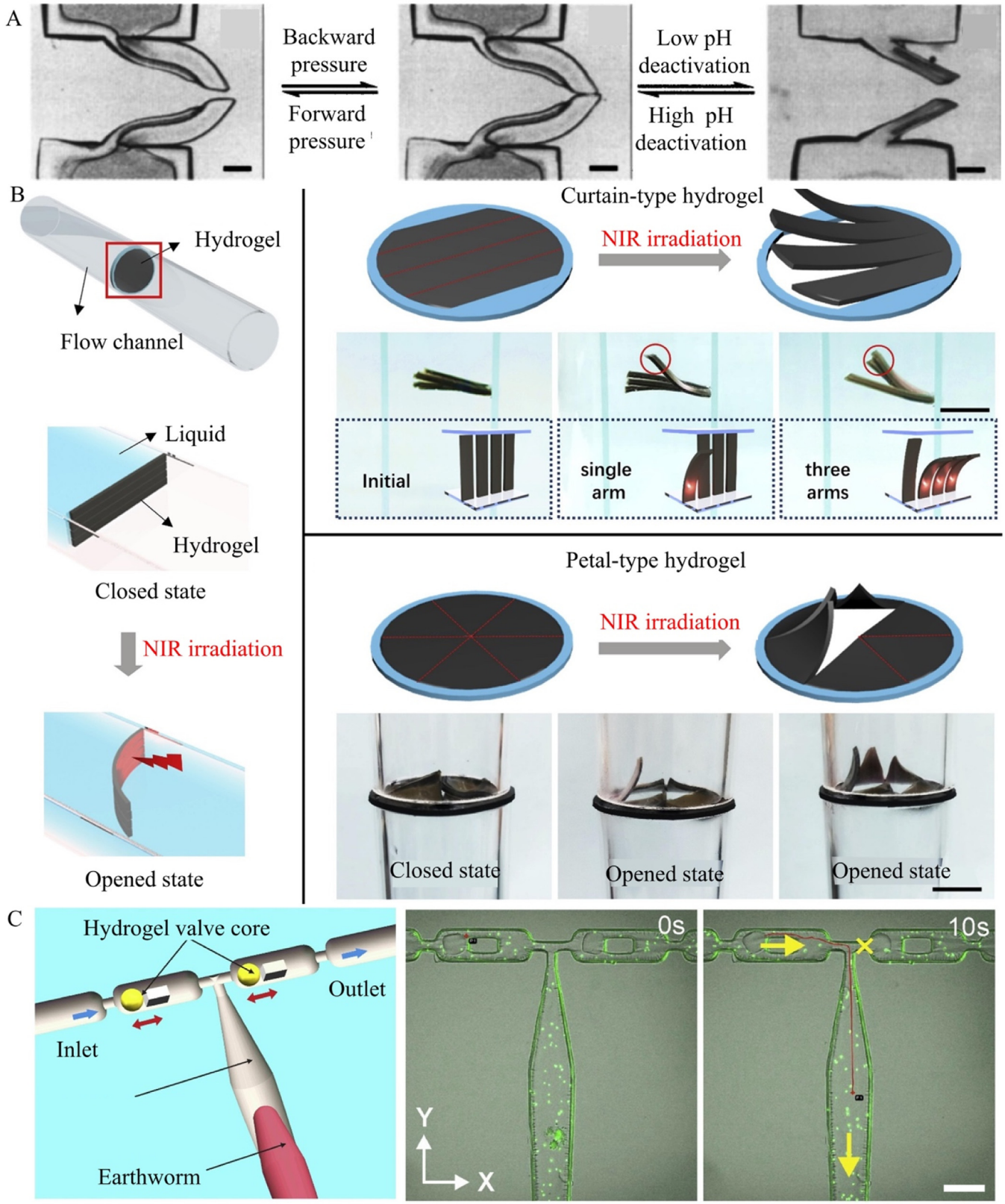



**Fig. 21.** Hydrogel actuators acting as valves functionality. (A) Images of the responsive biomimetic hydrogel used for valves. Scale bars, 500 μm. [245], Copyright 2001. Reproduced with permission from the American Institute of Physics. (B) Schematics and photos of the self-healing graphene oxide-based hydrogel serving as light-driven valves. Scale bars, 1 cm. [246], Copyright 2019. Reproduced with permission from Elsevier Science Ltd. (C) Schematics and photos of the photo-patterned hydrogel using as a simple micro check valve. Scale bars, 200 μm. [247], Copyright 2020. Reproduced with permission from Elsevier Science Ltd.

light irradiation. To do this, the hydrogel disc is divided into six pieces, the initial state is closed, forming a "petal," and the petal is partially deformed by near-infrared light stimulation to open part of the valve. This hydrogel valve can be employed as a controlled response switch, solid/liquid transport, and has good barrier properties. In a subsequent investigation, the channel above the hydrogel was filled with a $MnO_2$ suspension. NIR (2.76 W) illumination was used to open the hydrogel valve and regulate the passage and throttling of $MnO_2$ particles. This ability to regulate particle delivery and valve opening and closing has inspired additional valve-related applications.

Based on the previously mentioned concept of a response valve, Wang et al. [247] created a novel bio-driven micro-pump with hydrogel check valves, as shown in Fig. 21C, which is a T-shaped structure with the drive channel between the two channels, the inlet channel, and the outlet channel. They also created two hydrogel balls to serve as check valves. The pump operates on the same principle as a piston pump. A specially designed microchannel traps a hydrogel piston inside of it, allowing it to move back and forth between the two ends of the channel. When the piston moves backward in the channel, fluid enters through the inlet valve and is drawn back by the outlet valve from the return flow at the outlet. The flow process of fluorescently labeled microspheres from the inlet channel to the outlet channel is shown in detail in Fig. 21C (red trajectory), where the check valve quickly reacts to piston motion and generates a directional fluid flow in the channel. The aforementioned range of control and response actuation behaviors based on valves and microfluidic pumps serve as a useful benchmark for related future study.

#### 13.2.2. Microfluidics

Microfluidics is a science that deals with regulating and modifying fluids at incredibly small scales. It is extensively utilized in biomolecular and cellular research, high-throughput screening, diagnostics, and therapies [248,249]. In order to supply unconstrained, miniaturized, low-power, low-cost guided fluids, microfluidic devices typically need tiny smart components. Therefore, the integration of soft and stimulus-responsive hydrogels into microfluidic devices is an excellent idea [250].

The idea of fluids in microfluidic devices being driven by responsive hydrogels is intriguing. However, the device's progress over the past 20 years has been hampered by constraints in the device's capacity to attain adequate spatial resolution, speed, dependability, and integration. D'Eramo et al. [251] developed and patterned PNIPAM hydrogel films on planar substrates successfully using this as their foundation. They demonstrated devices with up to 7,800 actuated microcages that sequester and released solutes, and individual drives using this technology for the first time, with off and on switching periods for each channel being 0.6±0.1, 0.25±0.15 s, respectively. The microfluidic valve is made in the manner depicted in Fig. 22A. By including a rectangular gel sheet perpendicular to the length of the microchannel, the hydrogel sheet, which is longer than the channel width, functions as a sealing valve. The channel is closed, preventing leakage, by giving a low-power stimulus to the material on the base plate. The valve's open and closed states as well as the matching morphology are depicted in fluorescent microscopy pictures in Fig. 22A. The hydrogel valve opens at a system temperature over LCST at 40°C, and it closes when the temperature decreases to 25°C as the hydrogel film expands. The technology can be applied to single cell therapy and nucleic acid amplification assays in the genetic field.

Furthermore, Takeuchi et al. [252] described a programmable material in the form of a microfiber for a microfluidic device. In addition to these fluidic microchannels, this device also has a pneumatic valve with a membrane that regulates the switching state by applying pneumatic pressure through the other two microchannels. These microchannels are for the pre-gel solution and the crosslinker. A computer-controlled coding sequence can be used to design the switching of the valves on the microfibers. Fig. 22B displays the image of valve-controlled microfluidic device. The programming control is due to pressure-based air valve opening and closing. First, device is filled with the two different types of pre-gel solutions. Several pre-gel solutions are used to divert the convergence point following the pattern of the micro-channel. Finally, these tributaries will be joined at the second merger point of the cross-linked agent $CaCl_2$ solution. Hydrogel microfibres with an axial pattern were finally achieved. This offers the possibility to realize complex hydrogel actuator-controlled reactors and precise control of fluids.

### 13.3. Medical engineering

#### 13.3.1. Navigation locators

Researchers have created a wide variety of hydrogel navigation locators for use in tissue engineering since biocompatible hydrogel materials are widely used in the field. For example, Wang et al. [253] described a hydrogel actuator with a sensitive response that is made of magnetic nanoparticles and a PNIPAM network. And Fig. 23A illustrates a schematic of the magnetic hydrogel actuation. It uses magnetic field to drive its motion when it is enclosed in a device, and it can exhibit complex deformation behavior in response to changes in the environment's temperature, opening up a wider range of applications. The application of direct and alternating magnetic fields allowed the hydrogel actuator to perform navigation and shape deformation. A magnet is utilized to direct the actuator from the tube to the opposite end, which is encircled by a coil, of a star actuator that is positioned inside a water-filled, curved glass tube. An alternating magnetic field is applied once it reaches the coil's center, and it doesn't take long for the actuator to bend and deform upward and release the object. This provides some ideas for the application of hydrogel actuators in line navigation and motion delivery.

In industrial applications, confined space operations—typically closed spaces with limited access—are prevalent. However, the constrained space presents a significant problem for soft robot motion. In order to address this issue, Cheng et al. [167] described adding trivalent iron ions ($Fe^{3+}$) to polymers as a dynamic backbone for carboxyl cross-linking to produce transparent and soft polymers, adding neodymium magnets (NdFeB) to the pre-gel to create a homogeneous dispersion, and finally creating hydrogel actuators with excellent responsiveness through additional polymerization. The navigational components can be disassembled in order to address the size limitation issue. To effectively access the enclosed space, the bulk actuator can be divided into several parts, all of which have non-contact magnetic controllable properties, as shown in Fig. 23B. Narrow passages are provided within the enclosed space, along with a trench to prevent the hydrogel soft robot from transporting the cargo through the passages to its destination. The soft robot is first magnetized and then cut into rod-shaped pieces. The magnetic field is then used to control each piece into the "S" tube channels. Based on the magnetic assembly and rapid self-healing properties, numerous pieces are assembled and welded into a multi-legged robot, and this multi-legged robot can deliver the goods to the destination. This actuator successfully overcomes the limitations imposed by the size of the channel by displaying intricate assembly and task delivery capabilities, the combination of actuation and self-healing can go beyond repair of the actuator to enable the in-situ assembly of devices. This inspired us that we could look beyond this to start thinking about using a Lego-approach to build different classes of complex actuators from a set of simple parts.

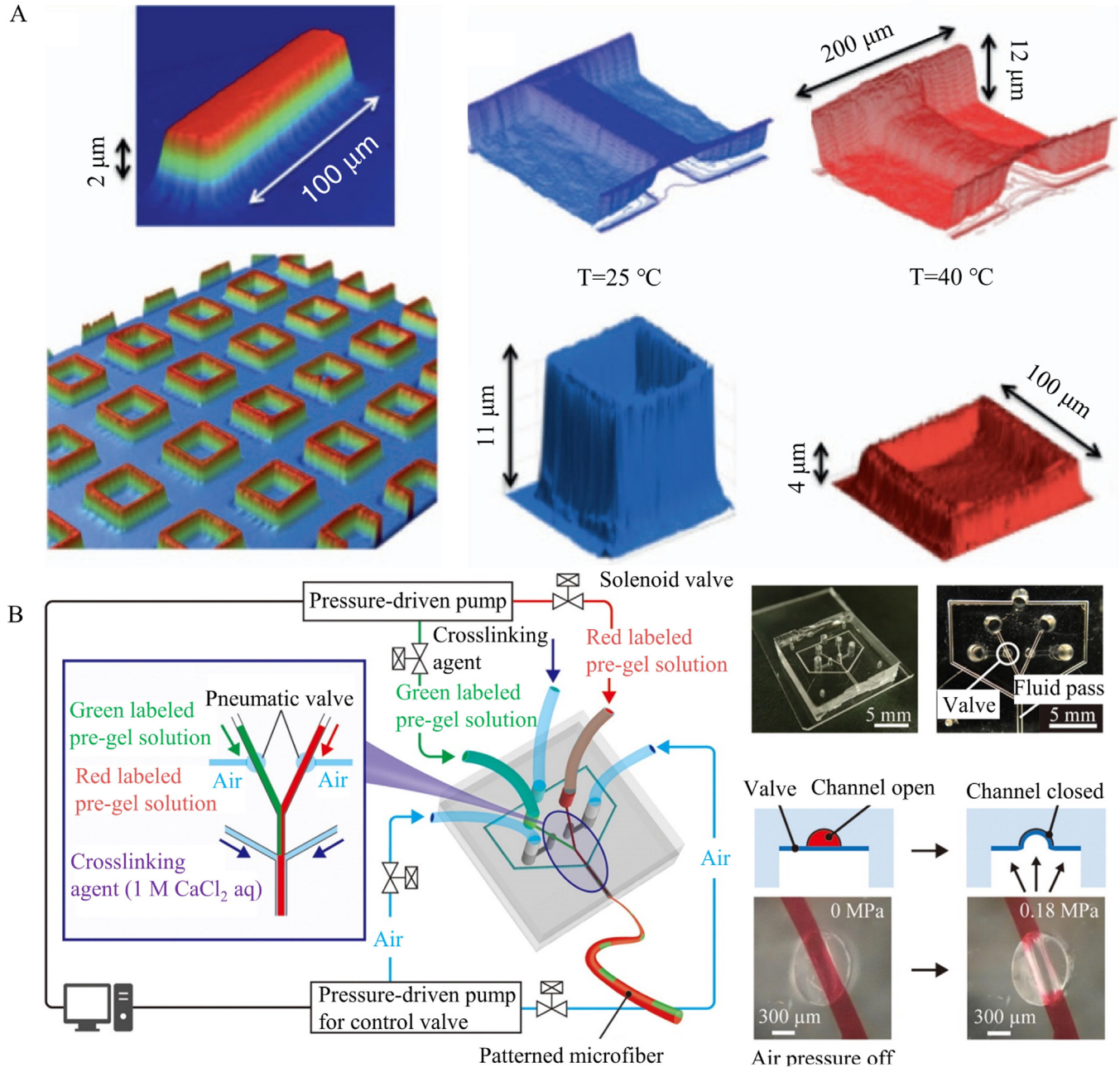



**Fig. 22.** Hydrogel actuators acting as microfluidics functionality. (A) The mechanism of the temperature-responsive hydrogels used as microfluidic actuators. [251], Copyright 2018. Reproduced with permission from the Nature Publishing Group. (B) Schematics and photos of the programmable stimuli-responsive hydrogel microfiber acting as a valve-controlled microfluidic system. [252], Copyright 2020. Reproduced with permission from the Mary Ann Liebert, Inc., publishers.

*13.3.2. Foreign body removal & drug delivery*

Injury-free foreign body removal has always been a challenge in medical treatment, but the advent of hydrogel actuators has made this operation possible. For example, Tang et al. [241] developed a reinforced polyacrylamide (PAAM) hydrogel based on neodymium iron boron (NdFeB) magnetic particles that can be utilized as a 3D printing ink to produce complex shapes. This hydrogel actuator may use a template-assisted magnetization technique to program the magnetic domain of a microrobot, and the programmable microrobot exhibits finely controlled deformation in response to an external magnetic field. The authors next show how a six-armed hydrogel robot might be used in foreign body removal research from organs. They do this in four steps: positioning the robot, moving it using magnetic navigation, grabbing and carrying the object, and releasing it (Fig. 24A). The soft-bodied robot was controlled by a handheld endoscope, which was also utilized to take inside pictures and serve as the foreign body. Prior to the experiment, a live/dead test using mouse embryonic fibroblasts revealed that the magnetic hydrogel had a low degree of surface toxicity and could be employed. After 24 hours of incubation, the relative cell survival rate was 90%. An external magnetic field is used to direct the micro-robot downward and toward the interior of the organ after it has been inserted into the organ's entrance. When the hydrogel robot reaches the predetermined position, it is distorted and catches the foreign object by managing the temperature. The foreign object is then moved to the predetermined position, all of which takes about 10 seconds. Repeating this procedure allows the hydrogel robot to traverse easily through the folded channels while

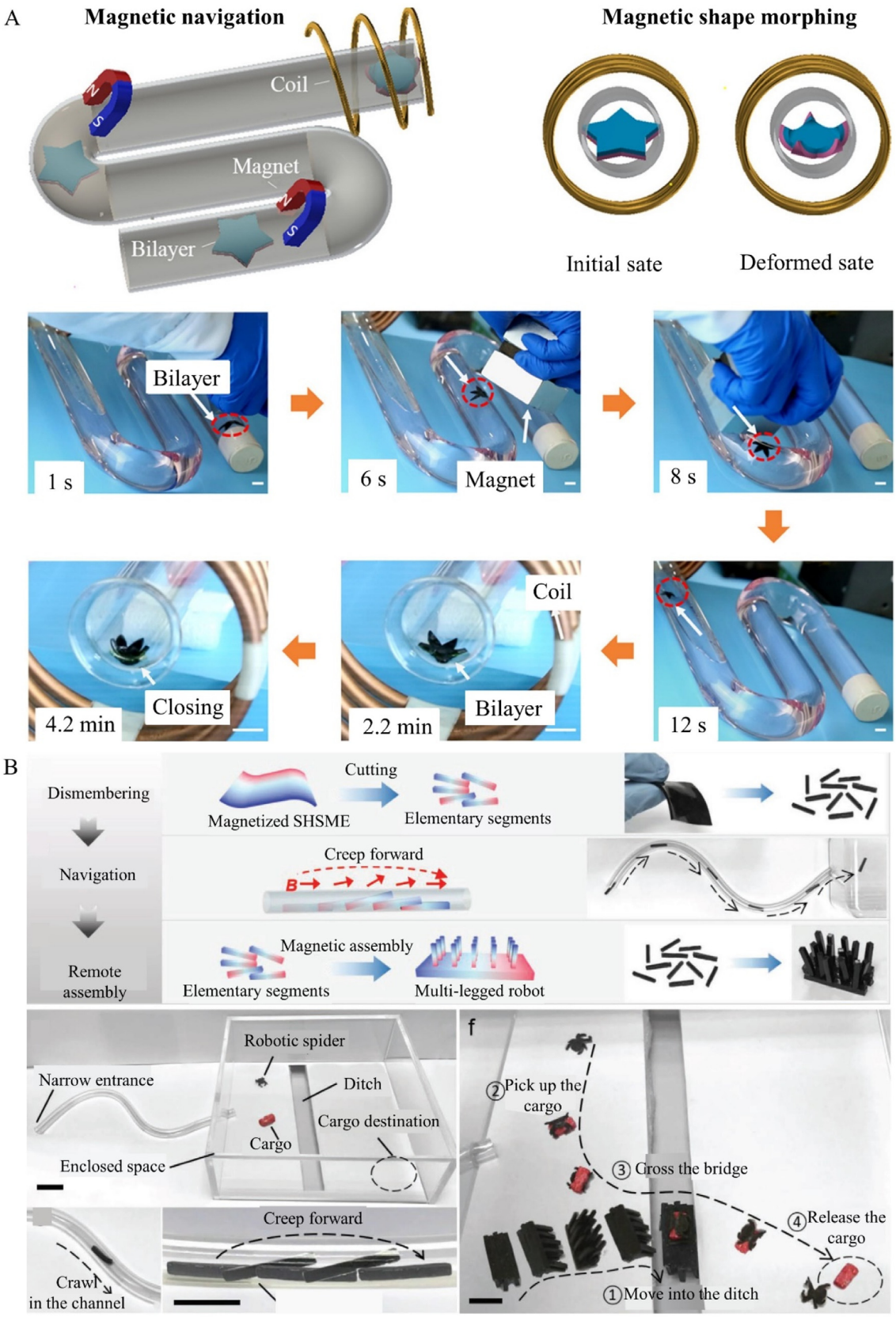



**Fig. 23.** Hydrogel actuators acting as navigation locators' functionality. (A) The mechanism and performance of the magnetothermal sensitive hydrogel for magnetic navigation of a starlike bilayer and its shape morphing. All scale bars are 10 mm. [253], Copyright 2019. Reproduced with permission from the American Chemical Society. (B) Schemes and photographs of the autonomous healing magnetic actuator used as a dismembering–navigation–assembly strategy. Scale bars, 10 mm. [167], Copyright 2021. Reproduced with permission from John Wiley & Sons Inc.

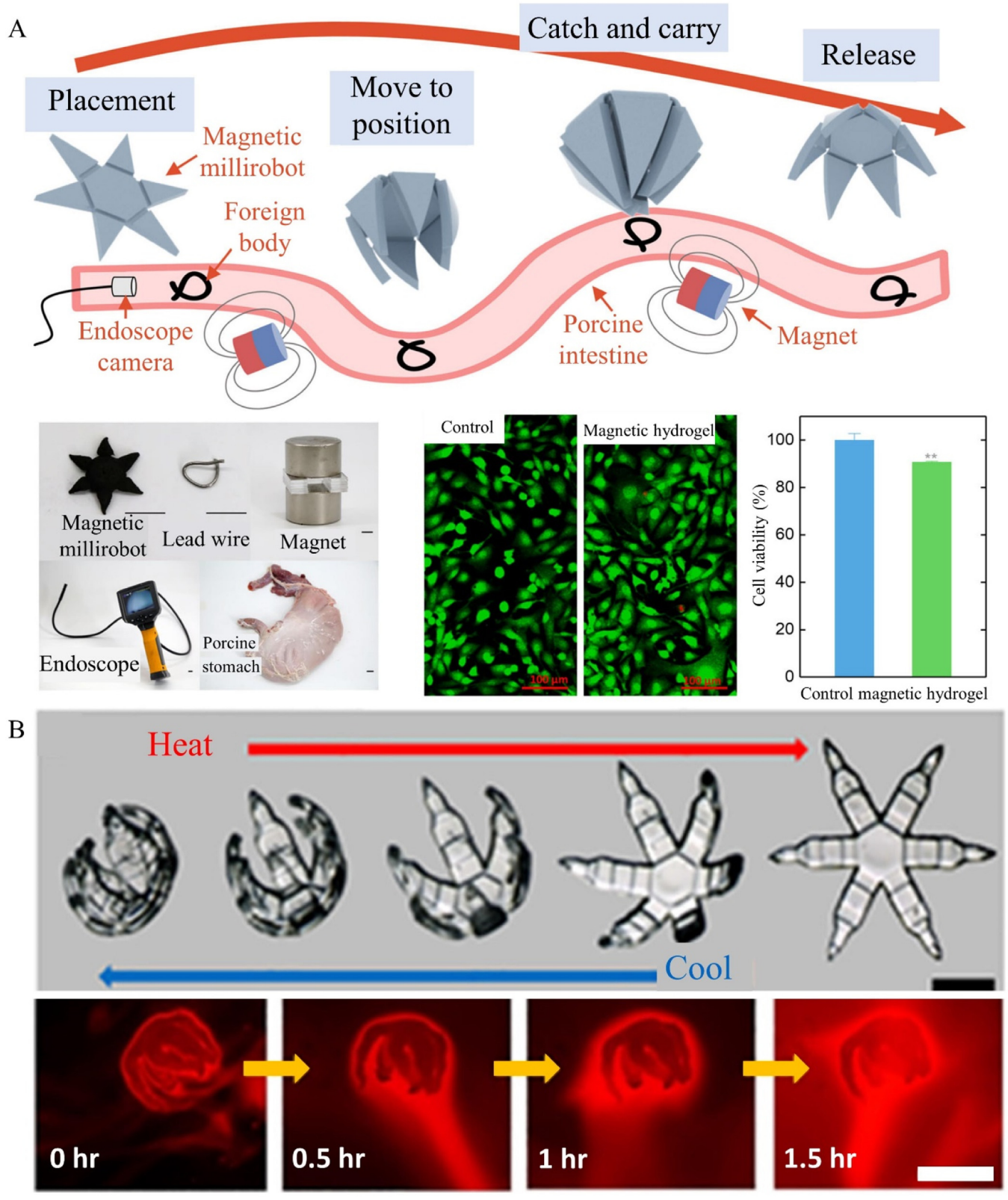



**Fig. 24.** Hydrogel actuators acting as drug delivery functionality. (A) Schematics and images of the 3D-printed magnetic six-armed millirobot used for foreign body removal. [241], Copyright 2021. Reproduced with permission from John Wiley & Sons Inc. (B) Schemes and photographs of the thermo-magnetically responsive hydrogel gripper used for drug delivery. Scale bars, 2 mm. [254], Copyright 2019. Reproduced with permission from the American Chemical Society.

also fully exhibiting its ability to remove foreign objects from inside an organ that is filled with water. Although magnetic hydrogel robots have shown practical applications in different organs, stability remains to be further investigated. In addition, a functional coating can be put to NdFeB particles to reduce their toxicity, and combining more functionalized biocompatible hydrogels with improved 3D printing holds promise for the creation of more complex robots.

Usually, drug delivery requires an accurate control of the timing and volume of drug release, which is a capability that is missing from traditional responsive hydrogels. Due to their delicate responsiveness to the environment, hydrogel actuators could also be used as drug transporters. Kobayashi et al. [254] prepared thermally responsive optically crosslinked highly soluble poly(oligoethylene glycol methyl ether methacrylate-bis(2methacryloyl)oxyethyl disulfide) P(OEGMA-DSDMA) gel layers and poly(acrylamideN,N′-bis(acyloyl)cystamine) P(AAM-BAC) gel layer doped with $Fe_2O_3$ nanoparticles, where the P(OEGMA-DSDMA) gel layer has LCST response performance adjustable from 20 to 90°C. A gripper that may be utilized for drug distribution in addition to picking and placing duties was then created in the form of a star using hydrogel (Fig. 24B). This gripper first is folded closed, then it opens progressively when heated, and refolds closed when the temperature drops. The multi-finger actuator, like the gripper that was previously discussed, may grasp the drug and enable slow release of medication in vivo. It can also be loaded for thermally powered drug patch applications. These above hydrogel actuators offer new solutions for applications such as drug delivery and foreign body removal in complex pipelines or in vivo, but there will be some issues that need to be addressed by future researchers due to the limitations in material selection.

*13.3.3. Cell manipulation*

Recently, various studies on the using of hydrogel actuators for particulate control and cell capture have been published [165,255]. The actuators can be utilized to catch particles and cells, as demonstrated by Zhang et al., [177] who created a pH stimulus-responsive actuator made of flexible hydrogel microtubules. Fig. 25A depicts this gel actuator, which consists of four hydrogel microtubules that can be continuously switched between straight (open state) and bent (closed state) in order to perform the function of capturing and releasing the target object. Each hydrogel microtubule has a diameter of 10 m and a height of 60 m, and these parameters can be changed depending on the size of the controlled particles. To show off the actuator's ability to capture particles, a solution of PS (polystyrene) microspheres (13 m in diameter) was dropped into an open microstructure. Next, a diluted acid solution (pH = 7), which excited the microtubules to deform and prevent the particles from being washed away, was added. Finally, a diluted alkaline solution (pH > 9) was added, which caused the clamps to open and release the particles. More crucially, the apparatus has the ability to isolate individual cells. As shown in Fig. 25A, the actuator is in its swelling state (open) initially which is used to protect the cells from destroyed by external force. Then the diluted hydrochloric acid (pH = 7) was added to the solution before the cells sink into the trap, which could help to drive the actuator to close and capture the cells. The following day, the live/dead cells are measured to determine the collected cell status. According to the final data, which revealed that 75% of the cells survived, this pH-triggered capture experiment can successfully catch cells. Thus, this miniature hydrogel actuator offers a new approach to cell and particle manipulation, but it also has the drawback of requiring a wide pH modulation range that results in considerable cytotoxicity.

To control biological processes, attention must be paid to the cytotoxicity and degradation of manipulators. Due to this, Du et al. [256] reported a biodegradable shape memory polymer called poly(L-lactide-co-D, L-lactide) (PLLADLLA) shape memory layer and a bilayer gel microarray actuator made of a photothermal layer with gold nanorods (AuNRS). The AuNRS layer was heated using NIR irradiation to produce a phase transition in the PLLADLLA layer, and the upper shape memory layer returned from a curved array morphology to a vertical microscopic state, providing control and influence on cell growth (Fig. 25B). First, on a static platform without NIR illumination, the cytoskeletal organization and cell nucleation from the micro-actuator arrays are unrestricted, and after 10 s of NIR illumination, the nucleation of the cytoskeletal organization exhibits significant changes in alignment, having changed from anisotropic to homogeneous. Thus, it can be inferred that at physiological temperature (37°C), the NIR-controlled morphological transition of the dynamic platform can cause the non-spontaneous geometric retraction of human cells. The aforementioned microarray actuator platform can not only make it easier to build the next-generation devices for cell manipulation, but it can also play a part in the processes of tissue regeneration and wound healing.

## 14. Conclusions and perspectives

In this work, we systematically introduce the latest research on hydrogel actuators based on biomimetic systems. First, natural organisms with external stimulus-actuated behaviors in nature are discussed in detail, including wheat, pinecones, chameleons, mimosas, jellyfish and octopus, etc., with particular focus on internal mechanisms and application prospects. Then, different types of hydrogel actuators controlled by various external stimuli, such as heat, light, magnetism, electricity, pH, etc, are presented. A successful actuator should be resilient and typical approaches to improve the overall mechanical properties of hydrogels are compared using a classification in three different categories: improving the synthesis (creating more uniform polymer networks), the materials design (introduction of energy dissipation mechanisms) or combining the two. Finally, we focused on the application and development of such hydrogel actuators, including crawlers, deformers, Origami devices, valves, microfluidics, navigation positioners, drug release and cell manipulation. Although great progress has been made, there is still great room for improvement. In important area of future work is the promotion of the practical use supported by the fabrication of hydrogel devices for multi-scenario applications. In this respect, we believe future research will move towards endowing the materials with programmable controllable responsiveness, improving material durability, and further systematization of functions, as shown in Fig. 26.

i) Endowing hydrogel actuators with programmable responsiveness

With the increased research interest in multifunctional actuators, more and more research has focused on responsive hydrogels as they can better incorporate different stimulus-response modalities, such as temperature, light, electricity and magnetism. However, the development and application of hydrogel actuators are still hindered by the limitations in the implementation of the various stimuli. In order to ensure the reliability and controllability of stimulation, the actuationand release of hydrogel actuators should adapt to the actual situation. Advancements in computer programming should enable more precise control. The current limitations in our ability to program material properties and control external stimuli hamper the practical application. In response, optimization algorithms and artificial intelligence (AI) can now be applied to materials design and control of the external stimuli. Taking the hydrogel crawler as an example, in order to reach the desired high-precision control of complex movements, it is necessary to design carefully the physical and chemical properties of the material, as

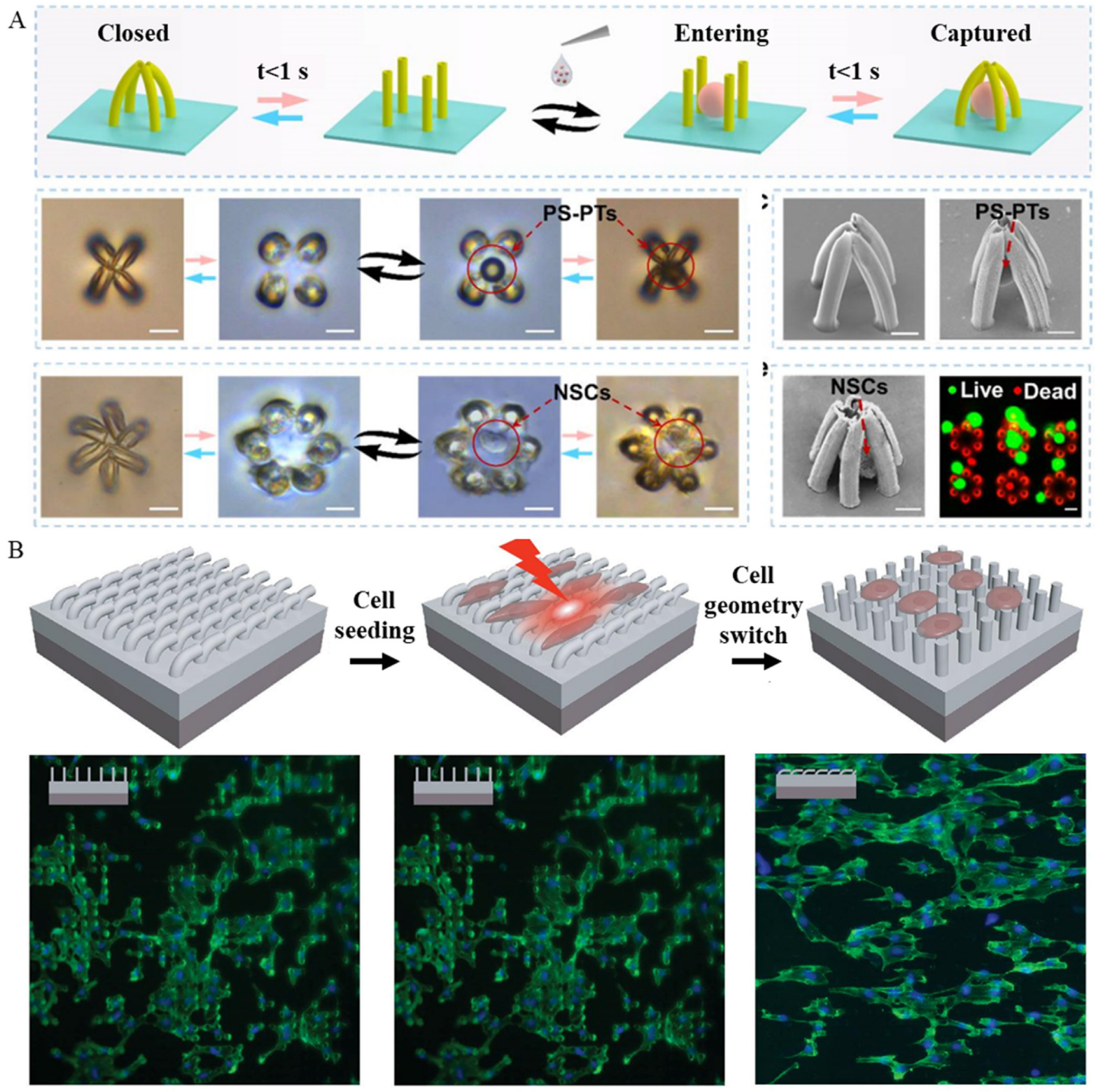



**Fig. 25.** Hydrogel actuators acting as cell manipulation functionality. (A) Schematics and images of the pH responsive hydrogel micro-pillar used to capture cell. Scale bars: 10 μm. [177], Copyright 2020. Reproduced with permission from the American Chemical Society. (B) Schematics and photos of the microstructure NIR triggered hydrogel platform for cell geometry switch. [256], Copyright 2020. Reproduced with permission from the Oxford University Press.

well as to manipulate accurately the external conditions. This may be difficult to achieve without the support of new technologies based on computer control and artificial intelligence.

i) Improving the durability of hydrogel actuators

Although there has been much progress in the improvement of the mechanical properties of hydrogels, few studies have been carried out on their durability, which is a key problem faced in practical applications. First, hydrogels are generally dehydrated in open systems due to the evaporation of internal moisture, resulting in the degradation of a variety of properties, including flexibility, transparency, conductivity, responsiveness, etc. Although there are practical examples of how to address this issue, the situation is not ideal. Second, the swelling problem under some solutions has been plaguing many researchers for years, and there is still room for improvement. Finally, the ability to cope with extreme conditions is another important issue, as hydrogel actuators needs to be used in practical scenarios which may be characterized by various extreme temperature/pressure conditions. Thus, the capability of hydrogel actuators to operate under these conditions would further widen the range of applications.

i) Further systematization

From the system point of view, the future trend is to allow hydrogel actuators to sense, respond, and complete programmed tasks autonomously, thereby making the system more intelligent.

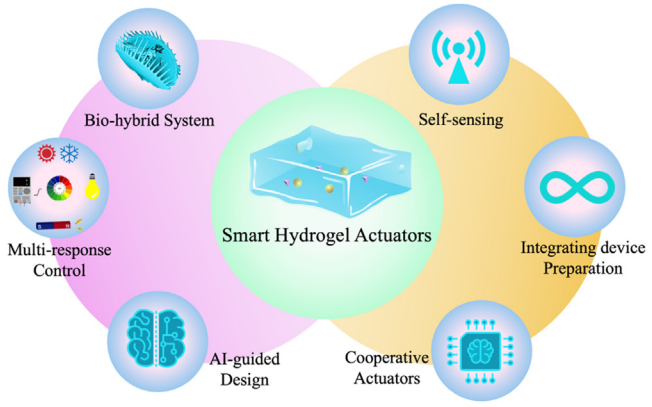



**Fig. 26.** Future directions to prepare intelligent and autonomous hydrogel actuators. [150], Copyright 2019. Adapted with permission from the Nature Publishing Group.

However, most of the current actuators are still in an open-loop control stage, which does not fit this requirement. Machine learning could help to achieve this goal, since autonomous control in different fields from self-driving vehicles to smart buildings has already been realized with its help. Therefore, the development of control systems with learning ability integrated into smart hydrogel machines is a promising research direction. It will require to map the general nonlinearity sensing signal into the actuation commands that control the hydrogel in the system. As a result, the sensor could get feedback from a closed-loop operation system and autonomously adjust its behavior.

In summary, the overall performance of functional devices depends on the synergy between different components. It is necessary to develop a comprehensive approach combining all the aspects involved in the design of new smart hydrogel actuators. It is foreseeable that the integration of technical applications with chemical design, artificial intelligence and machine learning will be particularly attractive. In the end, the development of smart hydrogel actuators is a long-term interdisciplinary research work that requires collaboration of researchers from different fields from chemistry to materials, electrical engineering or computer science.

## 15. Author contributions

Dr. Weijun Li and Dr. Qingwen Guan designed and composed the content of article, they contribute equally to this work. Dr. Ming Li conceived and guided the project. Prof. Eduardo Saiz and Prof. Xu Hou revised the content of article and provided useful suggestions. All authors discussed the contents and commented on the manuscript.

## Declaration of Competing Interest

The authors declare that they have no known competing financial interests or personal relationships that could have appeared to influence the work reported in this paper.

## Data availability

Data will be made available on request.

## Acknowledgments

This work was supported by the National Natural Science Foundation of China (grant nos. 52025132, 21975209, 21621091, 22021001 and 22121001), the National Key R&D Programme of China (grant no. 2018YFA0209500), the National Science Foundation of Fujian Province (2022J02059), the Fundamental Research Funds for the Central Universities in China (20720220085), the 111 Project (grant nos. B17027 and B16029), the Science and Technology Projects of Innovation Laboratory for Sciences and Technologies of Energy Materials of Fujian Province (grant no. RD2022070601), the Xplorer Prize (2022) and the EPSRC Program Manufacture Using Advanced Powder Processes (MAPP)EP/P006566. Qingwen Guan appreciates the support from the China Scholarship Council (grant no. 202006440011). Ming Li acknowledges financial assistance from Imperial College London in the form of "President Scholarship" (01790264).

## References

[1] Lee H, Um DS, Lee Y, Lim S, Hj Kim, Ko H. Octopus-inspired smart adhesive pads for transfer printing of semiconducting nanomembranes. Adv Mater 2016;28:7457–65.
[2] Spinks GM. Advanced actuator materials powered by biomimetic helical fiber topologies. Adv Mater 2020;32:1904093.
[3] Zhu QL, Du C, Dai Y, Daab M, Matejdes M, Breu J, et al. Light-steered locomotion of muscle-like hydrogel by self-coordinated shape change and friction modulation. Nat Commun 2020;11:1–11.
[4] Ren Z, Hu W, Dong X, Sitti M. Multi-functional soft-bodied jellyfish-like swimming. Nat Commun 2019;10:1–12.
[5] Zong L, Li X, Han X, Lv L, Li M, You J, et al. Activation of actuating hydrogels with WS2 nanosheets for biomimetic cellular structures and steerable prompt deformation. ACS Appl Mater Interfaces 2017;9:32280–9.
[6] Holmes DP, Crosby AJ. Snapping surfaces. Adv Mater 2007;19:3589–93.
[7] Ionov L. Biomimetic hydrogel-based actuating systems. Adv Funct Mater 2013;23:4555–70.
[8] Ma Y, Ma S, Yang W, Yu B, Pei X, Zhou F, et al. Sundew-inspired simultaneous actuation and adhesion/friction control for reversibly capturing objects underwater. Adv Mater Technol 2019;4:1800467.
[9] Le X, Lu W, Zhang J, Chen T. Recent progress in biomimetic anisotropic hydrogel actuators. Adv Sci 2019;6:1801584.
[10] Wong WS, Li M, Nisbet DR, Craig VS, Wang Z, Tricoli A. Mimosa Origami: A nanostructure-enabled directional self-organization regime of materials. Sci Adv 2016;2:e1600417.
[11] Xu Q, Su R, Chen Y, Theruvakkattil Sreenivasan S, Li N, Zheng X, et al. Metal charge transfer doped carbon dots with reversibly switchable, ultra-high quantum yield photoluminescence. ACS Appl Nano Mater 2018;1:1886–93.
[12] Ikejiri S, Takashima Y, Osaki M, Yamaguchi H, Harada A. Solvent-free photoresponsive artificial muscles rapidly driven by molecular machines. J Am Chem Soc 2018;140:17308–15.
[13] Lin H, Ma S, Yu B, Cai M, Zheng Z, Zhou F, et al. Fabrication of asymmetric tubular hydrogels through polymerization-assisted welding for thermal flow actuated artificial muscles. Chem Mater 2019;31:4469–78.
[14] Tian Y, Wei X, Wang ZJ, Pan P, Li F, Ling D, et al. A facile approach to prepare tough and responsive ultrathin physical hydrogel films as artificial muscles. ACS Appl Mater Interfaces 2017;9:34349–55.
[15] Guo M, Wu Y, Xue S, Xia Y, Yang X, Dzenis Y, et al. A highly stretchable, ultra-tough, remarkably tolerant, and robust self-healing glycerol-hydrogel for a dual-responsive soft actuator. J Mater Chem A 2019;7:25969–77.
[16] Qin H, Zhang T, Li N, Cong H-P, Yu S-H. Anisotropic and self-healing hydrogels with multi-responsive actuating capability. Nat Commun 2019;10:1–11.
[17] Wei S, Lu W, Le X, Ma C, Lin H, Wu B, et al. Bioinspired synergistic fluorescence-color-switchable polymeric hydrogel actuators. Angew Chem 2019;131:16389–97.
[18] Li C, Li M, Ni Z, Guan Q, Blackman BR, Saiz E. Stimuli-responsive surfaces for switchable wettability and adhesion. J R Soc, Interface 2021;18:20210162.
[19] Cheng Y, Chan KH, Wang X-Q, Ding T, Li T, Lu X, et al. Direct-ink-write 3D printing of hydrogels into biomimetic soft robots. ACS Nano 2019;13:13176–84.
[20] Duan X, Yu J, Zhu Y, Zheng Z, Liao Q, Xiao Y, et al. Large-scale spinning approach to engineering knittable hydrogel fiber for soft robots. ACS Nano 2020;14:14929–38.
[21] Wang X, Jiao N, Tung S, Liu L. Photoresponsive graphene composite bilayer actuator for soft robots. ACS Appl Mater Interfaces 2019;11:30290–9.
[22] Yuk H, Lin S, Ma C, Takaffoli M, Fang NX, Zhao X. Hydraulic hydrogel actuators and robots optically and sonically camouflaged in water. Nat Commun 2017;8:1–12.
[23] Liu J, Pang Y, Zhang S, Cleveland C, Yin X, Booth L, et al. Triggerable tough hydrogels for gastric resident dosage forms. Nat Commun 2017;8:1–10.
[24] Wen J, Jia Z, Zhang X, Pan M, Yuan J, Zhu L. Tough, thermo-Responsive, biodegradable and fast self-healing polyurethane hydrogel based on microdomain-closed dynamic bonds design. Mater Today Commun 2020;25:101569.
[25] Zheng SY, Shen Y, Zhu F, Yin J, Qian J, Fu J, et al. Programmed deformations of 3D-printed tough physical hydrogels with high response speed and large output force. Adv Funct Mater 2018;28:1803366.
[26] Chen G, Huang J, Gu J, Peng S, Xiang X, Chen K, et al. Highly tough supramolecular double network hydrogel electrolytes for an artificial flexible and low-temperature tolerant sensor. J Mater Chem A 2020;8:6776–84.

[27] Liang Y, Ye L, Sun X, Lv Q, Liang H. Tough and stretchable dual ionically cross-linked hydrogel with high conductivity and fast recovery property for high-performance flexible sensors. ACS Appl Mater Interfaces 2019;12:1577–87.
[28] Wang C, Zhang P, Xiao W, Zhao J, Shi M, Wei H, et al. Visible-light-assisted multimechanism design for one-step engineering tough hydrogels in seconds. Nat Commun 2020;11:1–9.
[29] Rao P, Sun TL, Chen L, Takahashi R, Shinohara G, Guo H, et al. Tough hydrogels with fast, strong, and reversible underwater adhesion based on a multiscale design. Adv Mater 2018;30:1801884.
[30] Xu L, Wang C, Cui Y, Li A, Qiao Y, Qiu D. Conjoined-network rendered stiff and tough hydrogels from biogenic molecules. Sci Adv 2019;5:eaau3442.
[31] Zhang HJ, Sun TL, Zhang AK, Ikura Y, Nakajima T, Nonoyama T, et al. Tough physical double-network hydrogels based on amphiphilic triblock copolymers. Adv Mater 2016;28:4884–90.
[32] Li M, Li W, Cai W, Zhang X, Wang Z, Street J, et al. A self-healing hydrogel with pressure sensitive photoluminescence for remote force measurement and healing assessment. Mater Horiz 2019;6:703–10.
[33] Long T, Li Y, Fang X, Sun J. Salt-Mediated Polyampholyte Hydrogels with High Mechanical Strength, Excellent Self-Healing Property, and Satisfactory Electrical Conductivity. Adv Funct Mater 2018;28:1804416.
[34] Pan C, Liu L, Chen Q, Zhang Q, Guo G. Tough, stretchable, compressive novel polymer/graphene oxide nanocomposite hydrogels with excellent self-healing performance. ACS Appl Mater Interfaces 2017;9:38052–61.
[35] Yang Y, Wang X, Yang F, Shen H, Wu D. A universal soaking strategy to convert composite hydrogels into extremely tough and rapidly recoverable double-network hydrogels. Adv Mater 2016;28:7178–84.
[36] Lai J-C, Jia X-Y, Wang D-P, Deng Y-B, Zheng P, Li C-H, et al. Thermodynamically stable whilst kinetically labile coordination bonds lead to strong and tough self-healing polymers. Nat Commun 2019;10:1–9.
[37] Sun W, Xue B, Fan Q, Tao R, Wang C, Wang X, et al. Molecular engineering of metal coordination interactions for strong, tough, and fast-recovery hydrogels. Sci Adv 2020;6:eaaz9531.
[38] Chen H, Liu Y, Ren B, Zhang Y, Ma J, Xu L, et al. Super bulk and interfacial toughness of physically crosslinked double-network hydrogels. Adv Funct Mater 2017;27:1703086.
[39] Kakuta T, Takashima Y, Nakahata M, Otsubo M, Yamaguchi H, Harada A. Preorganized hydrogel: self-healing properties of supramolecular hydrogels formed by polymerization of host-guest-monomers that contain cyclodextrins and hydrophobic guest groups. Adv Mater 2013;25:2849–53.
[40] Wang L, Cheng L, Li G, Liu K, Zhang Z, Li P, et al. A self-cross-linking supramolecular polymer network enabled by crown-ether-based molecular recognition. J Am Chem Soc 2020;142:2051–8.
[41] Haque MA, Kurokawa T, Kamita G, Gong JP. Lamellar bilayers as reversible sacrificial bonds to toughen hydrogel: hysteresis, self-recovery, fatigue resistance, and crack blunting. Macromolecules 2011;44:8916–24.
[42] Tuncaboylu DC, Sari M, Oppermann W, Okay O. Tough and self-healing hydrogels formed via hydrophobic interactions. Macromolecules 2011;44:4997–5005.
[43] Sun J-Y, Zhao X, Illeperuma WR, Chaudhuri O, Oh KH, Mooney DJ, et al. Highly stretchable and tough hydrogels. Nature 2012;489:133–6.
[44] Ducrot E, Chen Y, Bulters M, Sijbesma RP, Creton C. Toughening elastomers with sacrificial bonds and watching them break. Science 2014;344:186–9.
[45] Nakajima T. Generalization of the sacrificial bond principle for gel and elastomer toughening. Polym J 2017;49:477–85.
[46] Tong X, Du L, Xu Q. Tough, adhesive and self-healing conductive 3D network hydrogel of physically linked functionalized-boron nitride/clay/poly (N-isopropylacrylamide). J Mater Chem A 2018;6:3091–9.
[47] Wang L, Zhang X, Xia Y, Zhao X, Xue Z, Sui K, et al. Cooking-inspired versatile design of an ultrastrong and tough polysaccharide hydrogel through programmed supramolecular interactions. Adv Mater 2019;31:1902381.
[48] Li M, Li W, Guan Q, Dai X, Lv J, Xia Z, et al. A tough reversible biomimetic transparent adhesive tape with pressure-sensitive and wet-cleaning properties. ACS Nano 2021;15:19194–201.
[49] Chen Q, Zhu L, Chen H, Yan H, Huang L, Yang J, et al. A novel design strategy for fully physically linked double network hydrogels with tough, fatigue resistant, and self-healing properties. Adv Funct Mater 2015;25:1598–607.
[50] Rodell CB, Dusaj NN, Highley CB, Burdick JA. Injectable and cytocompatible tough double-network hydrogels through tandem supramolecular and covalent crosslinking. Adv Mater 2016;28:8419–24.
[51] Bin Imran A, Esaki K, Gotoh H, Seki T, Ito K, Sakai Y, et al. Extremely stretchable thermosensitive hydrogels by introducing slide-ring polyrotaxane cross-linkers and ionic groups into the polymer network. Nat Commun 2014;5:1–8.
[52] Zhang YS, Khademhosseini A. Advances in engineering hydrogels. Science 2017;356:eaaf3627.
[53] Chen Z, Zhao D, Liu B, Nian G, Li X, Yin J, et al. 3D printing of multifunctional hydrogels. Adv Funct Mater 2019;29:1900971.
[54] Deng Z, Hu T, Lei Q, He J, Ma PX, Guo B. Stimuli-responsive conductive nanocomposite hydrogels with high stretchability, self-healing, adhesiveness, and 3D printability for human motion sensing. ACS Appl Mater Interfaces 2019;11:6796–808.
[55] Merino S, Martín C, Kostarelos K, Prato M, Vázquez E. Nanocomposite hydrogels: 3D polymer–nanoparticle synergies for on-demand drug delivery. ACS Nano 2015;9:4686–97.
[56] Zhao Z, Fang R, Rong Q, Liu M. Bioinspired nanocomposite hydrogels with highly ordered structures. Adv Mater 2017;29:1703045.
[57] Elkhoury K, Russell CS, Sanchez-Gonzalez L, Mostafavi A, Williams TJ, Kahn C, et al. Soft-Nanoparticle functionalization of natural hydrogels for tissue engineering applications. Adv Healthc Mater 2019;8:1900506.
[58] Shi K, Xue B, Jia Y, Yuan L, Han R, Yang F, et al. Sustained co-delivery of gemcitabine and cis-platinum via biodegradable thermo-sensitive hydrogel for synergistic combination therapy of pancreatic cancer. Nano Res 2019;12:1389–99.
[59] Huang W, Tarakanova A, Dinjaski N, Wang Q, Xia X, Chen Y, et al. Design of multistimuli responsive hydrogels using integrated modeling and genetically engineered silk-elastin-like proteins. Adv Funct Mater 2016;26:4113–23.
[60] Keidel R, Ghavami A, Lugo DM, Lotze G, Virtanen O, Beumers P, et al. Time-resolved structural evolution during the collapse of responsive hydrogels: The microgel-to-particle transition. Sci Adv 2018;4:eaao7086.
[61] Wang Y, Yu X, Li Y, Zhang Y, Geng L, Shen F, et al. Hydrogelation landscape engineering and a novel strategy to design radically induced healable and stimuli-responsive hydrogels. ACS Appl Mater Interfaces 2019;11:19605–12.
[62] Lei Z, Wang Q, Wu P. A multifunctional skin-like sensor based on a 3D printed thermo-responsive hydrogel. Mater Horiz 2017;4:694–700.
[63] Matsumoto K, Sakikawa N, Miyata T. Thermo-responsive gels that absorb moisture and ooze water. Nat Commun 2018;9:1–7.
[64] Zhang X, Soh S. Performing logical operations with stimuli-responsive building blocks. Adv Mater 2017;29:1606483.
[65] Ding H, Li B, Liu Z, Liu G, Pu S, Feng Y, et al. Decoupled pH-and thermo-responsive injectable chitosan/PNIPAM hydrogel via thiol-ene click chemistry for potential applications in tissue engineering. Adv Healthc Mater 2020;9:2000454.
[66] Huang J, Jiang X. Injectable and degradable pH-responsive hydrogels via spontaneous amino–yne click reaction. ACS Appl Mater Interfaces 2018;10:361–70.
[67] Kahn JS, Hu Y, Willner I. Stimuli-responsive DNA-based hydrogels: from basic principles to applications. Acc Chem Res 2017;50:680–90.
[68] Yesilyurt V, Webber MJ, Appel EA, Godwin C, Langer R, Anderson DG. Injectable self-healing glucose-responsive hydrogels with pH-regulated mechanical properties. Adv Mater 2016;28:86–91.
[69] Jiang Z, Tan ML, Taheri M, Yan Q, Tsuzuki T, Gardiner MG, et al. Strong, self-healable, and recyclable visible-light-responsive hydrogel actuators. Angew Chem 2020;132:7115–22.
[70] Li L, Scheiger JM, Levkin PA. Design and applications of photoresponsive hydrogels. Adv Mater 2019;31:1807333.
[71] Wang M, Zhou L, Deng W, Hou Y, He W, Yu L, et al. Ultrafast response and programmable locomotion of liquid/vapor/light-driven soft multifunctional actuators. ACS Nano 2022;16:2672–81.
[72] Zhang H, Zeng H, Priimagi A, Ikkala O. Programmable responsive hydrogels inspired by classical conditioning algorithm. Nat Commun 2019;10:1–8.
[73] Downs FG, Lunn DJ, Booth MJ, Sauer JB, Ramsay WJ, Klemperer RG, et al. Multi-responsive hydrogel structures from patterned droplet networks. Nat Chem 2020;12:363–71.
[74] Manjua AC, Alves VD, JoG Crespo, Portugal CA. Magnetic responsive PVA hydrogels for remote modulation of protein sorption. ACS Appl Mater Interfaces 2019;11:21239–49.
[75] Li Y, Sun Y, Xiao Y, Gao G, Liu S, Zhang J, et al. Electric field actuation of tough electroactive hydrogels cross-linked by functional triblock copolymer micelles. ACS Appl Mater Interfaces 2016;8:26326–31.
[76] Qu J, Zhao X, Ma PX, Guo B. Injectable antibacterial conductive hydrogels with dual response to an electric field and pH for localized “smart” drug release. Acta Biomater 2018;72:55–69.
[77] Liu H, Rong L, Wang B, Xie R, Sui X, Xu H, et al. Facile fabrication of redox/pH dual stimuli responsive cellulose hydrogel. Carbohydr Polym 2017;176:299–306.
[78] Qiao L, Wang X, Gao Y, Wei Q, Hu W, Wu L, et al. Laccase-mediated formation of mesoporous silica nanoparticle based redox stimuli-responsive hybrid nanogels as a multifunctional nanotheranostic agent. Nanoscale 2016;8:17241–9.
[79] Shigemitsu H, Fujisaku T, Onogi S, Yoshii T, Ikeda M, Hamachi I. Preparation of supramolecular hydrogel–enzyme hybrids exhibiting biomolecule-responsive gel degradation. Nat Protoc 2016;11:1744–56.
[80] Li C, Feng S, Li C, Sui Y, Shen J, Huang C, et al. Synthesizing organo/hydrogel hybrids with diverse programmable patterns and ultrafast self-actuating ability via a site-specific “in situ” transformation strategy. Adv Funct Mater 2020;30:2002163.
[81] Li M, Wang X, Dong B, Sitti M. In-air fast response and high speed jumping and rolling of a light-driven hydrogel actuator. Nat Commun 2020;11:1–10.
[82] Zhang M, Wang Y, Jian M, Wang C, Liang X, Niu J, et al. Spontaneous alignment of graphene oxide in hydrogel during 3D printing for multistimuli-responsive actuation. Adv Sci 2020;7:1903048.
[83] Han X, Xiao G, Wang Y, Chen X, Duan G, Wu Y, et al. Design and fabrication of conductive polymer hydrogels and their applications in flexible supercapacitors. J Mater Chem A 2020;8:23059–95.
[84] Hines L, Petersen K, Lum GZ, Sitti M. Soft actuators for small-scale robotics. Adv Mater 2017;29:1603483.
[85] Wang B, Facchetti A. Mechanically flexible conductors for stretchable and wearable e-skin and e-textile devices. Adv Mater 2019;31:1901408.
[86] Ma Y, Lin M, Huang G, Li Y, Wang S, Bai G, et al. 3D spatiotemporal mechan-

ical microenvironment: a hydrogel-based platform for guiding stem cell fate. Adv Mater 2018;30:1705911.
[87] Weng W, Yang J, Zhang Y, Li Y, Yang S, Zhu L, et al. A route toward smart system integration: from fiber design to device construction. Adv Mater 2020;32:1902301.
[88] Zhu H, Yang H, Ma Y, Lu TJ, Xu F, Genin GM, et al. Spatiotemporally controlled photoresponsive hydrogels: design and predictive modeling from processing through application. Adv Funct Mater 2020;30:2000639.
[89] Forterre Y, Skotheim JM, Dumais J, Mahadevan L. How the Venus flytrap snaps. Nature 2005;433:421–5.
[90] Fratzl P, Barth FG. Biomaterial systems for mechanosensing and actuation. Nature 2009;462:442–8.
[91] Jiang Y, Korpas LM, Raney JR. Bifurcation-based embodied logic and autonomous actuation. Nat Commun 2019;10:1–10.
[92] Wang X, Khara A, Chen C. A soft pneumatic bistable reinforced actuator bioinspired by Venus Flytrap with enhanced grasping capability. Bioinspirat Biomimet 2020;15:056017.
[93] Le X, Lu W, Zheng J, Tong D, Zhao N, Ma C, et al. Stretchable supramolecular hydrogels with triple shape memory effect. Chem Sci 2016;7:6715–20.
[94] Volkov AG, Foster JC, Baker KD, Markin VS. Mechanical and electrical anisotropy in Mimosa pudica pulvini. Plant Signal Behav 2010;5:1211–21.
[95] Deng J, Li J, Chen P, Fang X, Sun X, Jiang Y, et al. Tunable photothermal actuators based on a pre-programmed aligned nanostructure. J Am Chem Soc 2016;138:225–30.
[96] Erb RM, Sander JS, Grisch R, Studart AR. Self-shaping composites with programmable bioinspired microstructures. Nat Commun 2013;4:1–8.
[97] Ko H, Javey A. Smart actuators and adhesives for reconfigurable matter. Acc Chem Res 2017;50:691–702.
[98] Taccola S, Greco F, Sinibaldi E, Mondini A, Mazzolai B, Mattoli V. Toward a new generation of electrically controllable hygromorphic soft actuators. Adv Mater 2015;27:1668–75.
[99] Burgert I, Fratzl P. Actuation systems in plants as prototypes for bioinspired devices. Philos Trans R Soc, A 2009;367:1541–57.
[100] Elbaum R, Gorb S, Fratzl P. Structures in the cell wall that enable hygroscopic movement of wheat awns. J Struct Biol 2008;164:101–7.
[101] Elbaum R, Zaltzman L, Burgert I, Fratzl P. The role of wheat awns in the seed dispersal unit. Science 2007;316:884–6.
[102] Motokawa T. Effects of ionic environment on viscosity of Triton-extracted catch connective tissue of a sea cucumber body wall. Comparat Biochem Physiol Part B: Comparat Biochem 1994;109:613–22.
[103] Trotter JA, Lyons-Levy G, Chino K, Koob TJ, Keene DR, Atkinson MA. Collagen fibril aggregation-inhibitor from sea cucumber dermis. Matrix Biol 1999;18:569–78.
[104] Szulgit GK, Shadwick RE. Dynamic mechanical characterization of a mutable collagenous tissue: response of sea cucumber dermis to cell lysis and dermal extracts. J Exp Biol 2000;203:1539–50.
[105] Trotter JA, Lyons-Levy G, Luna D, Koob TJ, Keene DR, Atkinson MA. Stiparin: a glycoprotein from sea cucumber dermis that aggregates collagen fibrils. Matrix Biol 1996;15:99–110.
[106] Miyawaki A, Llopis J, Heim R, McCaffery JM, Adams JA, Ikura M, et al. Fluorescent indicators for $Ca^{2+}$ based on green fluorescent proteins and calmodulin. Nature 1997;388:882–7.
[107] Shang L, Zhang W, Xu K, Zhao Y. Bio-inspired intelligent structural color materials. Mater Horiz 2019;6:945–58.
[108] Teyssier J, Saenko SV, Van Der Marel D, Milinkovitch MC. Photonic crystals cause active colour change in chameleons. Nat Commun 2015;6:1–7.
[109] Zhang Z, Chen Z, Wang Y, Zhao Y. Bioinspired conductive cellulose liquid-crystal hydrogels as multifunctional electrical skins. Proc Natl Acad Sci 2020;117:18310–16.
[110] Zhao P, Chen H, Li B, Tian H, Lai D, Gao Y. Stretchable electrochromic devices enabled via shape memory alloy composites (SMAC) for dynamic camouflage. Opt Mater 2019;94:378–86.
[111] Mather JA. How do octopuses use their arms? J Comp Psychol 1998;112:306.
[112] Sfakiotakis M, Kazakidi A, Tsakiris D. Octopus-inspired multi-arm robotic swimming. Bioinspirat Biomimet 2015;10:035005.
[113] Walker ID, Dawson DM, Flash T, Grasso FW, Hanlon RT, Hochner B, et al. Continuum robot arms inspired by cephalopods. Unman Ground Veh Technol VII: SPIE 2005:303–14.
[114] Calisti M, Giorelli M, Levy G, Mazzolai B, Hochner B, Laschi C, et al. An octopus-bioinspired solution to movement and manipulation for soft robots. Bioinspirat Biomimet 2011;6:036002.
[115] Cianchetti M, Arienti A, Follador M, Mazzolai B, Dario P, Laschi C. Design concept and validation of a robotic arm inspired by the octopus. Mater Sci Eng: C 2011;31:1230–9.
[116] Renda F, Cianchetti M, Giorelli M, Arienti A, Laschi C. A 3D steady-state model of a tendon-driven continuum soft manipulator inspired by the octopus arm. Bioinspirat Biomimet 2012;7:025006.
[117] McHenry MJ, Jed J. The ontogenetic scaling of hydrodynamics and swimming performance in jellyfish (Aurelia aurita). J Exp Biol 2003;206:4125–37.
[118] Nawroth J, Feitl K, Colin S, Costello JH, Dabiri J. Phenotypic plasticity in juvenile jellyfish medusae facilitates effective animal–fluid interaction. Biol Lett 2010;6:389–93.
[119] Nawroth JC, Lee H, Feinberg AW, Ripplinger CM, McCain ML, Grosberg A, et al. A tissue-engineered jellyfish with biomimetic propulsion. Nat Biotechnol 2012;30:792–7.
[120] Demont ME, Gosline JM. Mechanics of jet propulsion in the hydromedusan jellyfish, Polyorchis penicillatus: II. Energetics of the jet cycle. J Exp Biol 1988;134:333–45.
[121] Gu S, Guo S. Performance evaluation of a novel propulsion system for the spherical underwater robot (SURIII). Appl Sci 2017;7:1196.
[122] Marut K, Stewart C, Michael T, Villanueva A, Priya S. A jellyfish-inspired jet propulsion robot actuated by an iris mechanism. Smart Mater Struct 2013;22:094021.
[123] Spencer A, Satterlie RA. The action potential and contraction in subumbrellar swimming muscle ofPolyorchis penicillatus (Hydromedusae). J Comparat Physiol 1981;144:401–7.
[124] Capadona JR, Shanmuganathan K, Tyler DJ, Rowan SJ, Weder C. Stimuli-responsive polymer nanocomposites inspired by the sea cucumber dermis. Science 2008;319:1370–4.
[125] Dumais J, Forterre Y. Vegetable dynamicks": the role of water in plant movements. Annu Rev Fluid Mech 2012;44:453–78.
[126] Zhang Z-L, Dong X, Fan Y-N, Yang L-M, He L, Song F, et al. Chameleon-inspired variable coloration enabled by a highly flexible photonic cellulose film. ACS Appl Mater Interfaces 2020;12:46710–18.
[127] Guglielmino E, Tsagarakis N, Caldwell DG. An octopus anatomy-inspired robotic arm. In: IEEE/RSJ International Conference on Intelligent Robots and Systems; 2010. p. 3091–6.
[128] Montero de Espinosa L, Meesorn W, Moatsou D, Weder C. Bioinspired polymer systems with stimuli-responsive mechanical properties. Chem Rev 2017;117:12851–92.
[129] Gong C, Shi S, Dong P, Kan B, Gou M, Wang X, et al. Synthesis and characterization of PEG-PCL-PEG thermosensitive hydrogel. Int J Pharm 2009;365:89–99.
[130] Yao C, Liu Z, Yang C, Wang W, Ju XJ, Xie R, et al. Poly (N-isopropylacrylamide)-clay nanocomposite hydrogels with responsive bending property as temperature-controlled manipulators. Adv Funct Mater 2015;25:2980–91.
[131] Liu F, Urban MW. Recent advances and challenges in designing stimuli-responsive polymers. Prog Polym Sci 2010;35:3–23.
[132] Poly Schild HG. N-isopropylacrylamide): experiment, theory and application. Prog Polym Sci 1992;17:163–249.
[133] Taylor MJ, Tomlins P, Sahota TS. Thermoresponsive gels. Gels 2017;3:4.
[134] Tang L, Wang L, Yang X, Feng Y, Li Y, Feng W. Poly (N-isopropylacrylamide)-based smart hydrogels: Design, properties and applications. Prog Mater Sci 2021;115:100702.
[135] He X, Aizenberg M, Kuksenok O, Zarzar LD, Shastri A, Balazs AC, et al. Synthetic homeostatic materials with chemo-mechano-chemical self-regulation. Nature 2012;487:214–18.
[136] Kim YS, Liu M, Ishida Y, Ebina Y, Osada M, Sasaki T, et al. Thermoresponsive actuation enabled by permittivity switching in an electrostatically anisotropic hydrogel. Nat Mater 2015;14:1002–7.
[137] Nojoomi A, Arslan H, Lee K, Yum K. Bioinspired 3D structures with programmable morphologies and motions. Nat Commun 2018;9:1–11.
[138] Zhao C, Ma Z, Zhu X. Rational design of thermoresponsive polymers in aqueous solutions: a thermodynamics map. Prog Polym Sci 2019;90:269–91.
[139] Seuring J, Agarwal S. First example of a universal and cost-effective approach: Polymers with tunable upper critical solution temperature in water and electrolyte solution. Macromolecules 2012;45:3910–18.
[140] Koetting MC, Peters JT, Steichen SD, Peppas NA. Stimulus-responsive hydrogels: Theory, modern advances, and applications. Mater Sci Eng: R: Rep 2015;93:1–49.
[141] Asadujjaman A, Kent B, Bertin A. Phase transition and aggregation behaviour of an UCST-type copolymer poly (acrylamide-co-acrylonitrile) in water: effect of acrylonitrile content, concentration in solution, copolymer chain length and presence of electrolyte. Soft Matter 2017;13:658–69.
[142] Mirvakili SM, Hunter IW. Artificial muscles: Mechanisms, applications, and challenges. Adv Mater 2018;30:1704407.
[143] Hua L, Xie M, Jian Y, Wu B, Chen C, Zhao C. Multiple-responsive and amphibious hydrogel actuator based on asymmetric UCST-type volume phase transition. ACS Appl Mater Interfaces 2019;11:43641–8.
[144] Zhang Y, Xie S, Zhang D, Ren B, Liu Y, Tang L, et al. Thermo-responsive and shape-adaptive hydrogel actuators from fundamentals to applications. Eng Sci 2019;6.
[145] Roy D, Brooks WL, Sumerlin BS. New directions in thermoresponsive polymers. Chem Soc Rev 2013;42:7214–43.
[146] Li J, Ma Q, Xu Y, Yang M, Wu Q, Wang F, et al. Highly bidirectional bendable actuator engineered by LCST–UCST bilayer hydrogel with enhanced interface. ACS Appl Mater Interfaces 2020;12:55290–8.
[147] Zheng J, Xiao P, Le X, Lu W, Théato P, Ma C, et al. Mimosa inspired bilayer hydrogel actuator functioning in multi-environments. J Mater Chem C 2018;6:1320–7.
[148] Klajn R. Spiropyran-based dynamic materials. Chem Soc Rev 2014;43:148–84.
[149] Kloxin AM, Kasko AM, Salinas CN, Anseth KS. Photodegradable hydrogels for dynamic tuning of physical and chemical properties. Science 2009;324:59–63.
[150] Shi Q, Liu H, Tang D, Li Y, Li X, Xu F. Bioactuators based on stimulus-responsive hydrogels and their emerging biomedical applications. NPG Asia Mater 2019;11:1–21.
[151] Chen Y, Yang J, Zhang X, Feng Y, Zeng H, Wang L, et al. Light-driven bimorph soft actuators: design, fabrication, and properties. Mater Horiz 2021;8:728–57.
[152] Li Q, Fuks G, Moulin E, Maaloum M, Rawiso M, Kulic I, et al. Macroscopic contraction of a gel induced by the integrated motion of light-driven molecular motors. Nat Nanotechnol 2015;10:161–5.

[153] Park C, Lee K, Kim C. Photoresponsive cyclodextrin-covered nanocontainers and their sol-gel transition induced by molecular recognition. Angew Chem Int Ed 2009;48:1275–8.
[154] Shi Q, Xia H, Li P, Wang YS, Wang L, Li SX, et al. Photothermal Surface Plasmon Resonance and Interband Transition-Enhanced Nanocomposite Hydrogel Actuators with Hand-Like Dynamic Manipulation. Adv Opt Mater 2017;5:1700442.
[155] Yang H, Leow WR, Wang T, Wang J, Yu J, He K, et al. 3D printed photoresponsive devices based on shape memory composites. Adv Mater 2017;29:1701627.
[156] Sun Z, Yamauchi Y, Araoka F, Kim YS, Bergueiro J, Ishida Y, et al. An Anisotropic Hydrogel Actuator Enabling Earthworm-Like Directed Peristaltic Crawling. Angew Chem 2018;130:15998–6002.
[157] Xue P, Bisoyi HK, Chen Y, Zeng H, Yang J, Yang X, et al. Near-infrared light–driven shape-morphing of programmable anisotropic hydrogels enabled by MXene nanosheets. Angew Chem Int Ed 2021;60:3390–6.
[158] Shankar A, Safronov AP, Mikhnevich EA, Beketov IV. Multidomain iron nanoparticles for the preparation of polyacrylamide ferrogels. J Magn Magn Mater 2017;431:134–7.
[159] Kim Y, Yuk H, Zhao R, Chester SA, Zhao X. Printing ferromagnetic domains for untethered fast-transforming soft materials. Nature 2018;558:274–9.
[160] Roeder L, Bender P, Tschöpe A, Birringer R, Schmidt AM. Shear modulus determination in model hydrogels by means of elongated magnetic nanoprobes. J Polym Sci, Part B: Polym Phys 2012;50:1772–81.
[161] Kim Y, Zhao X. Magnetic soft materials and robots. Chem Rev 2022;122:5317–64.
[162] Shi W, Huang J, Fang R, Liu M. Imparting functionality to the hydrogel by magnetic-field-induced nano-assembly and macro-response. ACS Appl Mater Interfaces 2020;12:5177–94.
[163] Wu S, Hu W, Ze Q, Sitti M, Zhao R. Multifunctional magnetic soft composites: a review. Multifunct Mater 2020;3:042003.
[164] Liu Z, Liu J, Cui X, Wang X, Zhang L, Tang P. Recent advances on magnetic sensitive hydrogels in tissue engineering. Front Chem 2020;8:124.
[165] Li H, Go G, Ko SY, Park J-O, Park S. Magnetic actuated pH-responsive hydrogel-based soft micro-robot for targeted drug delivery. Smart Mater Struct 2016;25:027001.
[166] Podstawczyk D, Nizioł M, Szymczyk P, Wiśniewski P, Guiseppi-Elie A. 3D printed stimuli-responsive magnetic nanoparticle embedded alginate-methylcellulose hydrogel actuators. Addit Manufact 2020;34:101275.
[167] Cheng Y, Chan KH, Wang XQ, Ding T, Li T, Zhang C, et al. A fast autonomous healing magnetic elastomer for instantly recoverable, modularly programmable, and thermorecyclable soft robots. Adv Funct Mater 2021;31:2101825.
[168] Bassetti MJ, Chatterjee AN, Aluru N, Beebe DJ. Development and modeling of electrically triggered hydrogels for microfluidic applications. J Microelectromech Syst 2005;14:1198–207.
[169] Messing R, Schmidt AM. Perspectives for the mechanical manipulation of hybrid hydrogels. Polym Chem 2011;2:18–32.
[170] Osada Y, Okuzaki H, Hori H. A polymer gel with electrically driven motility. Nature 1992;355:242–4.
[171] Yang C, Liu Z, Chen C, Shi K, Zhang L, Ju X-J, et al. Reduced graphene oxide–containing smart hydrogels with excellent electro-response and mechanical properties for soft actuators. ACS Appl Mater Interfaces 2017;9:15758–67.
[172] Kang Y-W, Woo J, Lee H-R, Sun J-Y. A mechanically enhanced electroactive hydrogel for 3D printing using a multileg long chain crosslinker. Smart Mater Struct 2019;28:095016.
[173] Ko J, Kim D, Song Y, Lee S, Kwon M, Han S, et al. Electroosmosis-driven hydrogel actuators using hydrophobic/hydrophilic layer-by-layer assembly-induced crack electrodes. ACS nano 2020;14:11906–18.
[174] Albright V, Zhuk I, Wang Y, Selin V, van de Belt-Gritter B, Busscher HJ, et al. Self-defensive antibiotic-loaded layer-by-layer coatings: Imaging of localized bacterial acidification and pH-triggering of antibiotic release. Acta Biomater 2017;61:66–74.
[175] Guo W, Lu CH, Orbach R, Wang F, Qi XJ, Cecconello A, et al. pH-Stimulated DNA hydrogels exhibiting shape-memory properties. Adv Mater 2015;27:73–8.
[176] Duan J, Liang X, Zhu K, Guo J, Zhang L. Bilayer hydrogel actuators with tight interfacial adhesion fully constructed from natural polysaccharides. Soft Matter 2017;13:345–54.
[177] Li R, Jin D, Pan D, Ji S, Xin C, Liu G, et al. Stimuli-responsive actuator fabricated by dynamic asymmetric femtosecond bessel beam for in situ particle and cell manipulation. ACS nano 2020;14:5233–42.
[178] Xu Y, Bolisetty S, Drechsler M, Fang B, Yuan J, Ballauff M, et al. pH and salt responsive poly (N, N-dimethylaminoethyl methacrylate) cylindrical brushes and their quaternized derivatives. Polymer 2008;49:3957–64.
[179] Blackman LD, Gunatillake PA, Cass P, Locock KE. An introduction to zwitterionic polymer behavior and applications in solution and at surfaces. Chem Soc Rev 2019;48:757–70.
[180] Le X-X, Lu W, He J, Serpe MJ, Zhang J-W, Chen T. Ionoprinting controlled information storage of fluorescent hydrogel for hierarchical and multi-dimensional decryption. Sci China Mater 2019;62:831–9.
[181] Du X, Cui H, Zhao Q, Wang J, Chen H, Wang Y. Inside-out 3D reversible ion-triggered shape-morphing hydrogels. Research 2019 2019.
[182] Dawson C, Vincent JF, Rocca A-M. How pine cones open. Nature 1997;390:668.
[183] Kim H, Lee SJ. Stomata-inspired membrane produced through photopolymerization patterning. Adv Funct Mater 2015;25:4496–505.
[184] Lv C, Sun X-C, Xia H, Yu Y-H, Wang G, Cao X-W, et al. Humidity-responsive actuation of programmable hydrogel microstructures based on 3D printing. Sens Actuat, B 2018;259:736–44.
[185] Zheng Y, Huang H, Wang Y, Zhu J, Yu J, Hu Z. Poly (vinyl alcohol) based gradient cross-linked and reprogrammable humidity-responsive actuators. Sens Actuat, B 2021;349:130735.
[186] Wu S, Shi H, Lu W, Wei S, Shang H, Liu H, et al. Aggregation-induced emissive carbon dots gels for octopus-inspired shape/color synergistically adjustable actuators. Angew Chem Int Ed 2021;60:21890–8.
[187] Hubbard AM, Cui W, Huang Y, Takahashi R, Dickey MD, Genzer J, et al. Hydrogel/elastomer laminates bonded via fabric interphases for stimuli-responsive actuators. Matter 2019;1:674–89.
[188] Badeau BA, DeForest CA. Programming stimuli-responsive behavior into biomaterials. Annu Rev Biomed Eng 2019;21.
[189] Lin X, Wang X, Zeng L, Wu ZL, Guo H, Hourdet D. Stimuli-responsive toughening of hydrogels. Chem Mater 2021;33:7633–56.
[190] Ulijn RV, Bibi N, Jayawarna V, Thornton PD, Todd SJ, Mart RJ, et al. Bioresponsive hydrogels. Mater Today 2007;10:40–8.
[191] Cangialosi A, Yoon C, Liu J, Huang Q, Guo J, Nguyen TD, et al. DNA sequence–directed shape change of photopatterned hydrogels via high-degree swelling. Science 2017;357:1126–30.
[192] Chung HJ, Charaya H, Liu L, Li X. Tough hydrogels: toughening mechanisms and their utilization in stretchable electronics and in regenerative medicines. Hybrid Organ-Inorgan Interfaces: Toward Adv Funct Mater 2018:535–80.
[193] Bai R, Yang J, Suo Z. Fatigue of hydrogels. Eur J Mech A Solids 2019;74:337–70.
[194] Bouchbinder E, Goldman T, Fineberg J. The dynamics of rapid fracture: instabilities, nonlinearities and length scales. Rep Prog Phys 2014;77:046501.
[195] Delville MH, Taubert A. Hybrid organic-inorganic interfaces: towards advanced functional materials, 2. John Wiley & Sons; 2018. Volumes.
[196] Zhang T, Lin S, Yuk H, Zhao X. Predicting fracture energies and crack-tip fields of soft tough materials. Extrem Mech Lett 2015;4:1–8.
[197] Fuchs S, Shariati K, Ma M. Specialty tough hydrogels and their biomedical applications. Adv Healthc Mater 2020;9:1901396.
[198] Zhao X. Multi-scale multi-mechanism design of tough hydrogels: building dissipation into stretchy networks. Soft matter 2014;10:672–87.
[199] Furukawa H, Horie K, Nozaki R, Okada M. Swelling-induced modulation of static and dynamic fluctuations in polyacrylamide gels observed by scanning microscopic light scattering. Phys Rev E 2003;68:031406.
[200] Costa AM, Mano JF. Extremely strong and tough hydrogels as prospective candidates for tissue repair–a review. Eur Polym J 2015;72:344–64.
[201] Naficy S, Brown HR, Razal JM, Spinks GM, Whitten PG. Progress toward robust polymer hydrogels. Aust J Chem 2011;64:1007–25.
[202] Zhao X. Designing toughness and strength for soft materials. Proc Natl Acad Sci 2017;114:8138–40.
[203] Wang X, Wang H, Brown HR. Jellyfish gel and its hybrid hydrogels with high mechanical strength. Soft Matter 2011;7:211–19.
[204] Xu Q, McMichael P, Creagh-Flynn J, Zhou D, Gao Y, Li X, et al. Double-cross-linked hydrogel strengthened by UV irradiation from a hyperbranched PEG-based trifunctional polymer. Acs Macro Lett 2018;7:509–13.
[205] Buwalda SJ, Vermonden T, Hennink WE. Hydrogels for therapeutic delivery: current developments and future directions. Biomacromolecules 2017;18:316–30.
[206] Kolb HC, Finn M, Sharpless KB. Click chemistry: diverse chemical function from a few good reactions. Angew Chem Int Ed 2001;40:2004–21.
[207] Malkoch M, Vestberg R, Gupta N, Mespouille L, Dubois P, Mason AF, et al. Synthesis of well-defined hydrogel networks using click chemistry. Chem Commun 2006:2774–6.
[208] Truong VX, Tsang KM, Forsythe JS. Nonswelling click-cross-linked gelatin and PEG hydrogels with tunable properties using pluronic linkers. Biomacromolecules 2017;18:757–66.
[209] Akagi Y, Matsunaga T, Shibayama M, Chung U-i, Sakai T. Evaluation of topological defects in tetra-PEG gels. Macromolecules 2010;43:488–93.
[210] Kamata H, Chung U, Shibayama M, Sakai T. Anomalous volume phase transition in a polymer gel with alternative hydrophilic–amphiphilic sequence. Soft Matter 2012;8:6876–9.
[211] Nishi K, Fujii K, Katsumoto Y, Sakai T, Shibayama M. Kinetic aspect on gelation mechanism of tetra-PEG hydrogel. Macromolecules 2014;47:3274–81.
[212] Creton C. 50th anniversary perspective: networks and gels: soft but dynamic and tough. Macromolecules 2017;50:8297–316.
[213] Noda Y, Hayashi Y, Ito K. From topological gels to slide-ring materials. J Appl Polym Sci 2014:131.
[214] He Q, Wang Z, Yan Y, Zheng J, Cai S. Polymer nanofiber reinforced double network gel composite: strong, tough and transparent. Extrem Mech Lett 2016;9:165–70.
[215] Jordan AM, Kim S-E, Van de Voorde K, Pokorski JK, Korley LT. In situ fabrication of fiber reinforced three-dimensional hydrogel tissue engineering scaffolds. Acs Biomater Sci Eng 2017;3:1869–79.
[216] Kosik-Kozioł A, Costantini M, Bolek T, Szöke K, Barbetta A, Brinchmann J, et al. PLA short sub-micron fiber reinforcement of 3D bioprinted alginate constructs for cartilage regeneration. Biofabrication 2017;9:044105.
[217] Yodmuang S, McNamara SL, Nover AB, Mandal BB, Agarwal M, Kelly T-AN, et al. Silk microfiber-reinforced silk hydrogel composites for functional cartilage tissue repair. Acta Biomater 2015;11:27–36.

[218] Amaral AJ, Pasparakis G. Stimuli responsive self-healing polymers: gels, elastomers and membranes. Polym Chem 2017;8:6464–84.
[219] Lohani A, Singh G, Bhattacharya SS, Verma A. Interpenetrating polymer networks as innovative drug delivery systems. J Drug Deliv 2014 2014.
[220] Somya G, Nayyar P, Akanksha B, Kumar SP. Interpenetrating polymer network-based drug delivery systems: emerging applications and recent patents. Egypt Pharmaceut J 2015;14:75.
[221] Bakarich SE, Balding P, Gorkin III R, Spinks GM. Printed ionic-covalent entanglement hydrogels from carrageenan and an epoxy amine. RSC Adv 2014;4:38088–92.
[222] Chen Q, Chen H, Zhu L, Zheng J. Fundamentals of double network hydrogels. J Mater Chem B 2015;3:3654–76.
[223] Chen Q, Zhu L, Zhao C, Wang Q, Zheng J. A robust, one-pot synthesis of highly mechanical and recoverable double network hydrogels using thermoreversible sol-gel polysaccharide. Adv Mater 2013;25:4171–6.
[224] Carrow JK, Gaharwar AK. Bioinspired polymeric nanocomposites for regenerative medicine. Macromol Chem Phys 2015;216:248–64.
[225] Haraguchi K, Kimura Y, Shimizu S. Reversible generation of large retractive tensile forces in isometric chemo-mechanical actuators composed of nanocomposite hydrogels and aqueous NaCl solutions. Soft Matter 2018;14:927–33.
[226] Haraguchi K, Li H-J, Xu Y, Li G. Copolymer nanocomposite hydrogels: unique tensile mechanical properties and network structures. Polymer 2016;96:94–103.
[227] Hu J, Kurokawa T, Nakajima T, Wu ZL, Liang SM, Gong JP. Fracture process of microgel-reinforced hydrogels under uniaxial tension. Macromolecules 2014;47:3587–94.
[228] Kaspar C, Ravoo B, van der Wiel WG, Wegner S, Pernice W. The rise of intelligent matter. Nature 2021;594:345–55.
[229] Li M, Pal A, Aghakhani A, Pena-Francesch A, Sitti M. Soft actuators for real–world applications. Nat Rev Mater 2022;7:235–49.
[230] Yang C, Suo Z. Hydrogel ionotronics. Nat Rev Mater 2018;3:125–42.
[231] Dong Y, Wang J, Guo X, Yang S, Ozen MO, Chen P, et al. Multi-stimuli-responsive programmable biomimetic actuator. Nat Commun 2019;10:1–10.
[232] Yao Y, Yin C, Hong S, Chen H, Shi Q, Wang J, et al. Lanthanide-ion-coordinated supramolecular hydrogel inks for 3D printed full-color luminescence and opacity-tuning soft actuators. Chem Mater 2020;32:8868–76.
[233] Zhao H, Huang Y, Lv F, Liu L, Gu Q, Wang S. Biomimetic 4D-Printed Breathing Hydrogel Actuators by Nanothylakoid and Thermoresponsive Polymer Networks. Adv Funct Mater 2021;31:2105544.
[234] Yoon C. Advances in biomimetic stimuli responsive soft grippers. Nano Convergen 2019;6:1–14.
[235] Zhang A, Wang F, Chen L, Wei X, Xue M, Yang F, et al. 3D printing hydrogels for actuators: a review. Chin Chem Lett 2021;32:2923–32.
[236] Shang J, Le X, Zhang J, Chen T, Theato P. Trends in polymeric shape memory hydrogels and hydrogel actuators. Polym Chem 2019;10:1036–55.
[237] Cheng F-m, Chen H-x, Li H-d. Recent progress on hydrogel actuators. J Mater Chem B 2021;9:1762–80.
[238] Armon S, Efrati E, Kupferman R, Sharon E. Geometry and mechanics in the opening of chiral seed pods. Science 2011;333:1726–30.
[239] Zhao Q, Liang Y, Ren L, Yu Z, Zhang Z, Ren L. Bionic intelligent hydrogel actuators with multimodal deformation and locomotion. Nano Energy 2018;51:621–31.
[240] Ma C, Lu W, Yang X, He J, Le X, Wang L, et al. Bioinspired anisotropic hydrogel actuators with on–off switchable and color-tunable fluorescence behaviors. Adv Funct Mater 2018;28:1704568.
[241] Sun B, Jia R, Yang H, Chen X, Tan K, Deng Q, et al. Magnetic arthropod millirobots fabricated by 3D-printed hydrogels. Adv Intell Syst 2022;4:2100139.
[242] Fan W, Shan C, Guo H, Sang J, Wang R, Zheng R, et al. Dual-gradient enabled ultrafast biomimetic snapping of hydrogel materials. Sci Adv 2019;5:eaav7174.
[243] Wang W, Yao L, Cheng C-Y, Zhang T, Atsumi H, Wang L, et al. Harnessing the hygroscopic and biofluorescent behaviors of genetically tractable microbial cells to design biohybrid wearables. Sci Adv 2017;3:e1601984.
[244] Rivera ML, Forman J, Hudson SE, Yao L. Hydrogel-textile composites: Actuators for shape-changing interfaces. In: Extended Abstracts of the 2020 CHI Conference on Human Factors in Computing Systems; 2020. p. 1–9.
[245] Yu Q, Bauer JM, Moore JS, Beebe DJ. Responsive biomimetic hydrogel valve for microfluidics. Appl Phys Lett 2001;78:2589–91.
[246] Cheng Y, Ren K, Huang C, Wei J. Self-healing graphene oxide-based nanocomposite hydrogels serve as near-infrared light-driven valves. Sens Actuat, B 2019;298:126908.
[247] Wang Y, Toyoda K, Uesugi K, Morishima K. A simple micro check valve using a photo-patterned hydrogel valve core. Sens Actuat, A 2020;304:111878.
[248] Sackmann EK, Fulton AL, Beebe DJ. The present and future role of microfluidics in biomedical research. Nature 2014;507:181–9.
[249] Sontheimer-Phelps A, Hassell BA, Ingber DE. Modelling cancer in microfluidic human organs-on-chips. Nat Rev Cancer 2019;19:65–81.
[250] Ter Schiphorst J, Saez J, Diamond D, Benito-Lopez F, Schenning AP. Light-responsive polymers for microfluidic applications. Lab Chip 2018;18:699–709.
[251] d'Eramo Lc, Chollet B, Leman M, Martwong E, Li M, Geisler H, et al. Microfluidic actuators based on temperature-responsive hydrogels. Microsyst Nanoeng 2018;4:1–7.
[252] Takeuchi N, Nakajima S, Yoshida K, Kawano R, Hori Y, Onoe H. Microfiber-shaped programmable materials with stimuli-responsive hydrogel. Soft Robot 2022;9:89–97.
[253] Tang J, Yin Q, Qiao Y, Wang T. Shape morphing of hydrogels in alternating magnetic field. ACS Appl Mater Interfaces 2019;11:21194–200.
[254] Kobayashi K, Yoon C, Oh SH, Pagaduan JV, Gracias DH. Biodegradable thermomagnetically responsive soft untethered grippers. ACS Appl Mater Interfaces 2018;11:151–9.
[255] Malachowski K, Jamal M, Jin Q, Polat B, Morris CJ, Gracias DH. Self-folding single cell grippers. Nano Lett 2014;14:4164–70.
[256] Zhao Q, Wang J, Wang Y, Cui H, Du X. A stage-specific cell-manipulation platform for inducing endothelialization on demand. Natl Sci Rev 2020;7:629–43.